UCRL-17853

University of California

Ernest O. Lawrence Radiation Laboratory

BEHAVIOR OF SOME TRANSITION METAL PORPHYRINS

Linda Kanner Phillips
(Ph.D. Thesis)

December 1967

Berkeley, California

DISCLAIMER

UCRL-17853

UNIVERSITY OF CALIFORNIA

Lawrence Radiation Laboratory

Berkeley, California

AEC Contract No. W-7406-eng-48

BEHAVIOR OF SOME TRANSITION METAL PORPHYRINS

Linda Kanner Phillips

(Ph.D. Thesis)

December 1967

TABLE OF CONTENTS

TABLE OF CONTENTS (continued)

TABLE OF CONTENTS (continued)

BEHAVIOR OF SOME TRANSITION METAL PORPHYRINS

Linda Kanner Phillips

Lawrence Radiation Laboratory
University of California
Berkeley, California

December 15, 1967

ABSTRACT

In order to study the influence of porphyrin-type ligands on the chemistry of transition metal ions, the behavior of manganese in chelates with phthalocyanine, methyl pheophorbide-a, etioporphyrin I -- members of three distinct classes of porphyrins -- has been investigated.

Oxidation and reduction reactions of the methyl pheophorbide-a and etioporphyrin complexes have been studied both in solutions and in the solid state. The compounds are light sensitive: the chelated manganese(III) is reduced to manganese(II) under irradiation by white light. (Methyl pheophorbide-a)manganese(IV) has been produced. Its reduction has been studied to learn whether this reaction can serve as a model for the mysterious but crucial role of manganese in photosynthetic oxygen evolution. However, no formation of free oxygen was detected.

Adducts with pyridine acetic acid, water, and other vapors were studied using a quartz helix microbalance which was designed so that atmosphere and temperature could be controlled. One pyridine per manganese is strongly bound and another weakly adsorbed by μ-oxobis (phthalocyaninomanganese), in agreement with the structure of this compound which was determined by Vogt and co-workers (Vogt, Zalkin

and Templeton, Science, 151, 569 (1966). Similarly, etioporphyrin I acetotatomanganese(III), with a single vacant axial coordination position, forms 1:1 adducts with pyridine, acetic acid, or acetone. Phthalocyaninomanganese(II) adds two equivalents of pyridine, in a reaction whose rate depends on the history of the sample.

The electron paramagnetic resonance of phthalocyaninomanganese(II), the only easily prepared manganese(II) compound among those studied, has been investigated in glasses at 90°K. The manganese appears to be in its rare low-spin state ($S = 1/2$) and shows anisotropic hyperfine and spectroscopic splitting tensors: $A = 151 \times 10^{-4}$, $B = 25 \times 10^{-4}$ cm^{-1}; $g_{\parallel} = 1.90$, $g_{\perp} = 2.16$. The unpaired electron is probably in the d_{xy} orbital of manganese. The energy ordering of levels is believed to be $d_{xz}, d_{yz} < d_{xy} < d_{z^2} < d_{x^2-y^2}$.

ACKNOWLEDGEMENTS

Many members of the Biodynamics group and the Chemistry Department have given me ideas and advice, taught me new techniques, or obtained, made or maintained experimental apparatus and chemicals. In particular, I thank my advisor, Professor Melvin Calvin, for his patience with a wayward student; Professor Rollie Myers, for a critical reading of Chapter VI; and Professor Sumner P. Davis, for his continued interest and encouragement. My early work was done under the tutelage of Dr. Akio Yamamoto. The synthesis of tetrasulfophthalocyanine complexes was done in collaboration with Dr. David Samuel. In connection with EPR experiments and their interpretation, I am grateful to Dr. Robert T. Ross, Dr. M. P. Klein, Mrs. Ann Kirkwood (nee Maksim), and Dr. William Blumberg. My thanks go to Miss Lucille McCormick and Mmes. Marilyn Taylor, Johanna Onffroy, and especially Evie Litton. They managed my affairs in Berkeley and typed my thesis via mail and long-distance phone calls. To Mrs. Litton and Mr. A. Korda of UCSB I owe many excellent figures.

I am deeply grateful to my husband, Dr. David Turner Phillips, who has helped me in so many ways and has even allowed me to litter his desk with my papers and books; and to Daviel Alan Phillips, who so actively and vocally spurred me on towards the finish.

This work was done under auspices of the U. S. Atomic Energy Commission.

I. INTRODUCTION

Hemoglobin transports oxygen in the blood. Chlorophyll not only gives green plants their color, but also traps light energy to make photosynthesis possible. These vital compounds are the most famous members of the large and wide-spread family of porphyrins, which are macrocyclic tetrapyrrole pigments. Other members play a variety of biological roles: Hemes, iron porphyrins related to that in hemoglobin, are the active agents of many of the electron-transfer enzymes. Ooporphyrin tints eggshells; turacin colors the wing feathers of the Turaco bird.

The porphyrins are important for their inorganic chemistry as well as for their biological functions, because they form square planar coordination complexes with transition metals. These complexes are often extremely stable; the association constant of iron in hemes is about 10^{30}, and vanadium porphyrins have been found in ancient oils. Those metal ions which tend to be six-coordinate may readily add or exchange axial ligands without disturbing the chelate, and again a dramatic example is the oxygen-carrying ability of iron in hemoglobin.

Manganese too is essential in certain biological processes, although it is usually necessary in such small quantities that its precise role has been harder to define. Manganese deficiency hinders the production of oxygen by plants (see for instance Tanner et al., 1960). The smallest unit that can perform photosynthesis, known as the quantasome, contains two manganese atoms (Park and Biggins, 1964).

The manganese appears in the intractable protein fraction, and has so far frustrated all attempts to discover its molecular environment.

Several enzymes are specifically activated by Mn^{2+}. We know very little about the surroundings of the manganese in the enzymes, but it is almost certainly chelated (Martell and Calvin, 1952, p. 401 ff.). Red blood cells incorporate manganese when in the body (though oddly, not in a test tube), binding it very tightly in a compound which is isolated with crystallized hemin. Borg and Cotzias (1958) suggest that the manganese is present as a porphyrin complex, but do not speculate on its function.

Elvidge and Lever in 1959 reported that a manganese complex of phthalocyanine--first cousin to the porphyrins--could produce oxygen. Since then several man-years have been devoted to the study of various manganese porphyrins in the Chemical Biodynamics Laboratory (Engelsma et al., 1962; Calvin, 1965). While no evidence has been found for oxygen formation, even in Elvidge and Lever's system, we have learned much about the coordination chemistry, redox behavior, and electronic structure of these chelates. In this dissertation I will discuss some progress in each of the areas mentioned.

STRUCTURE AND NOMENCLATURE OF THE PORPHYRINS

Porphin is a fully conjugated macrocycle which contains four pyrrole rings (Fig. I-1a). Any compound having this basic structure is called a porphyrin. Many of these substances were discovered in nature long before their composition was known, and were named for where they occur (ooporphyrin, found in eggs) or for some property, particularly color (chlorophyll, light green; rhodoporphyrin, rose

a)

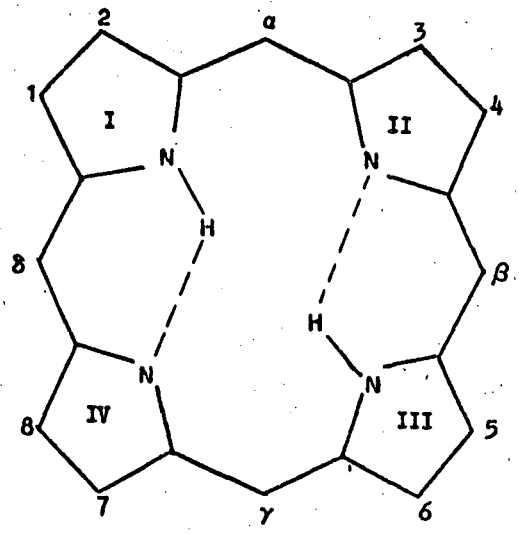

b)

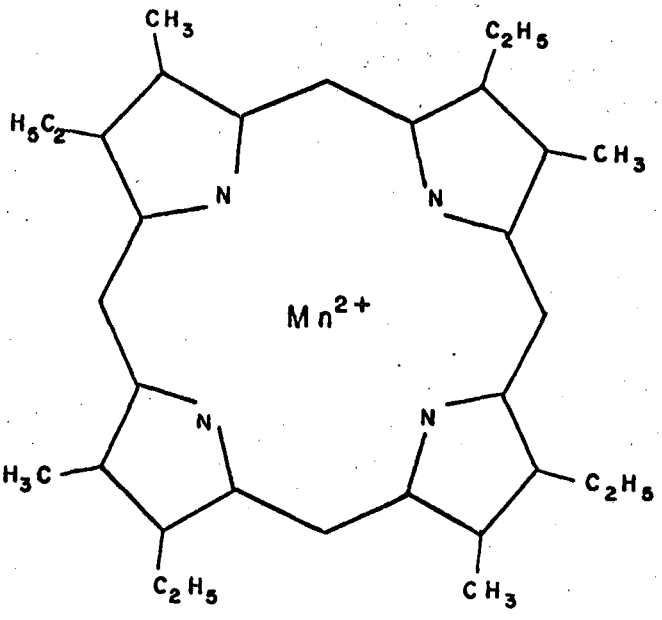

XBL 678-6132

Fig. I-1. Porphins. a) the parent molecule porphin, showing the numbering system conventionally used for naming porphyrins. The dashed lines indicate possible hydrogen-bonding; b) etioporphyrin I manganese(II). The "I" refers to the alternate ordering of methyl and ethyl groups around the ring.

red; porphyrin, from the Greek "porphyra", purple). The trivial names make it difficult to visualize the relationships among the porphyrins, but there is a reason for continuing to use them instead of systematic names. One of the simplest substituted porphyrins, etioporphyrin I (Fig. I-1b), is properly 2,4,6,8-tetraethyl-1,3,5,7-tetramethylporphin, and more complicated compounds have correspondingly intractable names.

The substituted, fully unsaturated molecules like those in Fig. I-1 are a class of porphyrins properly called porphins, but often known simply as porphyrins. The most important class of dihydroporphyrins, which have a single saturated bond in the ring, is the chlorins. In Fig. I-2 is shown a well-known chlorin: with M = Mg and R = phytyl, the chain of a long organic alcohol, this is chlorophyll-a. One of the compounds which we have studied, (methyl pheophorbide-a)manganese, is just the same molecule with R = methyl and M = Mn. As usual, the trivial names conceal the relationship between the compounds.

Azaporphyrins are formed by replacement of one or more of the bridge carbons by nitrogens. Tetrabenztetrazaporphin, better known as phthalocyanine, is a synthetic dye with a spectacular blue color. A manganese(III) complex of phthalocyanine, in which two of the planar moeities are joined by an oxygen atom, is illustrated in Fig. I-3.

Neutral porphyrins contain two protons attached to the central nitrogens, possibly with some hydrogen bonding, as indicated in Fig. I-1a. The terms "free-base" and "metal-free" porphyrins are often used to distinguish the porphyrins from the metalloporphyrins, in which the hydrogens are replaced by metal ions. With a few

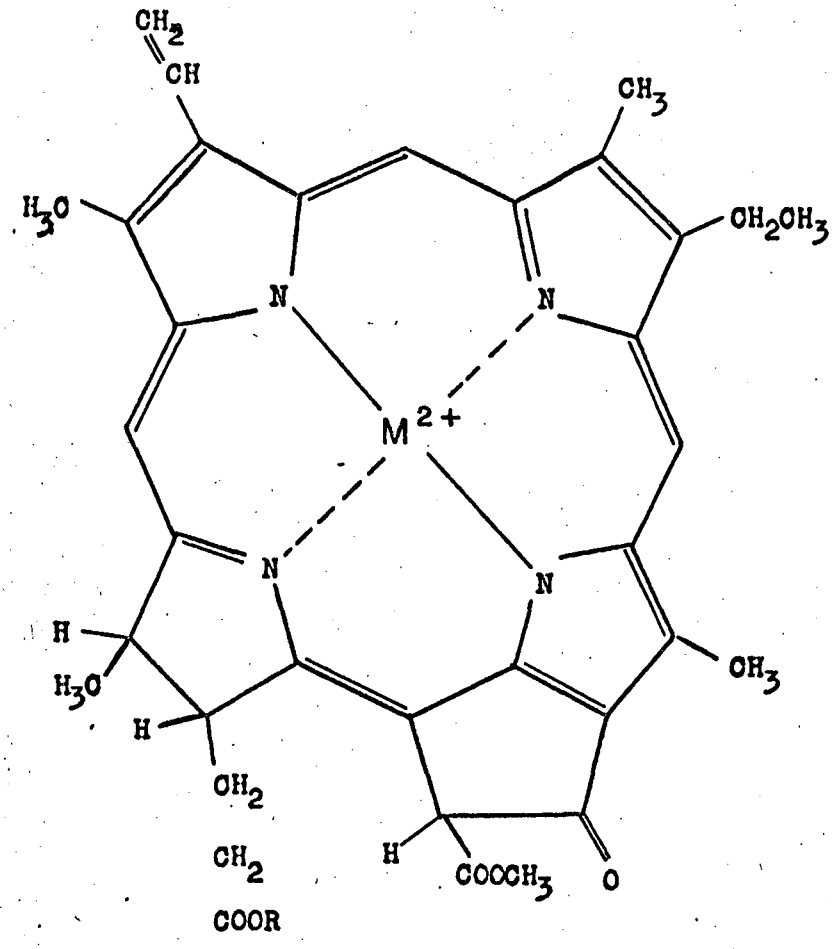

XBL 678-6133

Fig. I-2. Chlorophyll-a: M = Mg, R = phytyl ($C_{20}H_{39}$);
(Methyl pheophorbide-a)manganese: M = Mn, R = methyl.
Only one of the possible resonance structures is shown.

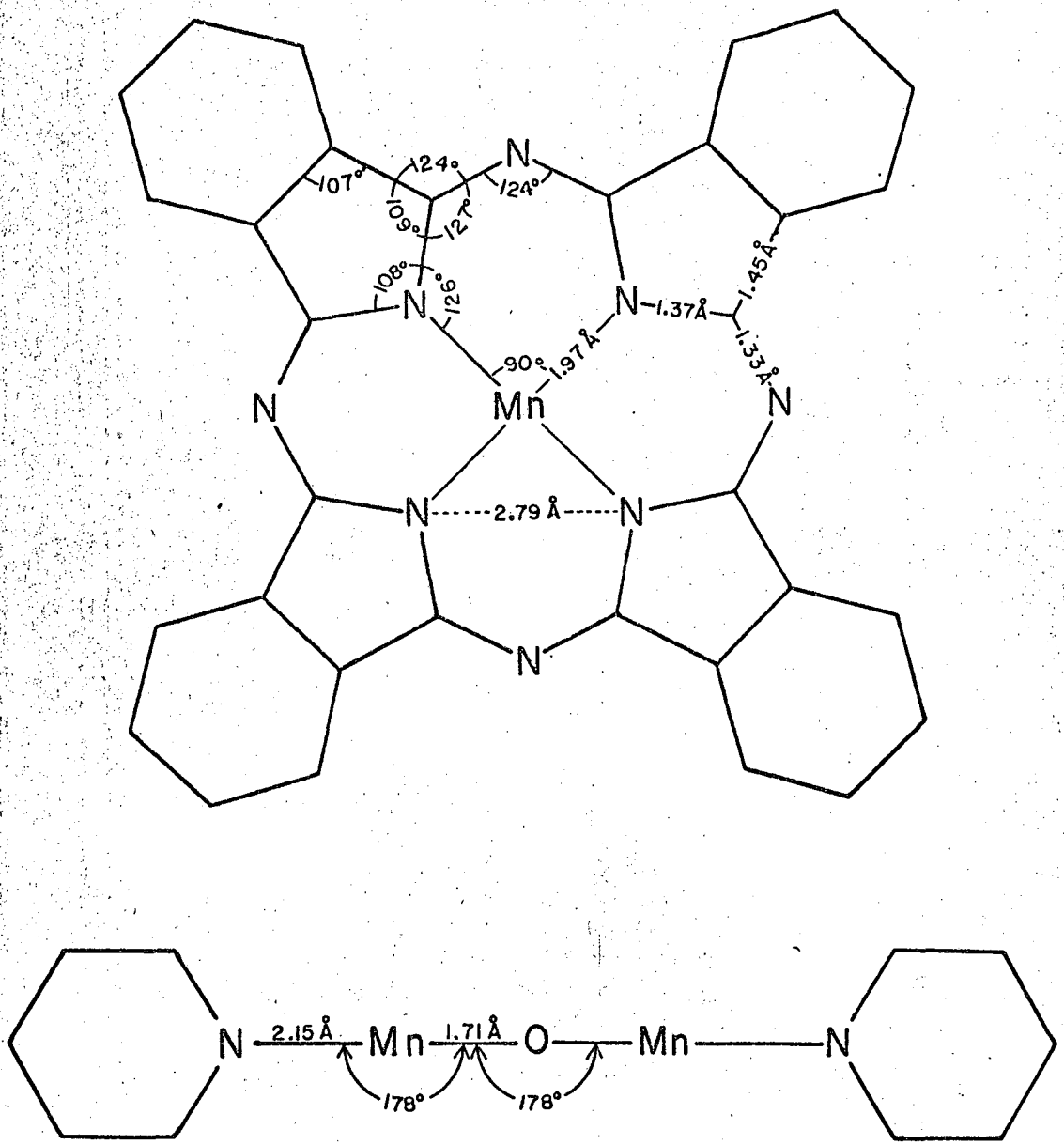

Fig. I-3. Molecular structure of μ-oxobis(phthalocyaninomanganese), (Vogt, Zalkin and Templeton, 1966, 1967).

exceptions, for instance the diberyllium and dilithium compounds, a single metal ion occupies the central hole in the porphyrin and is bound equally by all four nitrogens. This important fact is sometimes masked by the common practice of illustrating a single resonance form, as in Fig. I-2. There are several ways of naming metalloporphyrins, depending mainly on the author's orientations: hemin, iron protoporphyrin chloride, (protoporphyrin IX)chloroiron(III) are all the same. The last style, although more unwieldy than the others, conforms to the conventions set by IUPAC for inorganic chemical nomenclature, and makes it clear that we are dealing with a metal coordination compound.

We shall often abbreviate the names of porphyrins under discussion. H_2Etp refers to etioporphyrin I; Mn^{II}Etp, to (etioporphyrin I); manganese(II); Mn^{III}Etp(OAc), to (etioporphyrin I)acetatomanganese(III). Usually we shall include the oxidation state of the metal if it is known. Axial ligands, however, will not always be specified. Table I-1 lists the abbreviations used here.

Table I-1

Abbreviations for the names of porphyrins

Abbreviation	Trivial Name	Figure
Etp	Etioporphyrin I	I-1b
Pheo	Methyl pheophorbide-a	I-2
Pc	Phthalocyanine	I-3
PTS	Tetrasulfophthalocyanine	---
Hm	Hematoporphyrin IX	*
P	(general) Porphyrin	---

*See Loach and Calvin, 1963.

Robertson (1936) determined the structure of phthalocyanine by X-ray analysis, in a classic triumph for the method of isomorphous replacement. So formidable was the task* that until recently no complete three-dimensional analysis was accomplished on any porphyrin. Since Robertson reported convincing evidence that phthalocyanine is flat, all porphyrins were assumed to be planar. Several studies have now proved that, on the contrary, the porphyrin skeleton is remarkably flexible and will bend or pucker to fit a particular crystalline form, (Webb and Fleischer, 1965; Hamor, Caughey and Hoard, 1965). Even in phthalocyanine, the benzene rings can bend away from the molecular plane (Vogt, Zalkin and Templeton, 1966, 1967). Nor is the metal always coplanar with the porphyrin, as the references above show.

The literature in the porphyrin field is vast, scattered, and often conflicting. Fortunately it includes some rather thorough compilations. Falk's monograph, Porphyrins and Metalloporphyrins (1964), is recommended for its coverage of the general chemistry of these substances and of special techniques for handling them in the laboratory. Lever (1965a) has written a comprehensive review of the phthalocyanines.

---

*For the structure in Fig. I-3, each stage of refinement required three hours on an IBM 7044 computer (Vogt et al., 1966).

II. PREPARATIONS

A. ETIOPORPHYRIN I ACETATOMANGANESE(III)

Etioporphyrin I (0.47 g, 1.0 mmole) and manganese(II) acetate (0.63 g, 5.5 mmole) were heated for several hours at about 80° in 50 ml glacial acetic acid containing 8 ml acetic anhydride. Completion of the reaction was confirmed by the electronic spectrum, which showed that all of the etioporphyrin was in the form of its manganese (III) complex. The solution was evaporated to dryness and taken up in chloroform. The residue, excess manganese acetate, was filtered off, and the filtrate was concentrated to a small volume. Concentration of all chloroform solutions was accomplished by using a rotary evaporator at room temperature under vacuum.

Chromatography of the concentrated chloroform solution on a column of activated alumina (Woelm, activity grade I; or Merck, chromatographic grade) showed at least three distinct bands, one of which was nearly insoluble in chloroform but soluble in pyridine. The main, chloroform-soluble fraction was further purified by removing the solvent and then subliming the solid at 350-400°C, in vacuum. This procedure yields $Mn^{II}Etp \cdot HOAc$; impurities and by-products of the reduction do not sublime with the complex, which upon exposure to the atmosphere is oxidized to $Mn^{III}Etp(OAc)$. Probably the acetic acid is liberated during the reduction; as $Mn^{II}Etp$ condenses in a cool part of the vessel, it reabsorbs the acetic acid vapor. The infrared spectrum of the compound in air (see Chapter III) indicates the presence of acetate as well as some adsorbed acetic acid.

Calculated for $Mn^{III}Etp(OAc)$, $C_{34}H_{39}N_4O_2Mn$: C, 69.1; H, 6.7; N, 9.5; O, 5.4; Mn, 9.3%. Found: C, 68.1; H, 6.6; N, 9.7; O (by difference), 6.1; Mn, 9.5%. (Manganese content was estimated as ash, assuming that the ash consisted of Mn_3O_4 only.) Empirical formula: $C_{33}H_{38}N_4O_2Mn$.

B. (METHYL PHEOPHORBIDE-a)CHLOROMANGANESE(III)

An early preparation of $Mn^{III}Pheo$ gave a mixture of the chelate and metal-free methyl pheophorbide-a. Since the product was used in several experiments, however, the method is described here. About 25 mg of methyl pheophorbide-a was mixed with a tenfold excess of manganese acetate in chloroform. The electronic spectrum agreed with that of methyl pheophorbide-a (Zeiger and Witt, 1961), and did not change even after long standing and heating. The solvent was evaporated, and the residue dissolved in dimethylformamide to which was added some solid $NaHCO_3$. Again little reaction was observed until the mixture was heated on a steam bath. Water and benzene were now added, the plan being to extract the chelate and the unreacted chlorin into the benzene layer. Surprisingly, only the methyl pheophorbide-a appeared in the benzene, whereas the water layer exhibited an unfamiliar spectrum. To the eye both layers were the same dark green. From the water-soluble fraction the inorganic salts were removed by repeated evaporation and dissolution in ethanol. The final alcoholic solution was used without further purification. The sample was probably allomerized (although no accompanying spectral shifts were observed), and the methyl ester may have been replaced by ethyl. After a more nearly pure batch of $Mn^{III}Pheo$ was obtained (see below) it was obvious that

the electronic spectrum of this sample represented an approximately 50:50 mixture of complexed and uncomplexed chlorin.

A more satisfactory method for preparing Mn^{III}Pheo was a modification of that described by Loach and Calvin (1964b). Methyl pheophorbide-a, 110 mg or 0.18 mmole (Fluka AG Chemische Fabrik Buchs/SG, Switzerland; "puriss.") was dissolved in a 3:2 mixture of acetic acid and acetone. $MnAc_2 \cdot 4H_2O$, 548 mg or 2.24 mmoles (Matheson Coleman and Bell, reagent grade) was added, and the reaction was allowed to proceed for four days. The solution was then decanted from the undissolved manganese acetate. The solvent was removed by freeze-drying; the residue was extracted with chloroform, the resulting solution evaporated, and the solid leached with water. The aqueous solution was adjusted to pH about 7.35 with KOH and HCl; potassium chloride (Baker and Adams, reagent) was added to about 1 M. Instead of the hoped-for tractable precipitate, a colloid was formed, which refused to redissolve. The product was extracted into chloroform, from which it formed an oil rather than crystals.

In another attempt, the residue was leached with 95% ethanol instead of water. Leaching was done in small batches, and stopped when the electronic spectrum revealed that no more chelate was being extracted, but only the metal-free pheophorbide-a. The earlier fractions, containing Mn^{III}Pheo, and free of most inorganic salts, were evaporated down. The residue was extracted with chloroform, this solvent removed, and the final residue dissolved in 20% aqueous ethanol, from which it precipitated as small, dark green crystals. The product gave a spectrum similar to that reported by Loach and Calvin.

C. (METHYL PHEOPHORBIDE-a)MANGANESE(II): Attempted preparation.

Manganese acetate and methyl pheophorbide-a were placed in a cuvette similar to those illustrated in Fig. IV-1, but with an EPR tube as a side-arm. Acetic acid-acetone (3:2) was added and the vessel was glass-sealed. After 38 days in the dark a steady state had been reached; unfortunately the reaction did not go to completion. An electron paramagnetic resonance spectrum (see Chapter VI) revealed uncomplexed Mn^{2+}; any resonance from the chelate was too weak to detect.

D. TETRASULFOPHTHALOCYANINOIRON

This compound was prepared by a modification of Weber and Busch's method (1965). Mr. Bill Hart constructed for us a demountable three-neck boiling flask of about 300 ml volume (Fig. II-1). Around each half of the flask, near the flanges, was an adjustable hose connector to which three springs could be fastened. These springs held the flask together. A minimum amount of silicone grease was used. With this arrangement, leakage was negligible and the solid, friable product could easily be removed. To one neck of the flask was fitted a condenser; on another was a thermometer; the central neck was used for adding reagents and the rest of the time was corked.

Twenty ml of nitrobenzene was heated in this flask to about 170°C. Ammonium chloride (2.35 g, 45 mmole), monosodium 4-sulfophthalate (21.6 g, 81 mmole), urea (29 g, 490 mmole), ammonium molybdate (0.37 g, 0.3 mmole), and ferrous sulfate, $FeSO_4 \cdot 7H_2O$ (6.7 g, 24 mmole) were ground together in a mortar. The mixture was added slowly to the hot nitrobenzene, while the temperature was kept between about 160° and

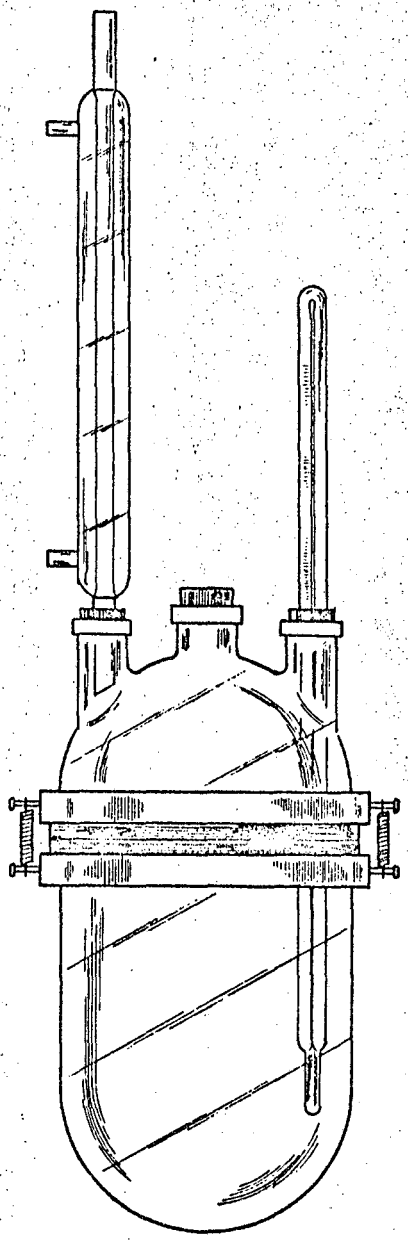

XBL 678-6126

Fig. II-1. Reaction vessel for the preparation of tetrasulfophthalocyanine complexes. The clamps are made from adjustable hose connectors; metal-glass contact is prevented by placing asbestos tape under the clamps.

200°. The reaction mixture soon became dark green and viscous, making temperature control rather difficult. NH_4Cl tended to clog the condenser; the most satisfactory arrangement was to use a straight condenser and occasionally scrape off the ammonium chloride with a long glass rod. After cooling, the green-black, cinder-like product was removed from the flask and ground in a mortar, then washed with methanol until the odor of nitrobenzene disappeared. The spectrum of the green methanol extract had a peak at 660 nm, with inflections at 630 and 600 nm and huge ultraviolet absorption. The residue was dissolved in 1 N hydrochloric acid, again giving a green solution; sodium chloride was added to salt out the tetrasulfophthalocyaninoiron. The spectra of diluted aliquots of this solution were taken for comparison with the known spectrum of $Fe^{II}PTS$ as reported by Kobayashi et al. (1960): 676 and 633 nm in detergent solutions. The product showed a peak at 637 nm with a shoulder at 676 nm; a broad shoulder centered at around 520 nm, and a very intense absorption around 325 nm. When this sample was further diluted, three peaks of nearly equal intensity appeared at 678, 637, and 330 nm.

A precipitate, formed upon heating the HCl solution, was filtered out; an aliquot of the supernatant diluted in water exhibited a spectrum similar to that above. The precipitate was dissolved in 0.1 N sodium hydroxide to give a very deep blue solution, whose main spectral peak was at 635 nm, with an inflection at about 580 nm and the usual ultraviolet peak at 328 nm. There was virtually no sign of any absorption at 670 nm, although on further dilution, a shoulder appeared at that wavelength.

The basic solution was heated to 90° and immediately filtered. A chocolate-colored precipitate remained on the filter, and was discarded. Salt was added to the solution. After about two hours some precipitate had appeared. The solution was again heated to 70-90° for about 15 minutes to remove ammonia, for which the classic test (smell) was given. As well as the odor of ammonia, there was another, yeast-like odor. Certainly yeast was not growing in the solution, as was confirmed by microscopic examination; the cause of the odor remains a mystery. Further heating did not remove the odor.

After storage in the dark for three days, the solution was again heated, and the extremely fine precipitate was filtered off. The precipitate was dissolved in 0.1 N NaOH, heated, filtered immediately to remove impurities, then cooled and filtered. The process was repeated twice, at which point filtration became frustratingly slow. A rubbery, dark blue pad remained on the filter; this was transferred to a beaker and 100 ml 80% ethanol was added. The remaining precipitate, after washing with more 80% ethanol, was Soxhlet-extracted with absolute ethanol. Yield, 5.5 g.

Analysis. The Chemistry Department's Microanalytical Laboratory performed analyses for C, H, N, and S. Iron content was determined by me by atomic absorption spectrophotometry.* The compound is very hygroscopic. Found: C, 34.3; H, 2.9; N, 8.4; S, 9.6; Fe, 4.2%. Empirical formula, $C_{38}H_{38}N_8S_4Fe$. The compositions $(C_{32}N_8H_{13}Na_3S_4O_{12})$; $Fe\cdot 3(C_2H_5OH)$ and $(C_{32}N_8H_{12}Na_4S_4O_{12})Fe\cdot 3(C_2H_5OH)$ fit the data equally

*A weighed sample was digested in 17:1 HNO_3-$HClO_4$ and the resulting solution diluted with water. The final solution was then compared with standard solutions of iron salts, on the Perkin-Elmer Model 303 Atomic Absorption Spectrophotometer. Measurements were taken at the 248 nm iron line.

well. The presence of ethanol, as well as water, was confirmed by mass spectrometry: A weighed sample of FePTS was warmed at about 60-80° for an hour, under vacuum; volatile matter was collected at liquid nitrogen temperature. A mass spectrogram of the latter (as vapor) revealed a large amount of water and at least one ethanol/10 Fe (estimated by peak area). Unfortunately, it is impossible to tell from the elemental analysis whether the iron is in the +2 or +3 state.

E. TETRASULFOPHTHALOCYANINOIRON(II): Attempted preparation.

To an aqueous solution of H_2PTS (10^{-3} - 10^{-4} M) under nitrogen atmosphere was added $FeCl_2 \cdot 4H_2O$ (1.5 - 2 equivalents). The mixture was kept and handled under nitrogen. After two weeks, the water was evaporated off and 95% ethanol added to dissolve any $Fe^{III}PTS$, which Kobayashi and co-workers (1960) report is slightly alcohol-soluble. To separate the dark residue from the aqua solution, the mixture was centrifuged in a nalgene tube with a close-fitting lid. The residue was washed two more times; washings were poured into a beaker in the nitrogen box. The product was nitrogen-dried. Spectra of both product and washings, in 50% aqueous ethanol, were unmistakeably that of H_2PTS.

When a large excess of ferrous sulfate was added to a solution of H_2PTS (the washings from the experiment above), under nitrogen, there was a definite change in the spectrum, presumably representing formation of $Fe^{II}PTS$. Introduction of air, rather surprisingly, caused no alteration in spectrum. When potassium hydroxide was added under nitrogen, the solution turned violet; on exposure to

air, it returned to its original blue color, and thereafter remained blue even in the absence of oxygen.. A similar effect of alkali on Fe^{II}PTS was observed by Glikman and co-workers (1959).

III. ELECTRONIC AND INFRARED SPECTRA OF METALLOPORPHYRINS

Porphin and chlorin complexes of manganese(III) exhibit visible and near-ultraviolet spectra which are quite different from those characteristic of other porphyrin chelates. The origin of the anomalous "Mn^{III} spectrum" has worried the writer for some time. It is so unusual that we have considered the possibility that the manganese greatly disturbs the porphyrin ring. The suggestion was made (M. Gouterman, private communication) that the "Mn^{III} spectrum" might instead be due to a radical cation of the porphyrin, stabilized somehow by the manganese: $Mn^{II}(P^{+})$.

If the porphyrin were a free radical, its bond orders would be different from those in the normal porphyrin. Then bond lengths and strengths would change as well, resulting in an anomalous infrared (vibration-rotation) spectrum. But the infrared spectrum of Mn^{III}Etp(OAc) is compared in Section III-B with those of other etioporphyrins, and shows no abnormal features.

Another critical experiment is the electron paramagnetic resonance of the compound. A free radical should show a strong resonance signal at g = 2.00. However, neither Mn^{III}Pheo nor Mn^{III}Etp gave any signal which could be attributed to a radical (see Section VI-B).

This negative evidence for the $Mn^{II}(P^{+})$ agrees with Gouterman's later calculations, which also rule out the cation. Another explanation for the anomalous spectrum has been advanced. It will be discussed in the next section, along with a general background of the theory of porphyrin spectra.

A. ELECTRONIC SPECTRA

1. The porphyrins and similar compounds have distinctive electronic spectra, with strong absorption extending from the near ultraviolet region through the visible, and in some cases into the near infrared as well. The visible bands give porphyrins their deep and often beautiful colors, and make the phthalocyanines valuable dyes.

An extremely strong band ($\varepsilon > 10^5$) at around 400 nm* is characteristic of porphyrins; it has been named for Soret, who discovered it in 1883. In the 500-600 nm region appear weaker bands (ε ca. 10^3-10^4) which are sensitive to the symmetry in the center of the molecule: Only two bands (one electronic transition with a vibrational sideband) are seen in this region (Fig. III-3) for the centrally square, or D_{4h}, metalloporphyrins (see Fig. III-1). The electronic transition splits in the neutral porphin, which contains two protons in the center and hence has the lower symmetry D_{2h} (Fig. III-1d). Of the four peaks observed, as shown in Fig. III-2, bands I and III are the 0-0 vibrations of the two electronic transitions, while bands II and IV are their respective 0-1 vibrational peaks.

The natures of the coordinated metal and of peripheral substituents affect intensity and energy of the Soret and visible transitions, but with few exceptions do not change the qualitative picture. Only in manganese(III) porphyrins does the Soret band split widely** (see for instance, Fig. IV-2).

---

*Following IUPAC convention, we will use the term nanometer (nm) rather than mμ.

**The Soret band is also split in the triplet-triplet spectra and in the radical ions--both of which are obtained only under special conditions--and to a very small extent in extremely assymetric porphyrins.

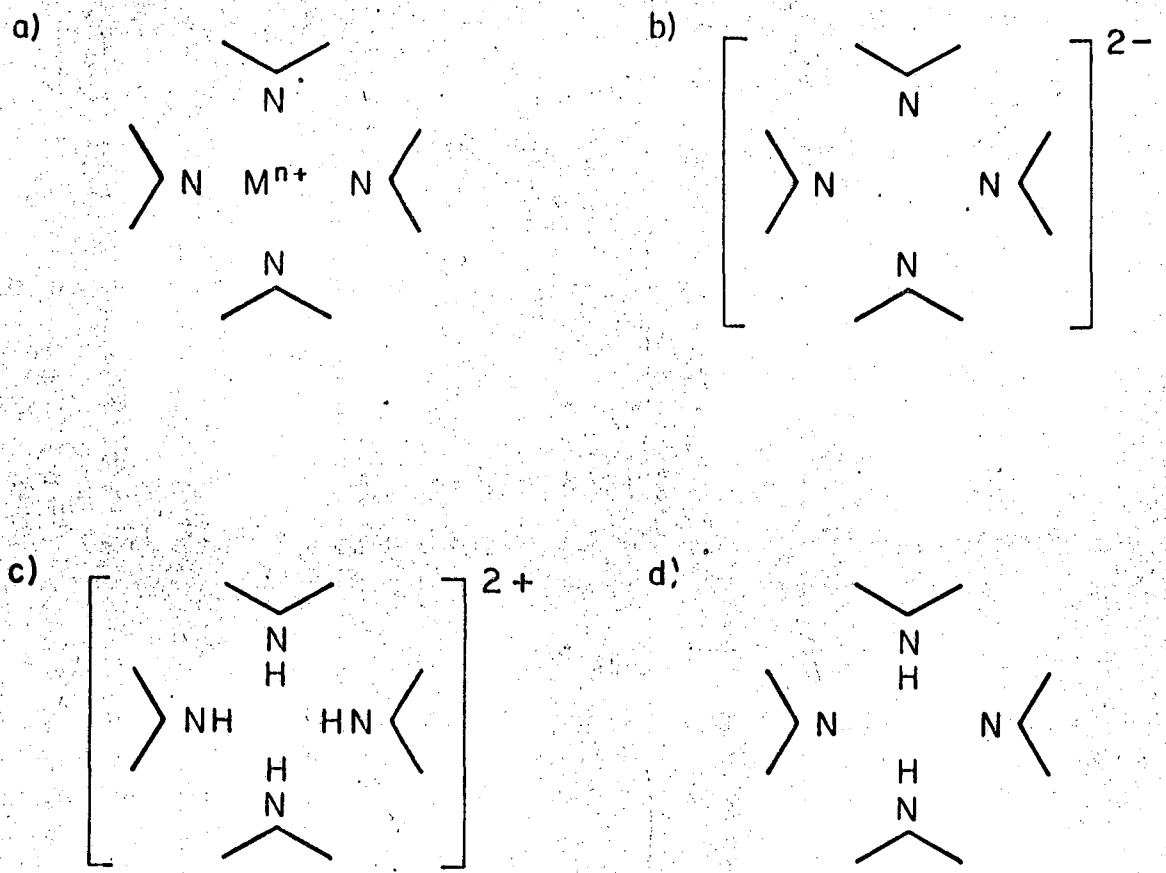

XBL 677-4531

Fig. III-1. Central structure in the porphyrins. In a), b), and c) the symmetry is D_{4h}; d) has D_{2h} symmetry.

a) Metalloporphyrin. b) Porphyrin di-anion; c) Porphyrin di-cation. d) Neutral porphyrin molecule.

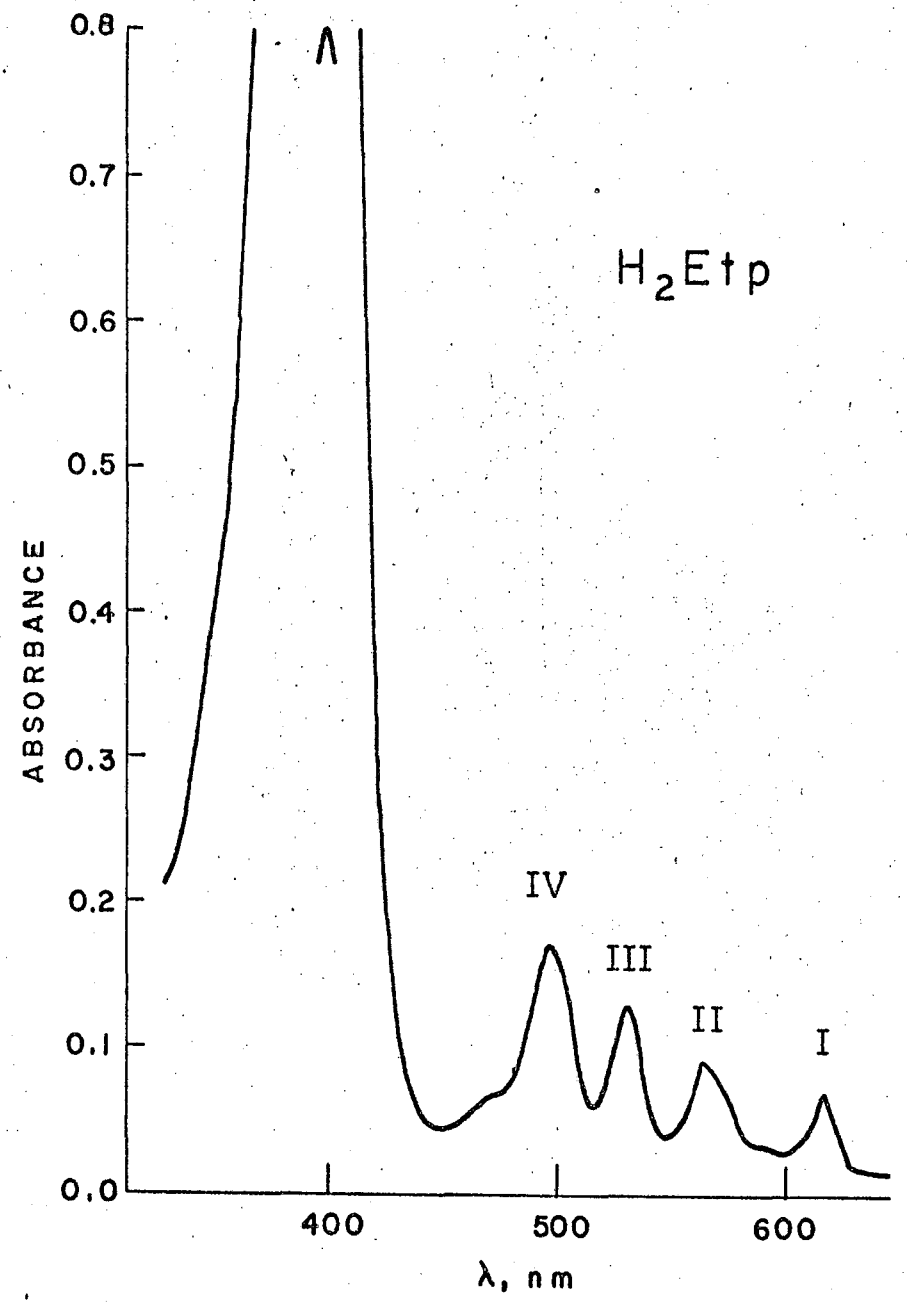

XBL 678-6130

Fig. III-2. Electronic spectrum of etioporphyrin I in chloroform solution.

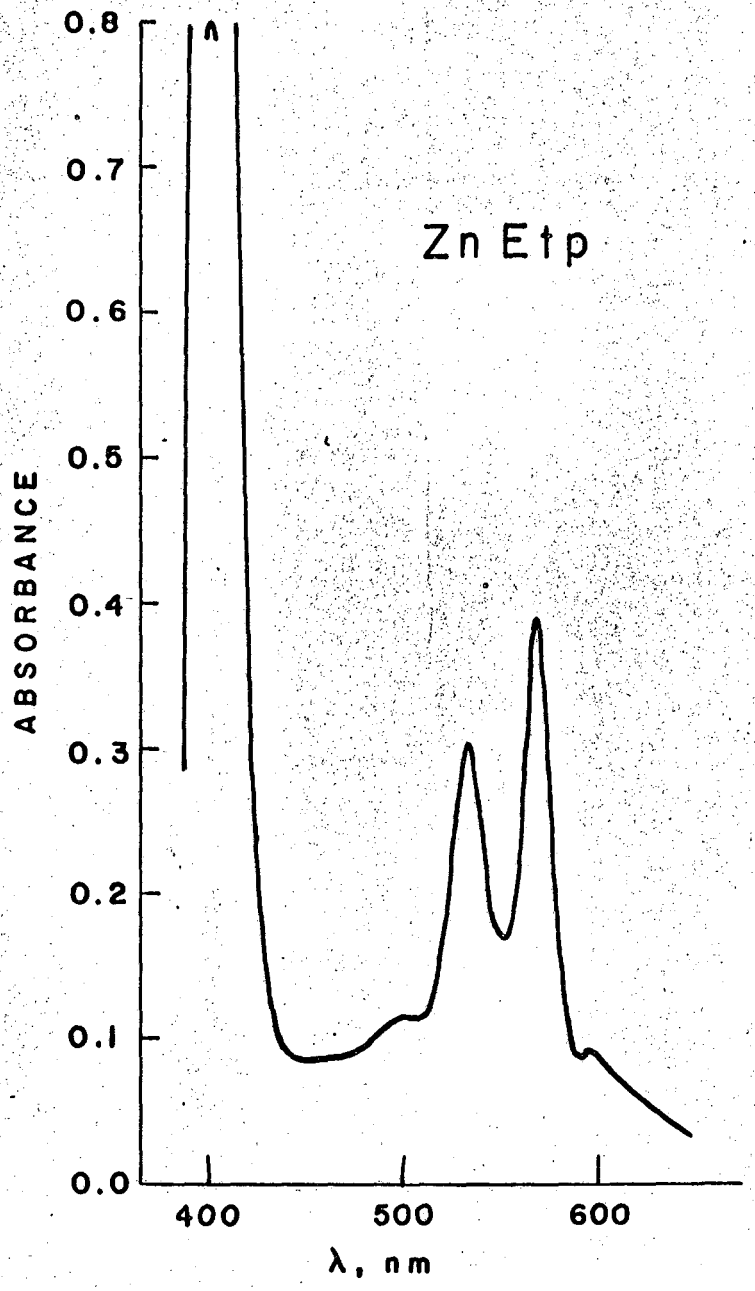

XBL 678-6131

Fig. III-3. Spectrum of a chloroform solution of etioporphyrin I zinc(II).

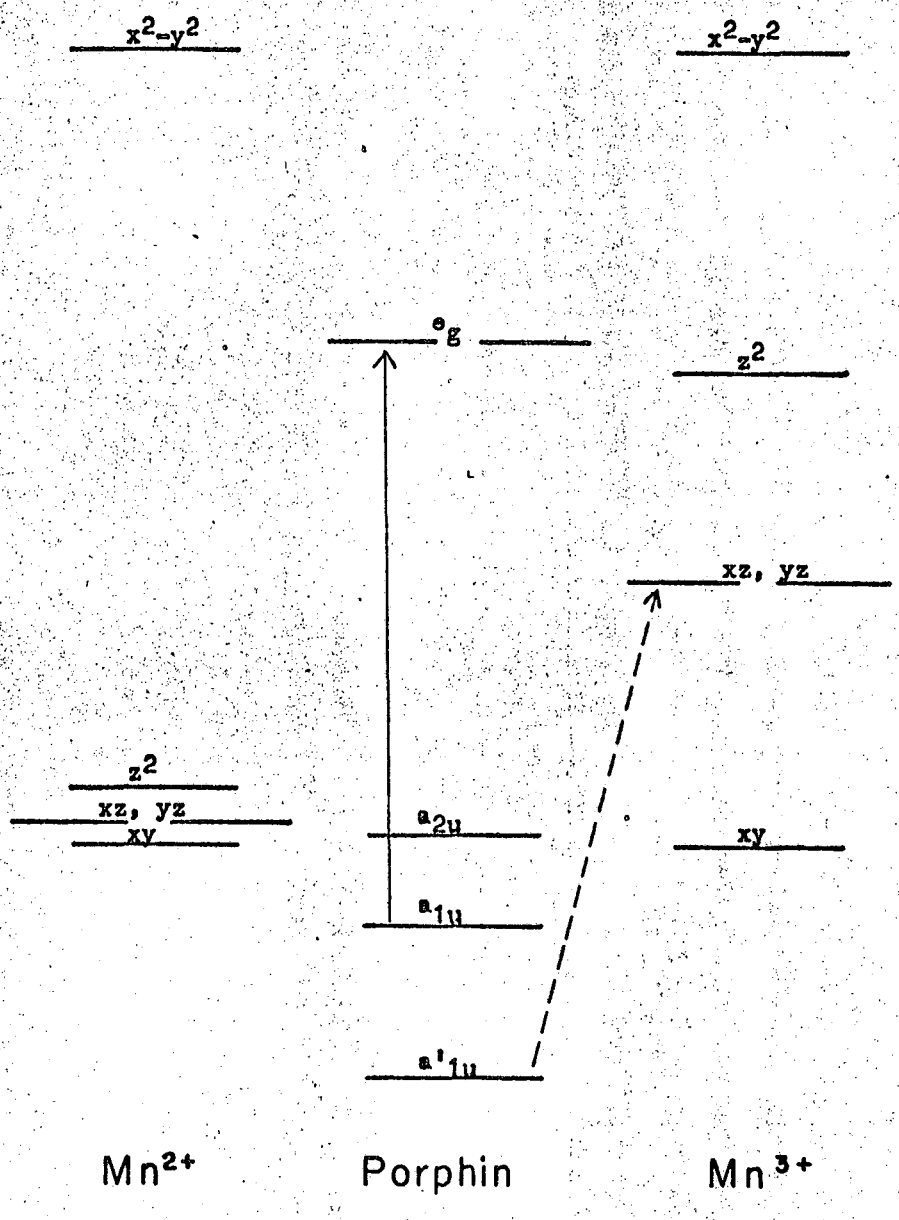

XBL 678-6129

Fig. III-4. Energy diagram for porphin and its manganese(II) and manganese(III) chelates. The solid arrow indicates the Soret transition; the dashed arrow, the resonance transition which occurs in the manganese(III) compounds. The Mn^{3+} levels are schematic only (M. Gouterman, private communication); the others are as calculated by Zerner, Gouterman and Kobayashi (1966).

Porphyrins contain a large pi-electron system which is cata-condensed: rings within the ring. The pi electrons can move over the entire porphyrin skeleton in molecular orbitals. Transitions among these molecular orbitals are responsible for the observed electronic spectra. The complicated nature of the system, the biological importance of the hemes, and the wealth of available spectral data have challenged theoreticians to elucidate the electronic structure of porphyrins. Successive refinements in the theory have brought it ever closer to the "truth"--that is, to a correct prediction of the electronic spectra. Early work on the subject is mainly of historical interest; recent calculations are highly technical and would take more than the available space to cover thoroughly. The most extensive investigation has been made by Gouterman and co-workers,* and their pertinent results will be briefly summarized below. We must warn the reader, as they do, that the theory is still far from perfect, and that the results must be taken with a grain of salt.

The spectral bands are generally due to transitions between one of the top two filled orbitals and the two (degenerate) lowest empty molecular orbitals. Gouterman (1961) has illustrated and discussed these orbitals. Suffice it here to say that the Soret band ($a_{1u} \rightarrow e_g$)** involves a movement of electrons toward those atoms nearest a chelated metal (the pyrrole nitrogens and bridging atoms), while the

---

*These authors have produced a monumental series of papers, of which Paper IV (Zerner and Gouterman, 1966) explores several transition metal complexes, including that of manganese. Paper VIII (Zerner, Gouterman and Kobayashi, 1966) is also pertinent, although limited to the iron complexes.

**Symmetries are those for the D_{4h} point group.

visible bands ($a_{2u} \rightarrow e_g$) move electrons away from these atoms. The calculated ordering of the orbitals is shown in Fig. III-4. Symmetry considerations allow the metal d_{xz}, d_{yz} (e_g) orbitals to mix with the excited porphyrin state. The only other metal orbital with the proper symmetry and anywhere near the right energy to mix with a porphyrin pi orbital is $4p_z$ (a_{2u}) which has the same symmetry as the next-to-top filled porphyrin level. There can also be some mixing between d orbitals and the nitrogen sigma orbitals, but these are not closely coupled to the pi system. The electrons on most metals studied--zinc is an exception--remain isolated from the porphyrin system to a surprising degree.

Thus a chelated metal chiefly affects the porphyrin spectrum by making the molecular center square, while the two hydrogens in the free porphyrin cause a small distortion into a rhombus. The spectrum is that of a squared porphyrin (compare Fig. III-1b,c) slightly perturbed by the presence of the metal. Because the metal orbitals do not interact extensively with those of the ligand, they do not affect a qualitative description of the spectrum. We cannot even observe their d-d transitions, which are so important in the spectra of many complexes, because the porphyrin bands occur in the same energy range and are at least 1000 times as intense.

2. Manganese(III) complexes. Why then does manganese(III) have such a profound effect on the spectrum? According to Gouterman (private communication) its uniqueness seems to stem from the energy of its $d_{xz,yz}$ level, which is of e_g symmetry. There are of course many filled pi orbitals in the porphyrin system, some of which are of a_{2u} symmetry, as is the next-to-top filled pi level

(Fig. III-4). The transition between the highest a_{2u} orbital and the excited pi state e_g gives rise to the Soret band. By chance another orbital which we shall call a'_{2u} is lower than $d_{xz,yz}$ by an energy very close to that of the Soret transition. Since $a'_{2u} \rightarrow e_g(d_{xz,yz})$ has the same symmetry properties as $a_{2u} \rightarrow e_g(pi)$, and the transition energies are nearly equal, a resonance occurs. What happens is a special case of two accidentally degenerate states: the states mix and their energies split. I am indebted to D. T. Phillips for the following phenomenological treatment of the problem.

Consider two electrons, each of which has two possible states:

	Location	State	Energy
Electron 1 in its ground state ---	ring	g	W_g
Electron 1 in its excited state ---	ring	e	W_e
Electron 2 in its ground state ---	ring	G	W_G
Electron 2 in its excited state ---	Mn	E	W_E

We assume that the energy differences between ground and excited states are equal:

$$W_e - W_g = W_E - W_G$$

then

$$W_e + W_G = W_E + W_g$$

so that there are two states of the total system with the same energy --either electron 1 or electron 2 excited, and the other in its ground state. The total wave function is

$$\phi = C_1 \mid eE > + C_2 \mid eG > + C_3 \mid gE > + C_4 \mid gG >$$

Let the Hamiltonian be

$$H = H_0 + \varepsilon H^*$$

where H_o contains the energies of the single-electron states and εH^* corresponds to some interaction which could lead to energy exchange between the two electrons. To find the possible states of the system, let

$$H \phi = W \phi .$$

Then:

$$H \phi = (W_e + W_E)\, C_1 \mid eE > + (W_e + W_G)\, C_2 \mid eG > + (W_g + W_E) x$$
$$C_3 \mid gE > + (W_g + W_E)\, C_4 \mid gG > + \varepsilon\, C_2 \mid Ge > + \varepsilon\, C_3 \mid eG >$$
$$= W (C_1 \mid eE > + C_2 \mid eG > + C_3 \mid gE > + C_4 \mid gG >)$$

Equating coefficients of each state gives these equations:

$$W C_1 = (W_e + W_E)\, C_1$$
$$W C_4 = (W_g + W_G)\, C_4$$
$$W C_2 = (W_e + W_G)\, C_2 + \varepsilon\, C_3$$
$$W C_3 = (W_g + W_E)\, C_3 + \varepsilon\, C_2$$

Clearly the double excited state and the double ground state are eigenstates of energy. The other two eigenstates are:

$$\phi_+ = 2^{-1/2} (\mid eG > + \mid gE >)$$
$$\phi_- = 2^{-1/2} (\mid eG > - \mid gE >) .$$

Their energies are $W_o + \varepsilon$ and $W_o - \varepsilon$ respectively.

Thus the accidental resonance can lead to excited states with an electron partly on the manganese, partly on the ring. That is, the states ϕ_+ and ϕ_- have <u>partial</u> $Mn^{II}P^+$ character. This partial charge transfer in the excited state could have interesting consequences for the chemistry of these compounds, and its implications deserve further study.

From the observed splitting of the Soret band (420 nm in $Mn^{II}Etp$ to 470, 370 nm in $Mn^{III}Etp$) we can estimate ϵ as about 2500 cm^{-1}.

This treatment is oversimplified, of course, since it assumes exact resonance. For the more likely situation in which the energy differences $W_e - W_g$ and $W_E - W_G$ are close but not exactly equal, the result is similar but more complicated. In particular, ϕ_+ and ϕ_- will no longer be exactly half-and-half mixtures.

3. Manganese(II) complexes. We should mention another feature of Fig. III-4, the relative energies predicted for the d levels in the manganese(II) porphins. Gouterman and his co-workers calculate that (at least in the absence of axial ligands) $d_{xy} < d_{xz,yz}$ in energy. They also suggest that the manganese(II) should be in the unusual intermediate spin state 3/2 (3 unpaired electrons). On the other hand, they obtain similar results for the iron(II) complexes under the same assumptions (no axial ligands, metal coplanar with ligand) but find that inclusion of axial ligands and allowing for nonplanarity* can considerably alter the conclusions.

Magnetic susceptibility measurements show that manganese(II) porphins tend to have 5 rather than the predicted 3 unpaired electrons (e.g., Loach and Calvin, 1963). Phthalocyaninomanganese(II) in the solid state may have spin 3/2 (Lever, 1965a; but see Weber and Busch, 1965). However, Weber and Busch find that $Mn^{II}PTS \cdot 2H_2O$ is low-spin with S = 1/2. Our paramagnetic resonance results described in Chapter VI indicate the same spin state for $MnPcPy_2$, and also a reversal of the energy levels: $d_{xz,yz} < d_{xy}$ in this compound.

---

*Iron may be as far as 0.5 Å out of the porphyrin plane; see Hoard et al., 1965.

Thus calculations based on a simplified model for manganese(II) porphin complexes are not borne out by experiments. The postulated planar compound may not even exist, and preliminary calculations (Gouterman, private communication) suggest that the predictions could be considerably altered if the manganese is out-of-plane. The phthalocyanine offers further complications. Its manganese may be in the plane as was shown for the similar compound $(MnPcPy)_2O$ (this structure, determined by Vogt et al., is illustrated in Fig. I-3). However, the axial pyridines will raise the d_{z^2} level, and the substitution of nitrogen for carbon at the bridges will raise d_{xy}--perhaps enough to effect a cross-over of energy levels.

A more sophisticated treatment of the electronic structure of manganese(II) porphyrins, along the lines of that done on the iron complexes by Gouterman's group, would be most useful. Such a study should include the effects of nonplanarity, of axial ligands, and of the bridging nitrogen or carbon atoms.

B. INFRARED SPECTRA OF ETIOPORPHYRIN AND ITS COMPLEXES

The infrared spectra of several metal complexes of etioporphyrin and of the free porphyrin were taken under the supervision of Akio Yamamoto. KBr pellets were examined using the Beckman IR7 spectrophotometer; no attempt was made to shield the samples from air or moisture while pressing the KBr pellets. A Beckman IR7 spectrophotometer was used, with a 1/15" mesh placed in the reference beam.

Absorption bands of etioporphyrin and its zinc(II), nickel(II), cobalt(II) and manganese(III) complexes are listed in Table III-1. The spectrum of H_2Etp is in fair agreement with that reported by Mason (1958).

The MnEtp(OAc) pellet contains far more water than any of the others, as its strong 3440 cm^{-1} band shows. Another peak at 1630 cm^{-1} is also assigned to water. The water is apparently not bound to the manganese, since the bands between about 1000 and 650 cm^{-1}, expected for coordinated water (Nakamoto, 1963; p. 156), are not seen. This sample also contains weakly adsorbed acetic acid, as is indicated by the band at 1714 cm^{-1} (Sidorov and Terenin, 1961). Two bands which appear only in the acetato-manganese complex, at 1594 and 1338 cm^{-1}, are in the proper regions for the antisymmetric and symmetric COO vibrations, respectively, of acetate (Ibid.). Another unique, but weak, band at 1695 cm^{-1}, has not been assigned.

The unusual electronic spectrum of manganese(III) porphyrins (Section III,A) raises the question of whether the macrocycle is normal or, say, a radical. In the latter case, we would expect changes in bond lengths and a peculiar infrared spectrum. Some of the vibrations of the pyrrole rings and of the bridge CH groups do vary with the metal ion (see Table III-1). However, none of these is exceptional for Mn^{III}Etp(OAc), strongly suggesting that the porphyrin ring is normal. M. Gouterman and P. Offenhartz (private communication) reach the same conclusion from their molecular orbital calculations.

Table III-1

Infrared absorption bands of etioporphyrin I complexes (3800-680 cm^{-1})

H_2Etp[c]	H_2Etp	ZnEtp	NiEtp	CoEtp	MnEtp(OAc)	Assignments
	3470wb	3520wvb	3460wb	3500wvb	3440sb	lattice H_2O (OH stretch)[g]
3314m	3330w					NH stretch[c]
	3200vw		3235vw	3230vw		
		3155w		3160w	3180vw	
3100w		3100vw			3120vw	CH deformation[c]
3052w	3075vw	3050w	3070w	3075w	3060vw	CH deformation[c] (?)
3030w						
3009w						
2963s	2975s	2970w	2960s	2970s	2965vs	methyl C-H[c]
2930s	2940m	2930wa	2933sa	2938sa	2925s	
2918s	2920wsh					
2867s	2880w	2870w	2865m	2875s	2865s	methyl C-H[c]
					1714w	weakly bound HOAc[d]
					1695w	
1670w	1675wb	1670wb	1669wb	1670wb	1665vwsh	
			1625vwb		1630mb	lattice H_2O (H-O-H bend)[g]
	1610wb					
					1594wb	assym. COO[f]
			1571wb	1568w	1550wb	-C=C- pyrrole (?)[e]
	1509w		1498w	1493w	1478m	
	1467w	1462s	1463msh	1467msh	1460sh	-C=N-[e]
1459	1455mb	1452s	1450s	1454s	1453s	
	1408w					
	1400wsh	1386s	1393m	1392s	1392m	
	1378m	1373m	1372w	1374m	1377m	=C-N- stretch (?)[e]
	1348vw	1356wsh	1359vw	1362wsh	1358vw	
					1338vw	sym COO[f]
1316w	1318w					
	1305vw	1308w	1310w	1312w	1308vw	

Table III-1 (Cont.)

H_2Etp[c]	H_2Etp	ZnEtp	NiEtp	CoEtp	MnEtp(OAc)	Assignments
1270w	1273w					
1262w	1265w	1265s	1266s	1269s	1265m	
1239w	1243w					
1221m	1223s	1223s	1233vs	1236vs	1223m	in-plane C-H deformation[c]
1192s	1192s					N-H[c]
1143m	1144wb	1150vs	1149s	1151s	1150vs	in-plane C-H def.[c]
			1126w	1132w	1125vw	
1115s	1115s					out-of-phase breathing
	1105msh	1101s	1107m	1107m	1104m	of opposite pyrroles[e]
1060s	1061s	1058s	1057s	1059s	1056s	
	1035vw	1028vw	1030vw	1030vw	1025vw	
987m	981m	982vs	989vs	991vs	987s	
981w						
956m	965s	968msh	974msh	975m	972m	
918w		921s	933s	935s	930s	
902m	900m					
885w	888w					
837s	837vs	835vs	832vs	836vs	835s	out-of-plane bridge C-H[c]
796w	808w	808w	812w	814w	808vw	
760w	768wsh	756s	758m	762m	755w	
744s	745vs	737m	730m	739w	732m	
730w	733msh	731wsh	724m			
722w	721w					N-H deformation[c]
708w	713w	712s	711s	710s	711s	out-of-phase comb. of in-plane pyrrole def.[c]
683s	685vs					

Intensities: a, assymetric; b, broad; sh, shoulder; s, strong; m, medium; w, weak; v, very.
References: c, Mason, 1958; d, Siderov and Terenin, 1961; e, Thomas and Martell, 1959; f, Bellamy; g, Nakamoto, 1963, p. 156.

IV. OXIDATION AND REDUCTION

The photo-oxidation and photoreduction of manganese complexes with phthalocyanine and etioporphyrin I and the influence of solvent on the oxidation state of phthalocyaninomanganese were earlier studied in this laboratory (Engelsma, Yamamoto, Markham, and Calvin, 1962). Similar experiments have now been carried out on various manganese porphyrins, and dark reactions with chemical oxidants and reductants have been studied as well. Attempts have been made to detect any free oxygen liberated in the reduction of (methyl pheophorbide-a)manganese(IV).

A. EXPERIMENTAL

Reaction Vessels. The vivid and distinctive colors of porphyrins make it convenient to follow the course of a reaction spectrophotometrically. Therefore, reactions have been carried out in cuvettes specially designed to allow us to evacuate the sample or expose it to a controlled atmosphere, and to permit addition of reagents when necessary. Those cuvettes illustrated in Fig. IV-1 were the most useful of several designs. The cuvettes were made by Bill Hart of the Biodynamics glass shop. Commercially obtained two- or four-sides-clear 1 cm square Pyrex tubing was used for most cuvettes; quartz cells were adapted from ordinary Beckman 1 cm square quartz cuvettes. Standard ground glass joints were fitted to vacuum-type stopcocks. Side-arms were useful for mixing reagents or when it was necessary to freeze water, which often breaks an improperly designed vessel as it expands. Attempts to isolate the side-arm from the cuvette by placing a stopcock between them proved all too effective; it is well-nigh impossible

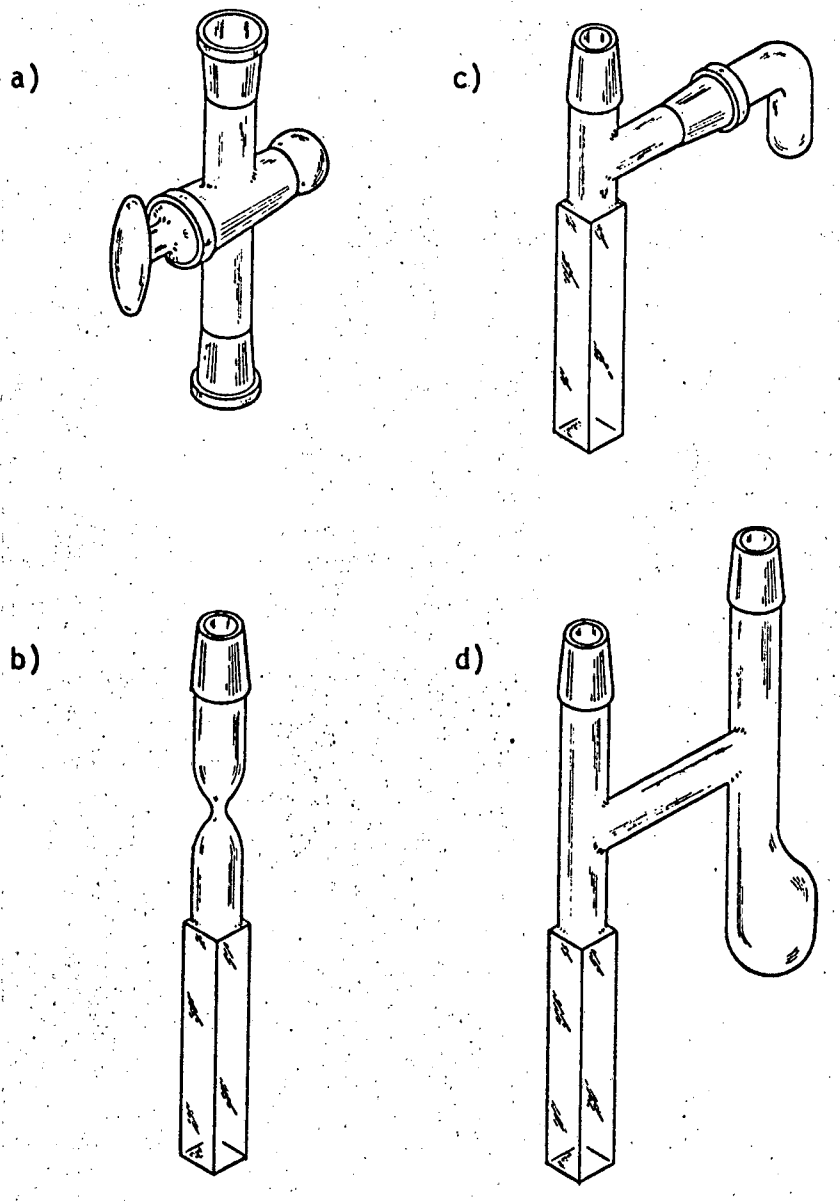

Fig. IV-1. Cells for redox reactions and spectrophotometry. a) Vacuum-type stopcock. b) Simple cuvette, with neck constricted for eventual sealing. c) Vessel with removable side-arm for addition of small portions of (usually solid) reagent. d) Cuvette with side-arm for mixing of sample with solid or liquid reagents, and for freezing of aqueous solutions.

XBL 678-6125

to pour a liquid through a narrow opening in an otherwise sealed container. For long term storage or unusually careful exclusion of air, vessels were glass-sealed on the vacuum line.

Spectrophotometers. Beckman DK-2 and Cary model 14 scanning spectrophotometers were used in the course of this work. To accommodate the vacuum cuvettes, which were up to about eight inches tall and often included a side-arm, tall extensions were added to the sample and reference compartments of the instruments. For the Cary 14, a simple vertical box was satisfactory; the Beckman sample compartment was more crowded, and required a more elaborate extension. At first this covered the entire compartment; however, the mirrors are sensitive to dust, fingerprints, and mis-alignment, so a new cover was built with a tall box which expanded the sample compartment only perpendicularly to the light beam, leaving the optics protected by a flat cover similar to the standard one.

Sample preparation. A solute concentration of around 10^{-5} M was dictated by the requirement that optical density be approximately 1. For the usual solution volume of 2-3 ml, a speck of solid sample barely large enough to see gave the proper concentration.

Some samples, particularly those containing water, were freed of oxygen by bubbling nitrogen through the solution. For pyridine solutions especially, however, it was nearly as important to keep the solvent out of the air as vice versa. And the composition of mixed solvents may be altered by differential evaporation in the nitrogen stream. Such solvents or solutions were de-gassed by freezing, evacuation to about 10^{-5} torr, and thawing. The process was repeated at least three times for each sample. It was often most convenient to

store the air-free solvent on the vacuum line, and vacuum-distil it over into a cuvette containing solid sample.

Thin films were formed on the walls of cuvettes by one of two methods: A few crystals of an easily sublimed compound, such as MnPc, were placed on the floor of a Pyrex cuvette, which was then evacuated. When the cuvette floor was heated gently with a torch, the compound sublimed and condensed on the walls. Compounds which could not be sublimed, such as H_2PTS, were first dissolved, and the solvent was then slowly vacuum-distilled over into a liquid nitrogen trap.

Photoreactions. An oxygen-free sample, in one of the cuvettes described above, was illuminated by one of three sources: a) bright sunlight, filtered through a glass window; b) a photoflood lamp (GE RS-2) about one foot from the sample, filtered through water to remove infrared; colored filters could also be used with this lamp; c) the unfiltered tungsten source of the spectrophotometer. Both photoreductions and back-reactions were usually slow enough (half-time minutes to days) that in most cases the sample could be removed from the spectrophotometer for exposure to light.

Reagents. Oxygen, commercial bleach (NaClO contaminated with Cl_2), reagent grade potassium ferricyanide, and $Ce(HSO_4)_4$ were used as oxidants. Reductants were ascorbic acid and sodium thiosulfate. In addition, autooxidation and autoreduction occurred in some of the compounds studied, and possibly the solvents pyridine (or its N-oxide), ethanol, or water participated in some reactions.

B. RESULTS

Etioporphyrin I manganese. In early experiments with this compound, no chemical reductants were added. When a pyridine solution of

Mn^{III}Etp(OAc) was evacuated to remove oxygen, and then illuminated with strong white light, Mn^{II}Etp was formed. In the dark the complex gradually reverted to its oxidized form even in vacuum; the oxidation was much faster in the presence of air. In all cases, the rate of photoreduction was apparently of first order. The rate varies by more than an order of magnitude (see Table IV-1), but the variation may well be due to differences in the intensity of light in the several experiments. Although Engelsma and co-workers (1962) observed that the photoreduction in pyridine solution of the 620 nm species* of MnPc was much more rapid in the presence of a trace of water, no such dependence has been seen for the etioporphyrin complex.

The dark back-reaction was more difficult to characterize. Even in a single sample, two successive re-oxidations might vary greatly in rate (Table IV-1). While back-reactions in some experiments were apparently first order, one was second order, and another defied analysis. The last was a sample containing 20% water, so the sparingly soluble Mn^{II}Etp may well have aggregated during the experiment.

Isobestic points (Fig. IV-2), which held throughout the reaction in almost every case, indicate that only two species absorbed in the visible region, and that their total concentration remained constant. Thus the porphyrin ring remained intact, and only reaction (1) occurred. Evidence that the metal rather than the ligand is involved is discussed in Chapter III; also, contrast this clean reaction with that of the less stable pheophorbide-*a* analog.

---

*At the time this was identified as Mn^{IV}PcO; recent work indicates that it is more likely a manganese(III) complex. See Vogt *et al.* (1966, 1967); Yamamoto, Phillips and Calvin.

Table IV-1

Rates of photoreduction and autoxidation

for manganese porphyrin complexes

Ligand	Solvent	k_1(reduction), sec^{-1}	k_1(oxidation), sec^{-1}
Etp I	anhydrous pyridine	4.2×10^{-4}	a
		6.8×10^{-4}	7.8×10^{-5}
		6.7×10^{-5}	c
		8.3×10^{-4}	(slow)
	pyridine, .001% H_2O	1.6×10^{-3}	a
	pyridine, 1% H_2O	3.7×10^{-4}	2.5×10^{-4}
	pyridine, 20% H_2O	1.4×10^{-4}	b
Pheo-a	EtOH	$(3.7 \pm .2) \times 10^{-4}$	3.2×10^{-5}
			1.2×10^{-5}
	20% aq. EtOH, pH 9.2	a	7×10^{-6} b

a) Insufficient data.

b) Order uncertain

c) Apparently second order, with $k_2 = 0.13$.

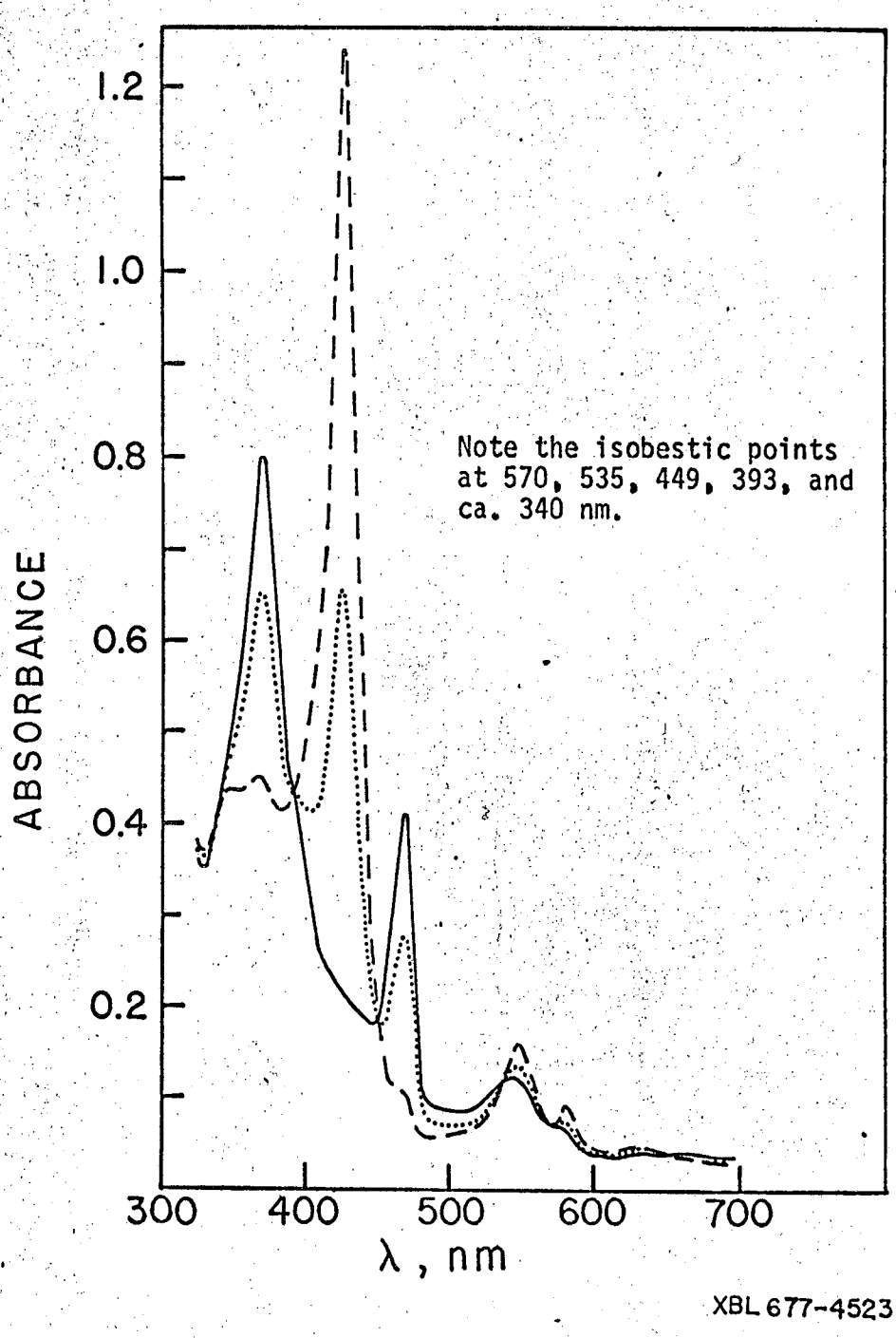

Fig. IV-2. Photoreduction and autoxidation of etioporphyrin I manganese.

———— $Mn^{III}Etp(OAc)$ in pyridine with 1% water, evacuated to 10^{-5} torr.

- - - - - - After 83 min. illumination with a photoflood lamp; almost complete reduction to $Mn^{II}Etp$.

..... After 21 hr. in the dark, in vacuum.

$$Mn^{III}Etp(OAc) \xrightarrow{\text{pyridine, } h\nu} Mn^{II}Etp \qquad (1)$$

When etioporphyrin I acetatomanganese(III) is sublimed in vacuum, most of the compound is reduced to etioporphyrin I manganese(II). The acetic acid group may remain coordinated (see Section III). Air immediately oxidizes such a sublimed film to $Mn^{III}Etp$ (Fig. IV-3). Water vapor does not alter the spectrum of this film; pyridine, on the other hand, shifts the 360 nm absorption band to about 345 nm, and a new shoulder appears at about 400 nm. The presence of both pyridine and water enhances the 400 nm shoulder.

The $Mn^{III}Etp$ film was illuminated under the various conditions above. When no gas was present, very slow and barely detectable photoreduction occurred. No photoreaction could be seen in the presence of water alone; with pyridine and water vapors together, the reaction was again very slow. More extensive photoreduction took place when pyridine alone was present, although even then the effect was too small for quantitative studies. Whenever the compound was reduced, there was eventually an autoxidation, which may have been due to an air leak. Though the data from this and similar experiments are rather poor, it is interesting that the reactions which are well characterized in solution can also occur in the solid state.

Preliminary attempts to chemically reduce or oxidize $Mn^{III}Etp$ were unsuccessful, even under conditions similar to those in which the compound is photoreduced, or in which other manganese porphyrins react with the reagents used. There was no reaction with solid $Na_2S_2O_4$, in pyridine or dioxane solution and under inert atmosphere (nitrogen); nor was any spectral change apparent when either sodium thiosulfate

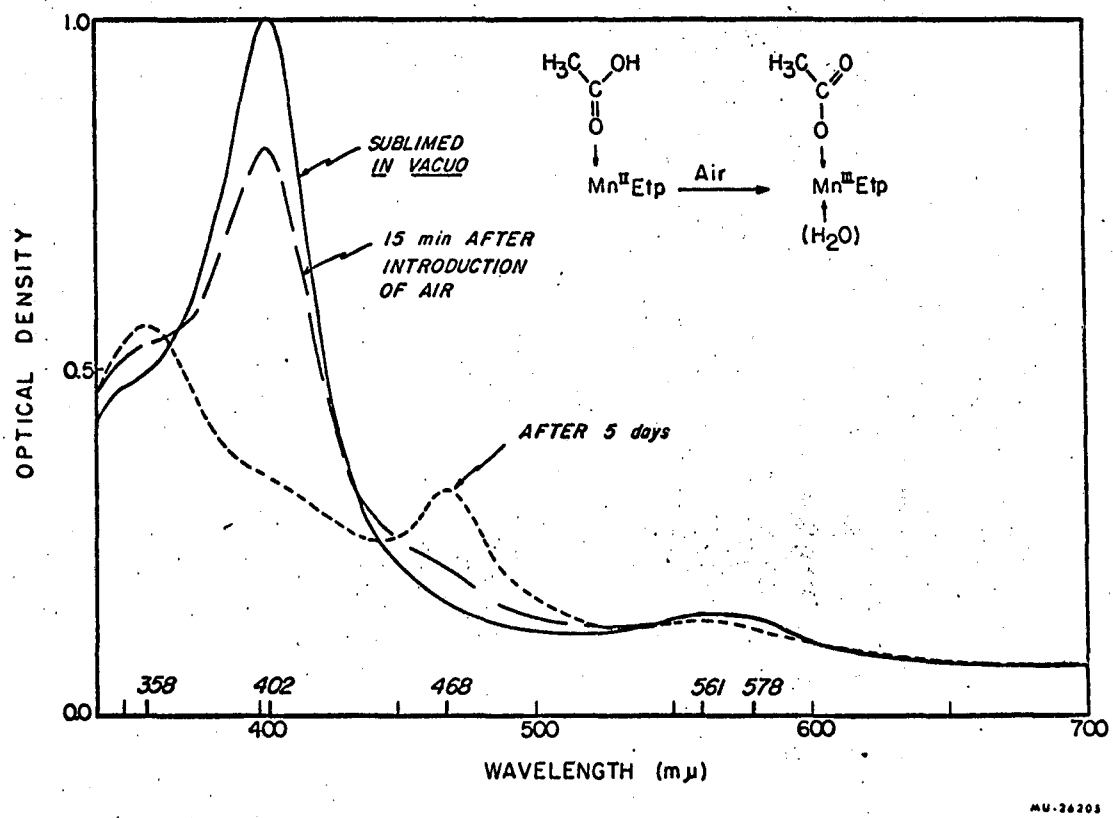

Fig. IV-3. Oxidation of a thin film of etioporphyrin I (acetic acid)manganese(II) by air.

_____ $Mn^{II}Etp(HOAc)$.

_ _ _ _ Mixture.

- - - - - - $Mn^{III}Etp(OAc)$.

or ascorbic acid was added to a solution in absolute ethanol, also under nitrogen atmosphere. Undiluted bleach did not bring about the hoped-for oxidation to Mn^{IV}Etp in either pyridine or ethanol solution. There was no sign of ring destruction.

(Methyl pheophorbide-a)manganese. As with other manganese porphyrins, the stable oxidation state in air for this chelate is Mn^{III}Pheo. When oxygen is absent, dithionite effects reduction to the manganese(II) complex in several solvents; ascorbic acid usually causes only incomplete reduction. In 20% aqueous ethanol, reduction by dithionite will proceed to some extent even in air. Three distinct reactions are observed:

$$Mn^{III}Pheo \underset{O_2}{\overset{e^-}{\rightleftharpoons}} Mn^{II}Pheo \qquad (2)$$

Ring destruction (3)

$$Mn^{III}Pheo^{+} + 2\ S_2O_4^{=} \dashrightarrow Mn^{III}Pheo(S_2O_4)_2^{3-} \qquad (4)$$

Extensive ring destruction did not always take place, and with luck and care to avoid excess reductant, a sample could be reduced and re-oxidized several times. However, the manganese-containing pheophorbide-a ring system is far less stable than is etioporphyrin, at least under the conditions studied. On the other hand, metal-free methyl pheophorbide-a in 95% ethanol did not react with either ascorbic acid or dithionite.

I attempted to measure the rate of reduction of Mn^{II}- to Mn^{III}Pheo. Under the conditions used by Loach (1964b) for this reaction (20%

aqueous ethanol, 10^{-5} M complex, titrated with 10^{-2} M sodium dithionite in the dark) , reaction is complete within 15 seconds. This upper limit was set by the time required for mixing the sample and reductant. Spectral characteristics of the manganese(II) and manganese(III) species (Fig. IV-4) are similar to those observed by Loach.

Upon addition of sodium dithionite, $Na_2S_2O_4$, and in nitrogen atmosphere, a solution of Mn^{III}Pheo in ethanol exhibited spectral changes corresponding to formation of Mn^{II}Pheo (Fig. IV-5). When air was again admitted to the solution, the resulting spectrum was slightly different from that of the original sample (Fig. IV-5, curve 3). A similar difference in spectrum can be obtained if $Na_2S_2O_4$ is added to such a sample in the presence of air; dithionite alone in ethanol is transparent in the visible region, and the metal-free methyl pheophorbide-a shows no spectral change under the same conditions. The data are consistent with reaction (4), with association constant $K = 4 \times 10^7\ l^2 mol^{-2}$ (see Table IV-2).

Mn^{III}Pheo is photoreduced to Mn^{II}Pheo very slowly by strong white light (sun or spotlight), in absolute or 95% ethanol, or in 20% aqueous ethanol buffered at pH 9.2. A pseudo-first order rate constant has been observed (Table IV-1). In 95% or unbuffered 20% ethanol, almost no reduction occurred on illumination by a 100-watt high pressure mercury lamp, which produced most of its intensity at 365 nm. Only a small fraction of the compound was reduced when a low-pressure mercury lamp was used, either unfiltered or filtered to select the 436 nm line. Perhaps the red transitions are responsible for the photoreaction, since they involve lowering porphyrin electron density in the vicinity of the metal ion (see Chapter III).

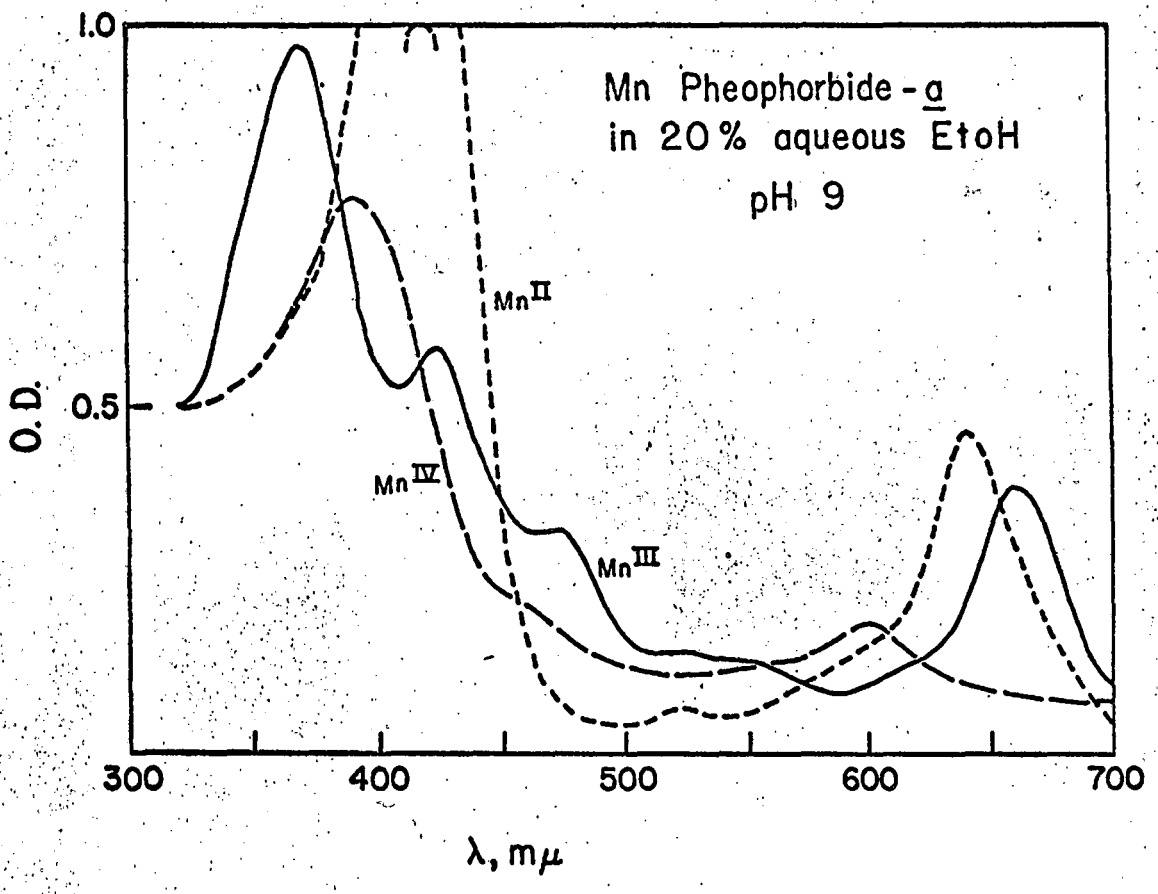

Fig. IV-4. Electronic spectra of the three oxidation states of (methyl pheophorbide-a)manganese in 20% aqueous ethanol, with 0.05 M borate buffer, pH 9.2. Concentrations of MnPheo species are nearly but not precisely equal, and are about 10^{-5} M.

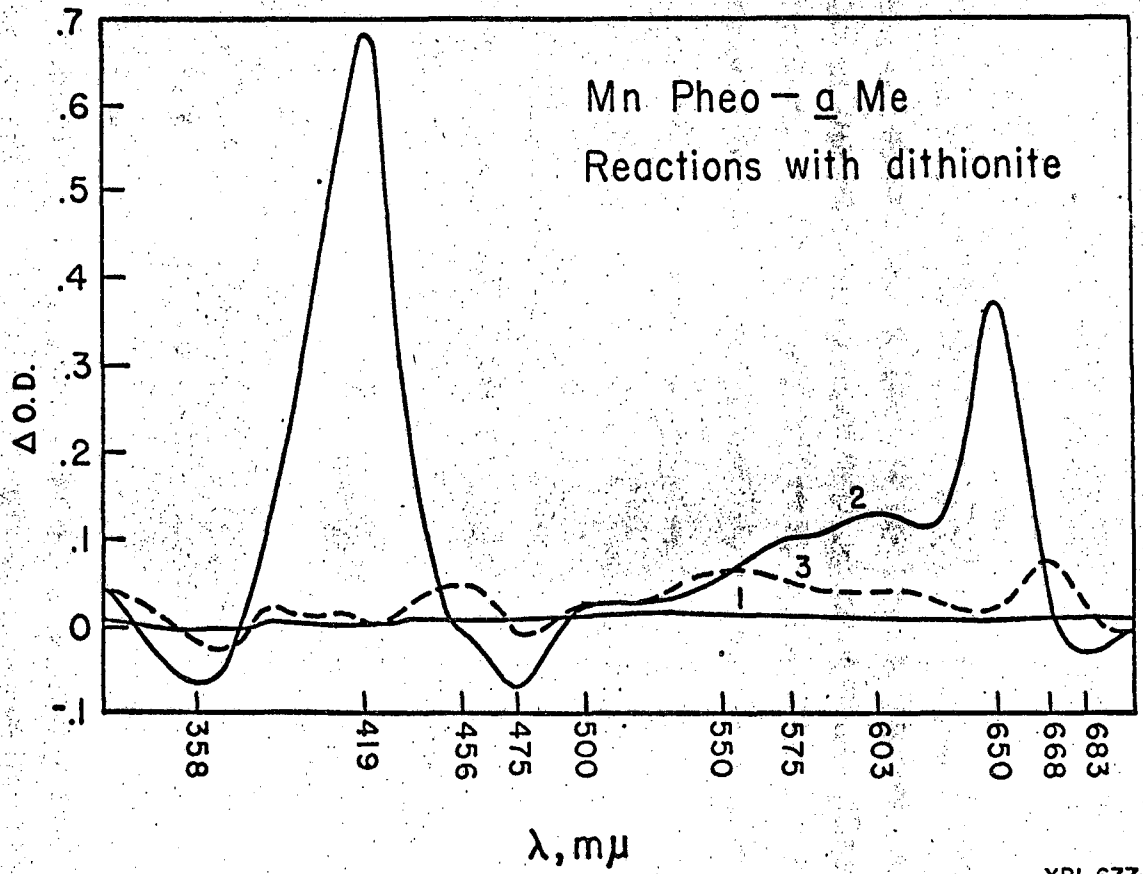

XBL 677-4524

Fig. IV-5. Reactions of (methyl pheophorbide-a)manganese with sodium dithionite. Reference cell contained an ethanol solution of Mn^{III}Pheo, in air. 1) Sample identical with reference; 2) After addition of solid $Na_2S_2O_4$ to sample, and under nitrogen atmosphere. The difference spectrum is that of Mn^{II}Pheo vs. Mn^{III}-Pheo. 3) After re-oxidation of sample by air.

Table IV-2

Complexation of dithionite with (methyl pheophorbide-a)manganese(III). Results were calculated at a peak (668 nm) and a minimum (365 nm) in the difference spectrum of adduct vs. Mn^{III}Pheo, in ethanol.*

$[S_2O_4^{=}]$, $\underline{M}x10^4$	Adduct / Mn^{III}Pheo 668 nm	365 nm	Average	10^{-3} K_1	10^{-7} K_2
0.21	0.33	0.27			
0.77	0.21	0.33	0.27	3.48	4.55
1.22	0.41	0.45	0.43	3.51	2.88
1.62	0.63	1.44	1.04	6.38	3.93
1.99	0.93	1.65	1.29	6.48	3.26
2.32	1.36	2.59	1.98	18.44	3.65
2.32*	3.34	3.36	3.35	14.50	6.22
Average					4.08

*After standing.

* $K_1 = \dfrac{[(MnPheo \cdot S_2O_4)^-]}{[MnPheo^+][S_2O_4^{=}]}$ $l\,mol^{-1}$

$K_2 = \dfrac{[(MnPheo \cdot 2S_2O_4)^{3-}]}{[MnPheo^+][S_2O_4^{=}]^2}$ $l^2 mol^{-2}$

Photoreduction was generally followed by a back-reaction in the dark. The rate of this back-reaction could be measured in two cases (Table IV-1), and was of apparent first order.

An account of the chemical and photoreductions of chlorophyllin-a and chlorin-a has been given by Oster et al. (1964). Red light sensitizes the reduction of chlorophyllin by ascorbic acid in 6% aqueous pyridine, at pH 7 (phosphate buffer). Blue light gave a quantum yield (7×10^{-4}) lower by a factor of five than that for red light. These authors claimed that their photoproduct did not depend on the presence of magnesium, although the product itself was neither isolated nor identified.

Similar experiments with Mn^{III}Pheo also resulted in reduction of the ring rather than the metal. Under the conditions above and an inert atmosphere, reduction to the unidentified product was accelerated somewhat by white light. The visible absorption peaks associated with MnPheo compounds, at 370 and 420 nm, decreased; on exposure to air, new peaks grew in at 350 and 400 nm (Fig. IV-6). Further investigation of this type of reaction might be of value in a study of the chlorin ring system.

Reduction of Mn^{III}Pheo by ascorbic acid in 20% ethanol, which produced Mn^{II} Pheo, was not affected by white light.

Loach and Calvin (1963) have shown that the stability of hematoporphyrinmanganese(IV) depends strongly upon pH. The potential at half-reduction to Mn^{III}Hm, E_m, is only 0.28 v. at pH 13.6, while at pH 9.9 it has risen to 0.635 v., high enough to oxidize water. Calvin (1965) has further predicted that the Mn^{IV}/Mn^{III}Pheo couple should have a reduction potential 100-200 mv higher than that for Mn^{IV}Hm.

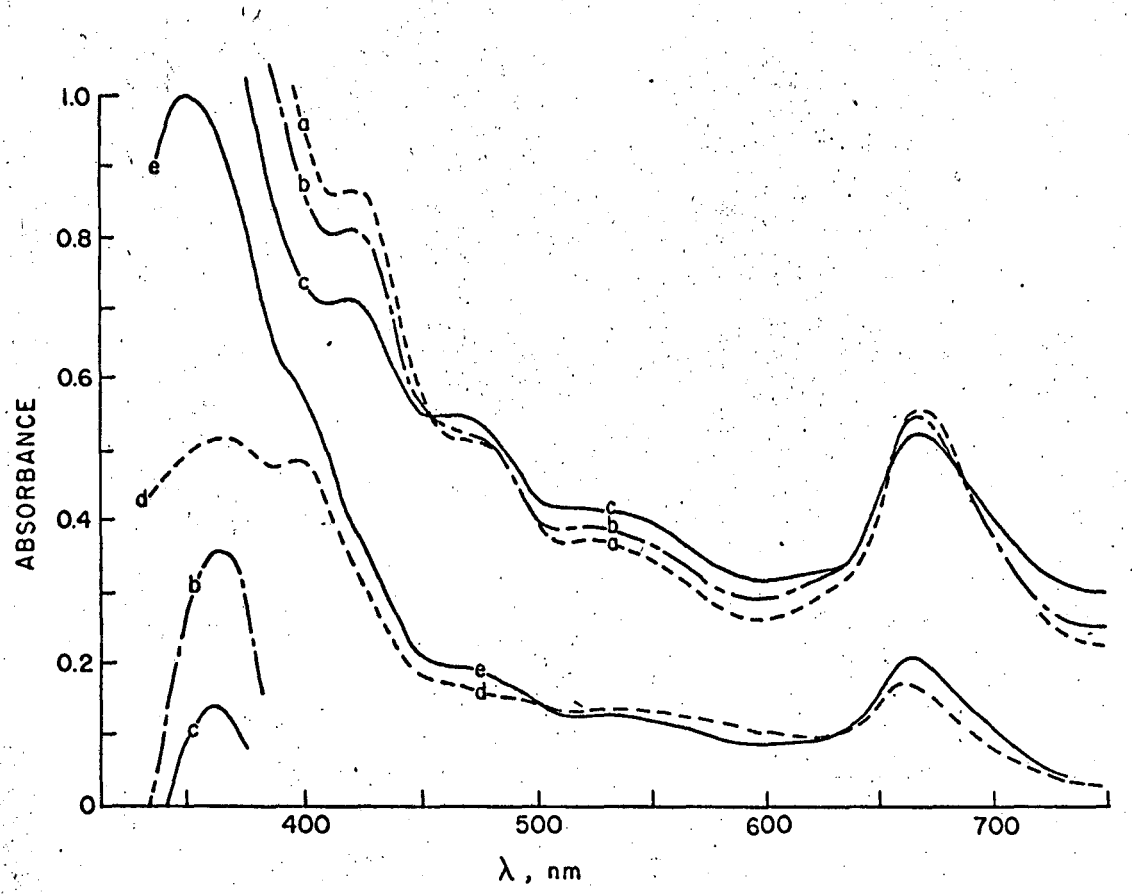

Fig. IV-6. Reaction of (methyl pheophorbide-a)manganese(III) with ascorbic acid in 6% pyridine. The ascorbic acid was 10^{-3} M; the pH was adjusted to 7 with phosphate buffer. a) Immediately after preparation; evacuated to 10^{-4} torr. b) and c) After illumination by white light. d) After standing overnight in the dark. e) After exposure to air.

Loach (1964b) was unable to obtain Mn^{IV}Pheo because the manganese(III) complex suffered major, irreversible changes in alkaline solution. In the present experiments no such changes were observed, although the spectrum of Mn^{III}Pheo is affected by pH (Fig. IV-7). Loss of a proton from a coordinated water molecule, forming Mn^{III}Pheo-(OH) at high pH, may cause the spectral change.

(Methyl pheophorbide-a)manganese(III) can be oxidized by commercial bleach (NaClO) or by ferricyanide in alkaline solutions. Spectral changes (Fig. IV-4) are reminiscent of those which occur in the hematoporphyrin complexes (Fig. IV-8), indicating that the metal and not the ring is oxidized. Mn^{IV}Pheo is unstable in 20% EtOH (pH 9.2) in the presence of bleach. A large excess of bleach destroys the ring, while when no excess oxidant is present the manganese reverts to the +3 state. Since the final Mn^{III} product is indistinguishable spectroscopically from Mn^{III}Pheo, it is possible that one of the two carboxylic acid substituents on pheophorbide-a has been converted to a per-acid, as is the case with hematoporphyrinmanganese (Loach and Calvin, 1964a). Since both carboxylates are isolated from the pi system, their reactions would not be expected to affect the spectrum.

If carried out with care, the oxidation of Mn^{III}Pheo by bleach was spectroscopically reversible either in aqueous KOH, pH 11.5 (Fig. IV-9), or in 20% aqueous pyridine, adjusted to pH 11.7 with KOH (Fig. IV-10; note the effect of pyridine on the spectra).

In contrast to its manganese salt, metal-free methyl pheophorbide-a was destroyed by bleach in 95% ethanol, with no qualitative spectral change.

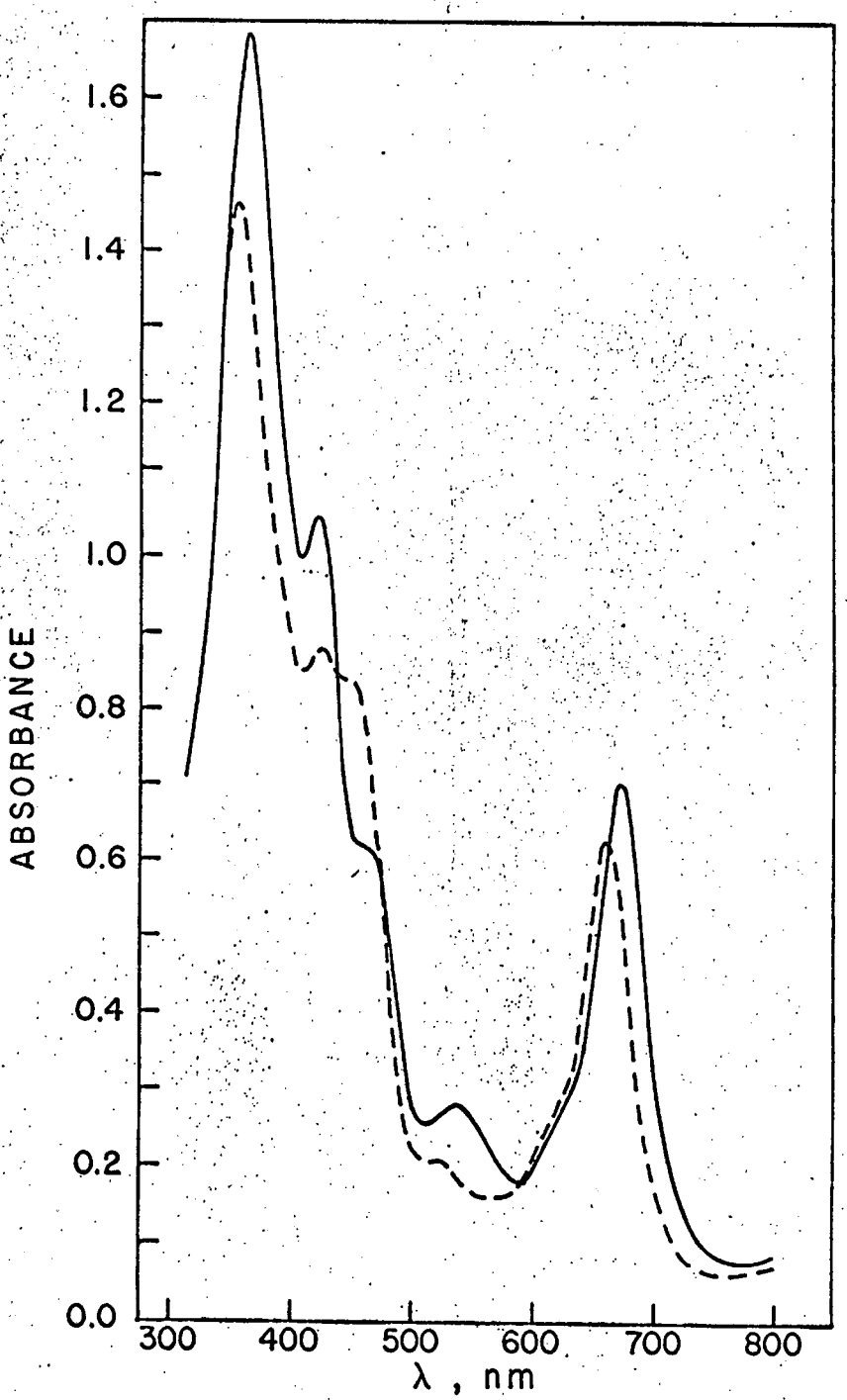

Fig. IV-7. Effect of pH on (methyl pheophorbide-a)manganese(III). The solvent was 20% aqueous ethanol; pH was adjusted by addition of HCl or KOH. _____ pH 5.1; ---------- pH 12.7.

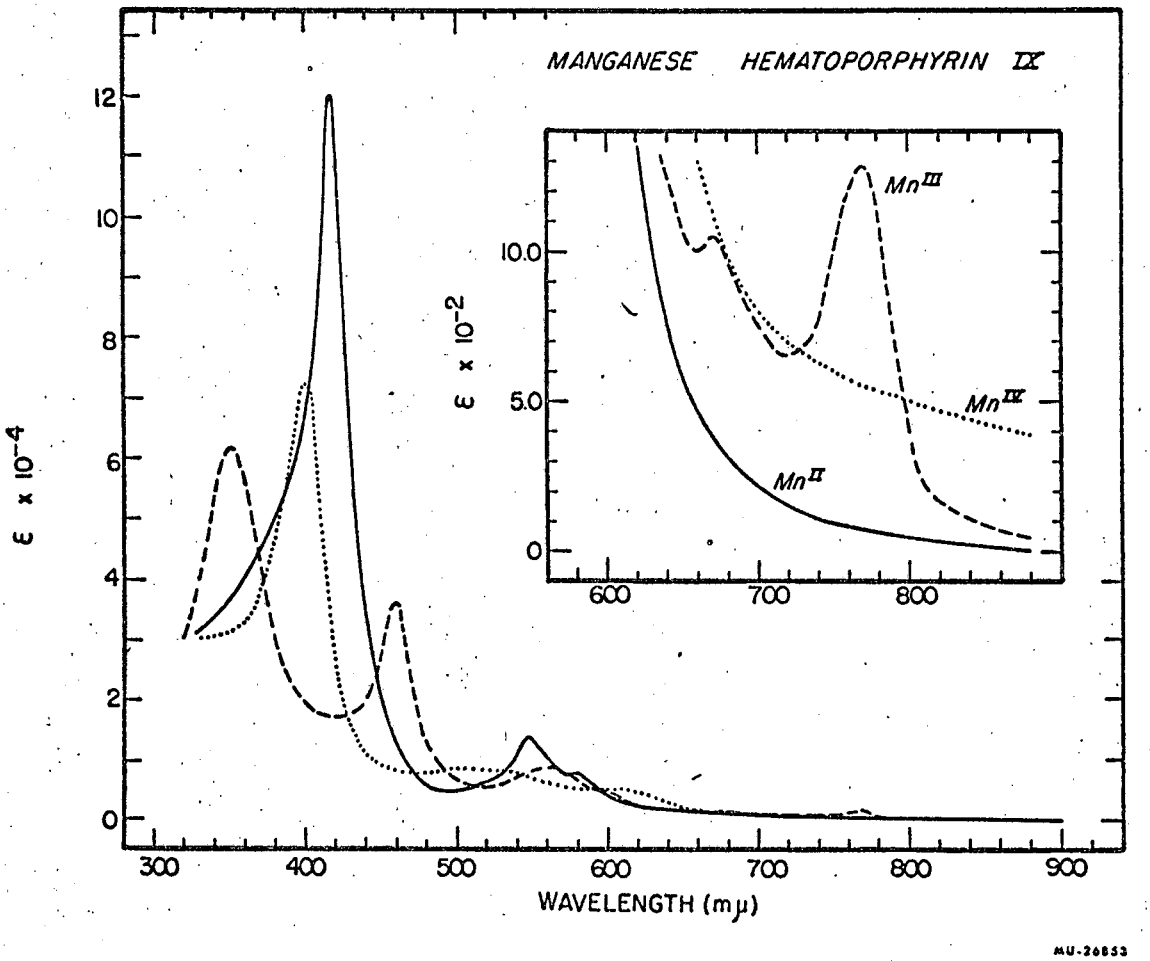

Fig. IV-8. Electronic spectra of the three oxidation states of hematoporphyrinmanganese in alkaline solution, pH 13. (Loach and Calvin, 1963).

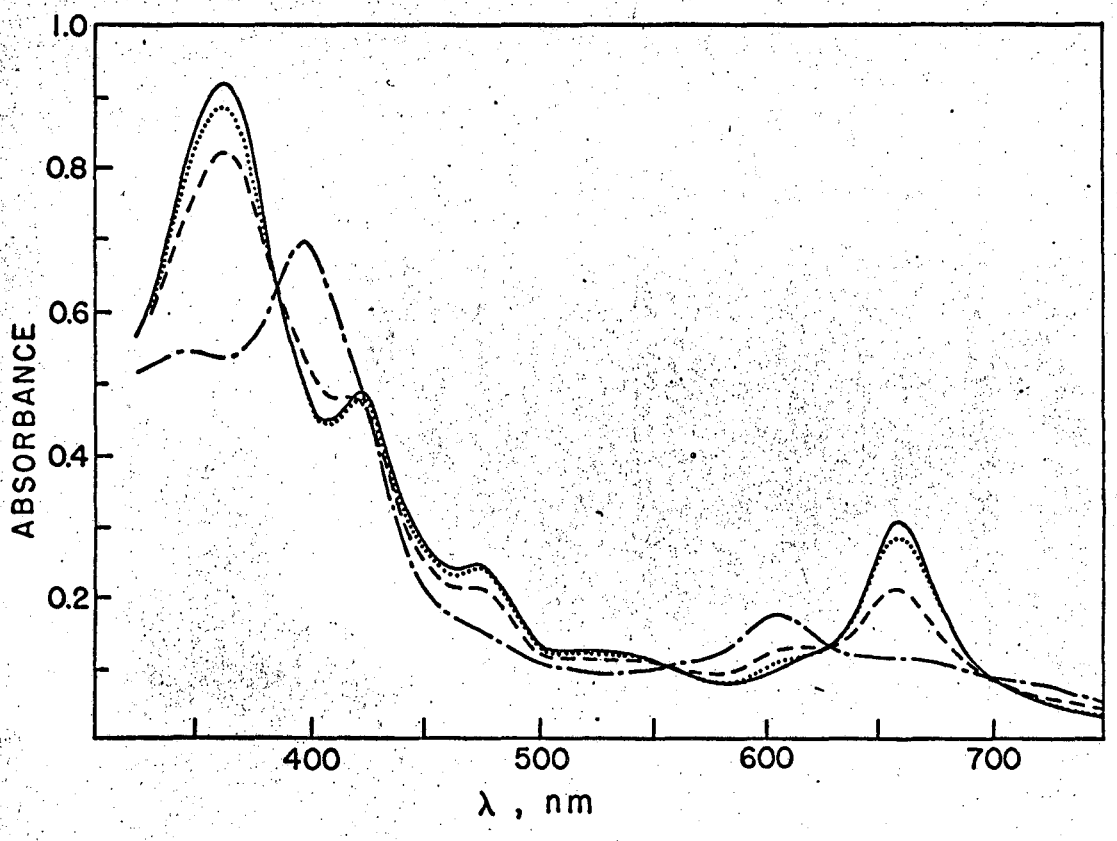

XBL 677-4518

Fig. IV-9. Oxidation of (methyl pheophorbide-a)manganese(III) to the manganese(IV) species by bleach. Aqueous KOH, pH 11.5. Note the isobestic points, which show that only two compounds absorb visible light. _____ Mn^{III}Pheo; _ _ _ _ Mn^{IV}Pheo.

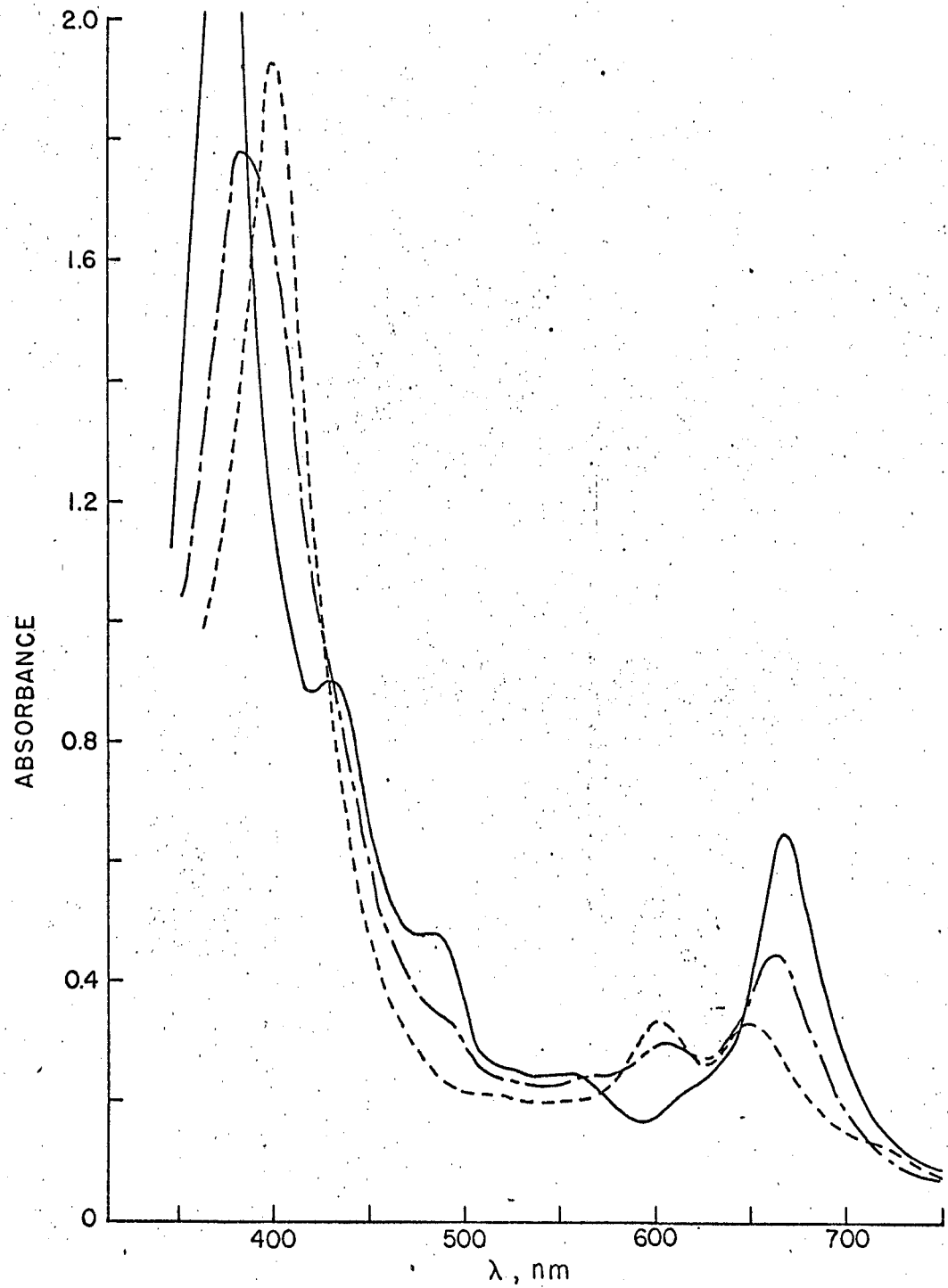

Fig. IV-10. Oxidation of (methyl pheophorbide-a)manganese(III) by bleach in 20% aqueous pyridine. The pH was adjusted to 11.7 by KOH. ——— Initial spectrum; — — — After addition of a small amount of bleach; ---------- After more bleach was added.

Potassium ferricyanide was added to a solution of Mn^{III}Pheo in dilute aqueous ethanol; there was a little pigment destruction but no other reaction. However, when KOH was added to this solution, Mn^{IV}-Pheo was formed. This reaction was studied in aqueous solution, with varying concentrations of KOH. At pH 8.2, almost no oxidation occurred; above pH 12, the manganese(IV) complex was relatively stable. It could be further stabilized by maintaining a constant oxidation potential with a mixture of ferro- and ferricyanide. This method was used to estimate the potential of the Mn^{III}/Mn^{IV}Pheo couple. Potential measurements were taken on a Beckman pH meter, using a platinum foil electrode with a saturated calomel reference electrode. The pH meter was calibrated with solutions of quinhydrone in Beckman standard buffers of pH 4 and 7, and in 0.1 N HCl. Relative concentrations of the manganese(III) and manganese(IV) species were estimated from their peaks at 656 and 602 nm, respectively. Results are shown in Table IV-3.

Note that under these rather alkaline conditions the potentials for the Mn^{IV}/Mn^{III}Pheo couple are not much higher than those for the Mn^{IV}/Mn^{III}Hm couple. This does not necessarily contradict Calvin's prediction for the behavior of the former in neutral medium; a more thorough study of the pH dependence of this reaction would be most interesting.

In 0.1 N KOH, one-half equivalent of $K_3Fe(CN)_6$ was added to a 2×10^{-5} M solution of Mn^{III}Pheo. The oxidation was stoichiometric and fast. Autoreduction of the Mn^{IV}Pheo formed, was followed spectrophotometrically (Fig. IV-11) and was apparent second order, $k_2 = 4 \times 10^2$ sec^{-1}. On addition of another half equivalent of ferricyanide, the expected oxidation occurred, but more slowly than before (half-time

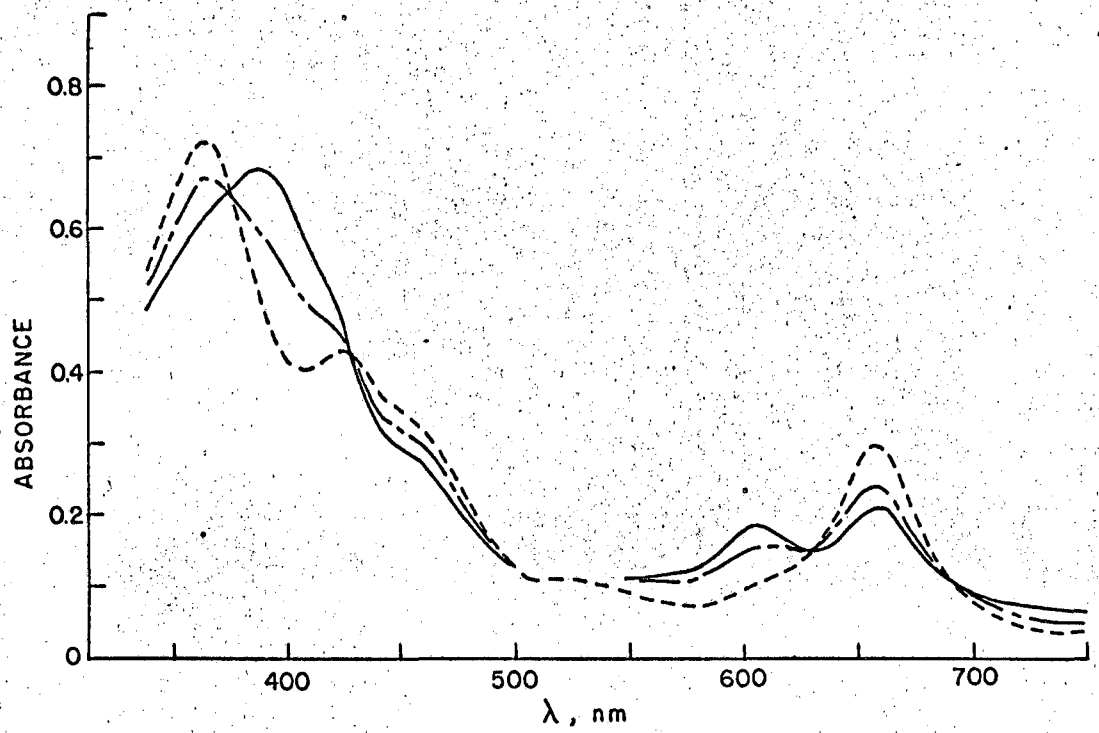

XBL 678-4591

Fig. IV-11. Autoreduction of (methyl pheophorbide-a)manganese(IV) at pH 13. --------- Mn^{III}Pheo, initial solution; _____ After addition of ferricyanide: a 50-50 mixture of the Mn^{III} and Mn^{IV} species. _ _ _ _ _ A few minutes later. After about 1 hour, most of the complex had reverted to Mn^{III}Pheo.

Table IV-3

Reduction potentials of (methyl pheophorbide-a)manganese(IV) in aqueous alkali.

pH	12.1	13.0
E_m,v	0.36 0.42 0.45	0.37 0.35
Ave.	0.41 ± .05	0.36 ± .05
MnHm* E_m,v	0.39	0.33

*Interpolated from Table VI in Loach and Calvin, 1963.

about 2 min); the rate of the subsequent autoreduction also decreased: $k_2 = 57.5\ sec^{-1}$. The reduction seemed to be catalyzed by white light. No satisfactory reaction scheme has been devised to explain these data.

Attempts to detect O_2 formation. Loach's potential measurements (Loach and Calvin, 1963) show that the Mn^{III}/Mn^{II} couple of the porphyrin chelates cannot oxidize water. Therefore, if we are to find any model among them for the direct role of manganese in photosynthetic oxygen production, we must invoke a different couple, such as Mn^{IV}/Mn^{III} or Mn^{IV}/Mn^{II}. This idea, of course, is not new; it was discussed during earlier work on phthalocyaninomanganese (see for example Engelsma et al., 1962). In that study, unsuccessful attempts were made to detect molecular oxygen from the reaction

$$2\ Mn^{IV}PcO \xrightarrow[\text{heat}]{\text{pyridine}} 2\ Mn^{II}Pc + O_2\ . \qquad (5)$$

Mass spectrometric measurements did not show any evolution of free oxygen. These authors also failed to demonstrate that exchange of ^{18}O between oxygen gas and ^{18}O-enriched water could be catalyzed by a mixture of Mn^{III}- and $Mn^{IV}Pc$.* The chief solvent in both these experiments was pyridine, and the suggestion was made that the pyridine might be oxidized to pyridine N-oxide. Since pyridine N-oxide is obtained by the reaction of pyridine with peroxides or peracids, its presence would indicate that in this system, as for the hemato-

*The compound previously identified as $Mn^{IV}PcO$ is, in the solid state, $(MnPc)_2O$ (Vogt et al., 1966); in solution it is probably, but not certainly, also a manganese(III) species.

porphyrin (Loach and Calvin, 1964a), the reduction of manganese(IV) in a porphyrin-type chelate is linked with the formation of a peroxide. Unfortunately, so far no evidence has been found for the presence of the N-oxide.

Since the desired reaction is the splitting of water, water-soluble compounds seem desirable for such experiments. Loach and Calvin, however, showed that when the water-soluble $Mn^{IV}Hm$ is reduced, the porphyrin's carboxylic acid substituents are converted to peracids; no free oxygen can be detected.

In the present study, the dependence of $Mn^{IV}Pheo$ stability on pH was utilized in an attempt to produce molecular oxygen. Into a double-necked vessel* were placed 0.9 micromole $K_3Fe(CN)_6$, 1.9 mg $Mn^{III}PheoCl$ (2.8 micromole), and 1.1 ml water enriched in ^{18}O (30.2% $H_2{}^{18}O$). A concentrated solution of KOH was made up in ordinary water. One drop of this solution from a No. 26 hypodermic needle, diluted to 1.1 ml, gave pH 13.0; a drop of the same size was added to the sample. The sample was immediately frozen and evacuated. A measured amount of concentrated hydrochloric acid was also evacuated, then distilled under vacuum into the sample to neutralize the base and cause reduction of the $Mn^{IV}Pheo$. The vessel was glass sealed. Had the reaction been

$$4\ Mn^{IV}Pheo(OH)_2 + 4H^+ \dashrightarrow 4\ Mn^{III}Pheo + O_2 + 6\ H_2O \qquad (6)$$

the oxygen pressure in the vessel would have been 0.6 torr, and the $^{32}O_2/^{34}O_2$ ratio would have been 4:1; background is approximately 200:1. A mass spectrogram revealed no significant deviation from the background

*One neck had a breakaway seal for mass spectroscopy; the other was eventually glass-sealed.

ratio. Thus, as expected from the arguments above but contrary to hopes, we must conclude that (methyl pheophorbide-a)manganese will not produce free oxygen.

On the other hand, in many cases reactions which occur with impunity *in vivo* cannot be duplicated *in vitro*. We should not lose sight of the fact that the models studied here are at best great oversimplifications of their biological counterparts.

V. COORDINATION OF AXIAL LIGANDS

Porphyrins act as tetradentate ligands which force chelated metals into a square-planar configuration.* Many of the metal ions which form stable porphyrin complexes tend to be six- rather than four-coordinated, and will readily pick up two more (monodentate) ligands to become nearly octahedral. The stability of the adducts varies widely, depending on both the metal ion and the added base; usually the formation of further complexes is reversible. In some cases five-coordinate, pyramidal complexes occur, particularly when the metal is in the 3+ or higher oxidation state and therefore requires a counter-ion.

Axial ligands can have important effects on the behavior of the entire complex: The metal ion may undergo a chemical reaction with an axial ligand; we have described in Chapter IV the reduction of manganese in Mn^{III}Pheo by coordinated dithionite. A ligand may affect the reactions of the metal with a second axial ligand or another compound, or it may stabilize a particular oxidation state of the metal; for instance, pyridine promotes the aerial oxidation of Mn^{II}Pc. There may even be interactions between axial ligands and the coordinated porphyrin, apparently through the metal's d orbitals which interact with both; thus, pyridine affects the visible spectra of manganese porphyrins.

Chemical analyses of several of the compounds discussed here indicate that axial ligands are present. And a structural analysis of an

---

*Sometimes there is a slight pyramidal distortion: the metal may be as far as 0.5 Å along the z axis from the plane of the surrounding nitrogens (Hoard et al., 1965).

oxidized form of phthalocyaninomanganese shows that it contains one coordinated pyridine and one pyridine of crystallization per manganese. So another aspect of the study of axial ligands is confirmation of these results.

The addition of pyridine to tetraphenylporphins and tetraphenylchlorins in benzene solution has been studied by Miller and Dorough (1952). They found that the chelates of divalent Zn, Cd, Hg, and Cu formed monopyridinates; that of Mg^{2+}, a dipyridinate.

The electronic spectra of solid phthalocyaninomanganese(II) or etioporphyrin I manganese(II) change in the presence of pyridine vapor (Yamamoto, Phillips and Calvin). The coordination of pyridine to Mn^{II}Etp causes an overall intensity increase and slight shifts in the bands, most markedly a shift of the Soret band from 402 nm to 442 nm (Fig. V-1). Pyridine also shifts the Soret band of Mn^{III}Etp(OAc) from 360nm to 345 nm, and a new shoulder appears at about 400 nm. In contrast, the spectrum of sublimed metal-free etioporphyrin is altered very little by pyridine vapor, supporting the contention that the base is bound to the metal rather than to the porphyrin ring.

The simplest means for measuring the stoichiometry of reactions giving a solid product is gravimetry. In the case of gas-solid reactions, this method is especially appropriate. We have measured the weight changes of solid manganese porphyrins when exposed to potential ligands in the vapor phase. The changes in weight are directly related to the stoichiometry, while the conditions under which they occur and their rates yield further information about the complexes. Experiments were performed using the quartz spring balance described below; the results will be discussed in Section V-B.

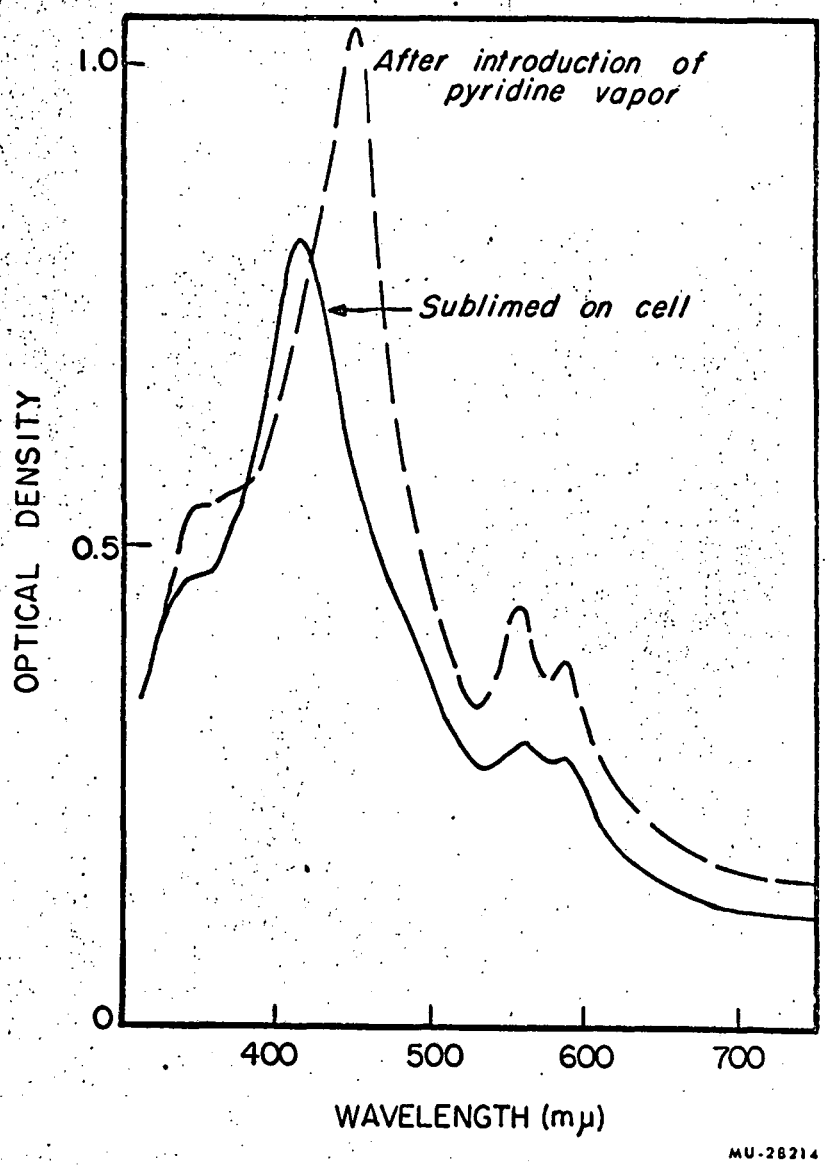

Fig. V-1. Effect of pyridine vapor on a sublimed film of etioporphyrin I (acetic acid)manganese(II).

A. QUARTZ HELIX MICROBALANCE: APPARATUS AND METHOD

Samples can be exposed to vacuum or to various gases while on the balance shown in Fig. V-2; temperature as well as pressure can be controlled. The samples are between 1 and 10 mg in weight; balance extension can be read to about 0.002 cm, or 2 μg. Various systematic errors which we will mention later lower the precision to about 10 μg.

The balance, obtained from Microchemical Specialties Company in Berkeley, California, consists of an extremely fine quartz fiber wound into the shape of a helix (k, Fig. V-2), whose extension is measured by observing the position of the crossbar (l). The helix terminates in a straight fiber (m) called the hangdown, with a hook on the end on which a panholder loop (p) is hung. A shallow pan made of aluminum foil rests on the loop of (p), and holds the powdered sample. The reference rod (j) extends through the center of the helix; its lower tip serves as the reference point (this was present only on the balance used for the most recent experiments).

The balance is enclosed in a cylindrical glass case connected to a vacuum system through an outlet in its main portion (d). A ground glass joint (f,h) allows the lower portion of the case (i) to be removed for loading and unloading the balance. With the balance completely unloaded, only the loop (n) is below the joint. The hangdown is long enough so that even with the heaviest load permitted (about 12 mg) the delicate helix is completely enclosed by (d). To avoid getting stopcock grease on the fiber and sample, a short length of glass tubing (g) extends through the joint (f,h). The cap (a), from which the balance hangs, can also be removed when necessary, providing

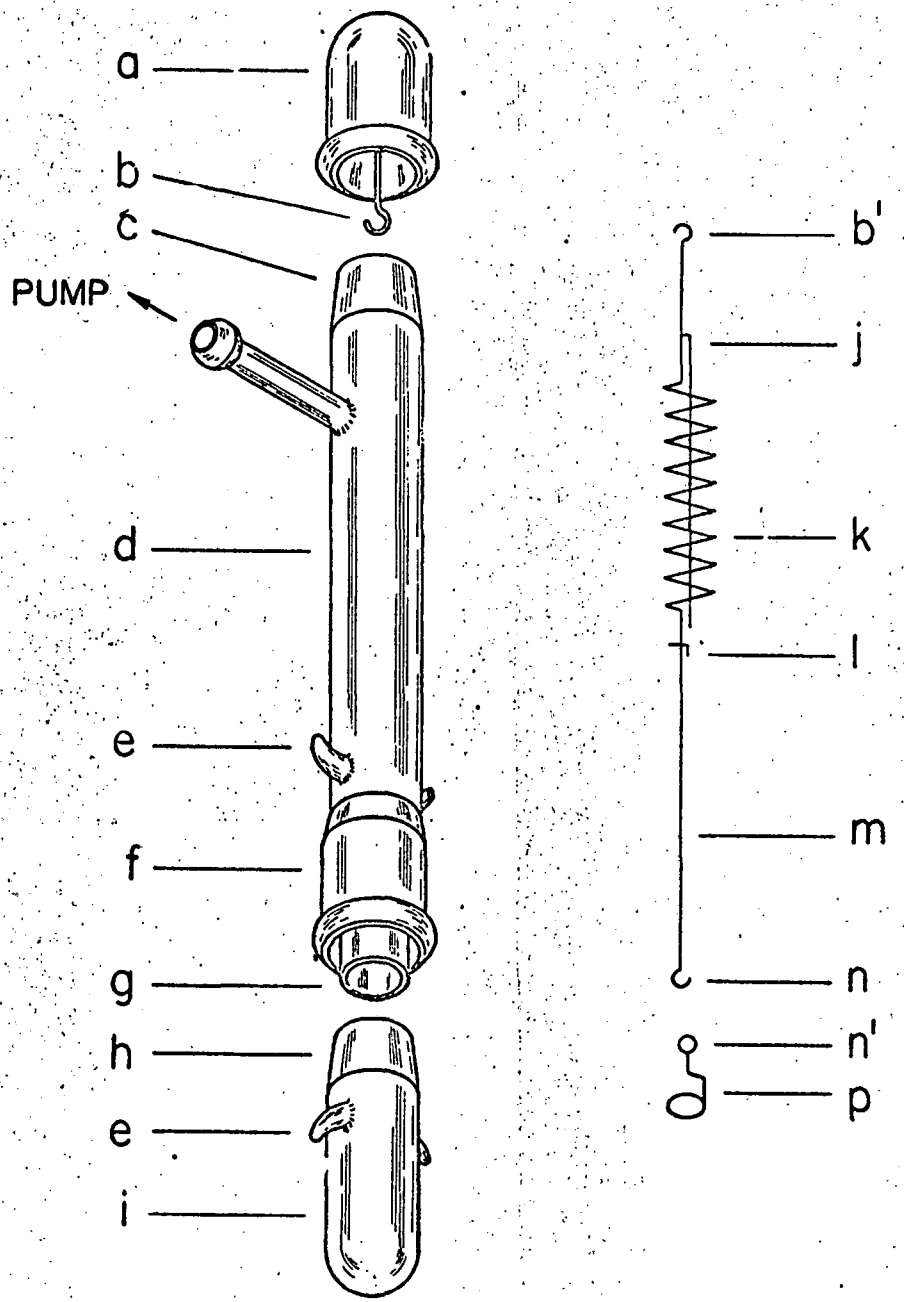

XBL678-4557

Fig. V-2. Quartz helix balance and case. The case: Into the cap (a) is fused a hook (b) from which the balance hangs by its hook (b'). The main portion of the case (d) is joined to (a) and the lower section (i) by ground glass joints. Springs between the ears (e,e) support (i). The balance includes the helix (k) and concentric reference rod (j) and hangdown (m). The panholder loop (p) is suspended below (m) by hooks (n), (n'). An aluminum foil pan, not shown, fits on the loop of (p).

access to the entire balance. Rings of conductive paint near the regions (c), (g), and (h) help reduce the violently disruptive effects of static electricity (see below).

In early experiments, spring extension was read on a simple scale with a mirror to prevent parallax error. Later, accuracy was increased by using a cathetometer. The reference has also been improved: at first the initial reading was used as the only reference point, relying on the immobility of the apparatus. Then crossed hairs held in place on the balance case provided a reference which could correct for any jarring of the cathetometer. Finally the reference rod was constructed as an integral part of the balance of itself. The internal reference remains accurate even if the case is tilted, which may happen during sample changes.

The extension of the helix is linear to ± 0.2 percent over the range 0-15 mg. The balances used have had extensions about 1 cm/mg; the final one stretches 0.980 ± 0.002 cm/mg. Mr. T. S. Nissen (AA Balance Sales and Service, Oakland, California) kindly lent me his 'M' tolerance weights for the calibration.

The sample can be heated by a tube furnace which surrounds the lower part of the balance case. Temperature is read from a thermocouple junction taped or glued to the outside of the case at about the height of the sample.

Pitfalls of the method. The hazards and sources of systematic error in microbalance techniques are well-known (Katz, 1961; Waters, 1965). Those particularly appropriate to the present study will be discussed here.

Since the quartz balance is a nonconductor of electricity and sensitive to forces on the order of a few micrograms, it is very susceptible to static electricity. The balance may cling to the side of the case, so that its extension cannot be read. More seriously, it may be suddenly attracted or repelled by some charged object, and the resulting violent motion will usually spill the sample and dislodge the pan and panholder loop. When handling the balance, one must carefully ground the balance, case, oneself, and so on; but especially on a dry day, this precaution has only limited effect. The problem was ameliorated by enlarging the case from 1" to 2" diameter. Since there can be no potential gradient inside a conducting shell, conductive rings were painted around the inside of the case at sensitive places, especially near the ground joints (regions c, g, and h in Fig. V-2). Rings about an inch wide, or narrow rings connected by conductive paint, seem equally effective. Unfortunately the ideal, inert paint has not yet been found. Deposited silver is far too fragile. Silver paint (Hanovia) tends to flake off (possibly due to amalgamation with traces of mercury from the diffusion pump) and is slightly soluble in the solvents used for cleaning. Conductive epoxy (silver "solder" No. 3022, Epoxy Products Inc.) is only slightly more durable. Occasionally the helix must be cleaned. Dust and vacuum grease, the most usual contaminants, can be removed by gently spraying with a solvent such as xylene, while touching the helix with a tissue. Of course the operation must be performed delicately and without rubbing or pinching the quartz fiber. Panholder loops are cleaned in the same way, with a solvent appropriate for the sample.

Small pressure gradients, such as those caused by a vigorous wave of the hand, may send the unprotected hangdown careening to the side of its case. Large pressure gradients, caused by too-sudden evacuation or introduction of gases, have been fatal to one entire balance and several hangdowns. This problem was less severe in the enlarged case, but remains a severe hazard. An important rule is that stopcocks must operate with absolute smoothness, and be opened with agonizing slowness.

The reference rod (j, Fig. V-2) as supplied by the manufacturer persistently twisted itself around the hangdown; to eliminate the twisting the reference rod had to be shortened. The balance was loaded with an empty sample pan, and the rod amputated at a point just below level with the bottom of the helix. This length has proved satisfactory. Sudden pressure changes, in addition to their other effects, invariably make the reference rod protrude through the coils of the helix; it is disengaged by gently pulling the spring down (using cork-tipped tweezers) until the rod is freed.

Errors in weighing may arise from such obvious sources as tangling of the helix; transient pressure gradients (even when small); or contamination. Temperature gradients cause less spectacular but equally annoying disturbances (Honig, 1961; Czanderna, 1961). Unfortunately, experiments often call for operating at pressures in the Knudson range, approximately 10^{-3} to 20 torr. At these pressures the mean free path is long enough for many gas molecules to strike the sample from regions of different temperatures (different kinetic energies), and the number of molecules is great enough for them to have considerable cumulative force. The balance is not thermostatted; neither has

any serious attempt been made to place the sample at the thermal center of the tube furnace, since there are generally weight changes (hence position changes) during heating. I have assumed that at room temperature the balance is in equilibrium with the room air, and that thermal gradients are negligible. However, discrepancies of around 10 micrograms occasionally occur during an experiment, probably because of temperature gradients.

Some gases, pyridine and water for instance, are adsorbed on both balance and pan; such effects are taken into account by exposure to the gas with no sample present. Some of these blank runs are shown in Fig. V-7b and V-10. True buoyancy corrections are negligible since the sample volume is very small. This was verified by exposing a sample of MnPc to nitrogen, which is not absorbed on the sample. At pressures of 18.5 and 159 torr, the apparent weight was the same as in vacuum.

B. RESULTS

1. Pyridine sorption. Pyridine has a profound effect on both the spectrum and the chemistry of phthalocyaninomanganese (Yamamoto, Phillips and Calvin; Engelsma et al., 1962). It is a good solvent for this compound as well as for etioporphyrin I manganese, and many of our chemical and EPR studies have been carried out in pyridine solution. We have therefore focussed our investigation of the addition of vapor-phase ligands by solid metalloporphyrins mainly on pyridine.

a. μ-Oxobis(phthalocyaninopyridinemanganese)-bispyridine, $(MnPcPy)_2O \cdot 2Py$, has the novel binuclear structure shown in Fig. I-3.

It contains two pyridines, one coordinated to each manganese ion so that the metal is surrounded by six ligands in a distorted octahedron. Two other pyridine molecules fill holes in the crystal but are not directly bonded to the complex (Vogt et al., 1966; 1967). The coordinated pyridine can be removed only by heating in vacuum; the pyridine of crystallization is gradually lost even in air at room temperature. We have studied the absorption and desorption of pyridine on $(MnPc)_2O$, and our results agree with Vogt's observations and with his formulation for the compound.

$(MnPcPy)_2O \cdot 2_A^{Py}$ is produced by aerial oxidation of $Mn^{II}Pc$ in pyridine solution. The crystals used in early work were prepared by A. Yamamoto; their pyridine content depended on how rigorously they were dried (Yamamoto, Phillips and Calvin). A sample of the material used for the X-ray structural determination (Vogt, Zalkin and Templeton, 1967) was kindly provided by L. H. Vogt, Jr.; his preparation differed from Yamamoto's mainly in that pains were taken to prevent it from drying.

In a typical experiment, the loss of pyridine is measured in vacuum, first at room temperature and then at 60-140°C. After the sample has cooled to about 23° again, pyridine vapor is admitted to the system and its absorption is followed. An experiment using crystals prepared by Yamamoto (I) and one using Vogt's preparation (II) are compared in Table V-1. They are illustrated graphically in Figures V-3 and V-4.

The interstitial pyridines are held so tenuously that Vogt found it necessary to seal his crystal in a capillary tube containing pyridine; otherwise the X-ray diffraction pattern showed crystalline

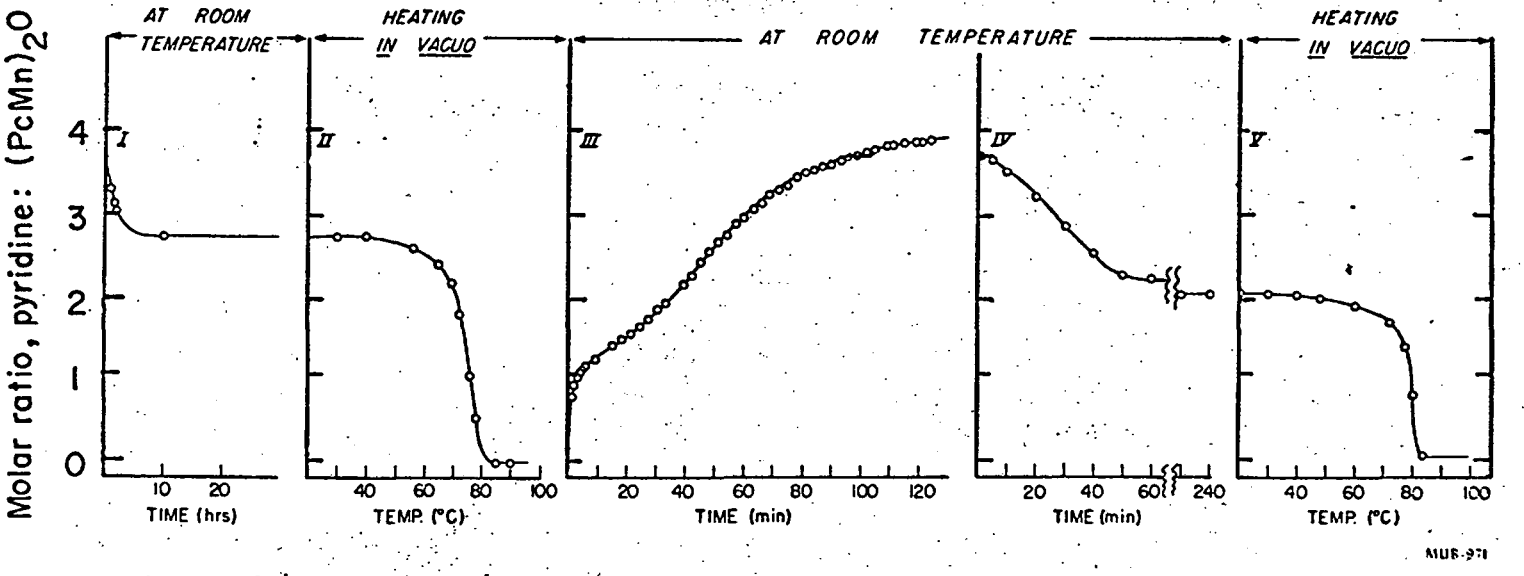

Fig. V-3. $(MnPcPy)_2O \cdot 2$ Py (Yamamoto): pyridine removal and resorption. I, IV. Evacuation at room temperature. II, V. Heating in vacuum. III. Exposure to pyridine vapor (15-17 torr).

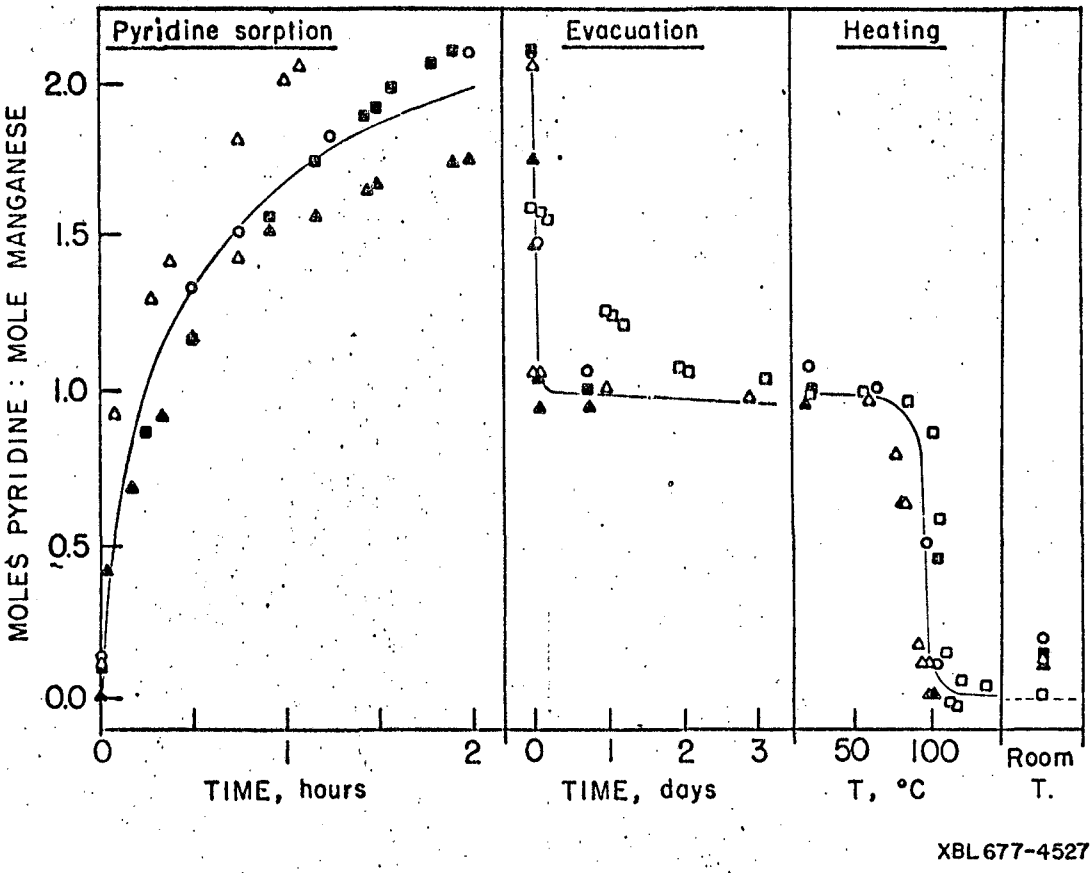

Fig. V-4. Repeated removal of pyridine from $(MnPcPy)_2O \cdot 2$ Py (Vogt), and its resorption. The compound after evacuation is $(MnPcPy)_2O$; after heating, $(MnPc)_2O$.. □, initial behavior; the sample was kept in air 80 days before evacuation, and was observed in vacuum 21 days before heating. Other symbols represent subsequent cycles, in which the sample was not exposed to air, and was evacuated for 1-3 days. Pyridine pressure during sorption cycle was 13.5-16 torr.

Table V-1

Pyridine adducts of

μ-oxobis(phthalocyaninomanganese)

Source: Vogt		Yamamoto[b]	
Treatment	Molar ratio[a]	Treatment	Molar ratio[a]
Initial	3.55		
In air 3 hours	3.45	In air	3.84
In air 80 days	3.21		
In vacuum 3 days	2.06	In vacuum 1 day	2.85
In vacuum 21 days	1.96		
Heated 7 hours in vacuum, to 116°	(0)	Heated 8 hours in vacuum, to 60°	(0)
Pyridine atmosphere	≥3.98[c]	Pyridine atmosphere	3.94
≥16 hours in vacuum	1.99[c]	1 hour in vacuum	2.35
Heated in vacuum (to about 110°)	0.27[c]	Heated in vacuum to 116°	0.05

a. $Py/(MnPc)_2O$.

b. Crystals prepared from MnPc by oxidation in pyridine were washed with pyridine and diethyl ether and dried in air.

c. Averages for four cycles.

disorder. However, the loss can be very slow: after 80 days in still air, II still contained 3.2 moles pyridine per mole of the binuclear complex (Table V-I). Even in vacuum (10^{-5} torr) many days were required to reach the composition $(MnPcPy)_2O$. I behaves in the same way (Yamamoto, Phillips and Calvin) although typically only 1 to 3 days were allowed for evacuation, so that the product often contained an intermediate amount of pyridine.

The coordinated pyridine can be removed by heating to 90-100°, or more slowly at 60°. If the $(MnPc)_2O$ is then exposed to pyridine vapor at room temperature, there is rapid absorption up to about the composition $(MnPcPy)_2O \cdot Py$, after which the weight gain is slower. On evacuation, the pyridines of crystallization are lost more readily than before. The coordinated pyridines, on the other hand, are desorbed in the same way on the first and second heatings.

The cycle of sorption, evacuation, and heating was repeated four times for II, and was reproducible (Fig. V-4). The difference between initial and subsequent rates of loss of interstitial pyridine may be explained by a change in crystal structure, which is not surprising in view of Vogt's observation that removal of pyridine leads to crystalline disorder.

b. In phthalocyaninomanganese(II), both of the metal's axial coordination positions are empty, so that it should be able to add two further ligands. Our results, although imperfect, tend to support this conclusion. Up to two equivalents of pyridine are strongly bound, and can be removed only by heating in vacuum (Yamamoto, Phillips and Calvin).

$Mn^{II}Pc$ itself is stable in air; its pyridine complex, however, is easily oxidized either in the solid state or in solution. Therefore our studies on the sorption of pyridine by solid $Mn^{II}Pc$ were always carried out in the absence of air.

The results were not reproducible; in particular, the rate of sorption varied tremendously from sample to sample, and was increased by heating for a given sample. We are dealing with two distinct phenomena: chemisorption, whose rate will be limited by such factors as diffusion into the crystal, or changes in crystal packing to provide large enough holes for the additional ligands; and physical sorption, which largely depends on surface characteristics. Thus even when kinetics can be obtained, they must be taken with a grain of salt. Certainly their dependence on the sample's history is not surprising. We have found in one case that results were determined by the force used in grinding a sample. However, no correlation with the phase of the moon has yet been observed.

In Fig. V-5, a typical experiment is shown. The $Mn^{II}Pc$ powder was exposed to pyridine vapor in the absence of air (stage I). Adsorbed pyridine was removed in vacuum at room temperature (stage II), while coordinated pyridine was lost only after heating to 50-60°C (stage III). The sample behaved differently in a second cycle (stages IV-VI). Note that the chemisorbed pyridine in the first cycle was 1.17 equivalents; in the second, 1.74; and in a third cycle (not shown), 2.05 equivalents, which was the amount expected, within experimental error.

An estimate of the coordinated pyridine can be made for a sorption run if the weight change levels off, as in Fig. V-5, stage IV.

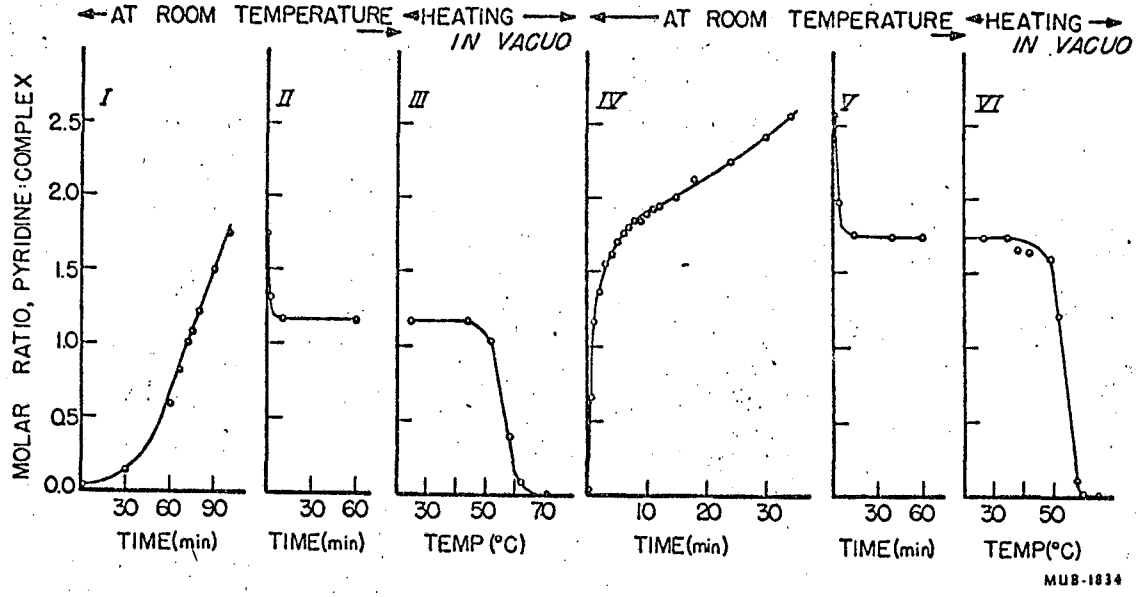

Fig. V-5. Sorption of pyridine vapor on phthalocyaninomanganese(II) powder. I, IV. Sorption of pyridine vapor (P = 15 torr). II, V. Evacuation at room temperature (ca. 10^{-5} torr). III, VI. Heating in vacuum: temperature increased at the rate of 1°/min.

We assume that the final slope is due to physical adsorption only, and the initial slope chiefly due to chemisorption. The intersection of these two lines then provides a rough estimate of the amount of adduct formed. Several samples were subjected to gradually increasing pressures of pyridine vapor, and the observations plotted on a log-log graph (Fig. V-6). For each series, the slope is close to 1/2, indicating that the reaction

$$MnPc + 2\ Py = MnPcPy_2 \qquad (7)$$

occurs. The equilibrium constant, $K = (MnPcPy_2) / (MnPc)(Py)^2$, where (Py) is expressed as pressure, is $(2.0 \pm 1.5) \times 10^3\ atm^{-2}$.

One specimen of MnPc (Vogt, sublimed) absorbed pyridine very slowly. When pyridine (13-16 torr) was admitted to the system, there was an immediate jump in weight of about 0.12 equivalent; then weight gain was linear with time for the rest of the run, up to nearly four hours. On evacuation, not all the pyridine was lost, showing that during each run there was some chemisorption. If the new weight in vacuum was taken as the zero point on the graph, the phenomenon was remarkably repeatable (Fig. V-7). At the end of seven cycles, a total of 1.65 equivalents of pyridine had been chemisorbed (Fig. V-8). If we assume that reaction (7) occurs during exposure to pyridine vapor, but is not reversed by evacuation at room temperature, then we obtain an apparent rate constant first order in (MnPc), $k_1 = 2 \times 10^{-5}\ sec^{-1}$. We note that the rate of physical sorption in this experiment is independent of MnPc concentration.

c. Although etioporphyrin I acetatomanganese(III) will take up a large amount of pyridine (Fig. V-9), only one equivalent is strongly

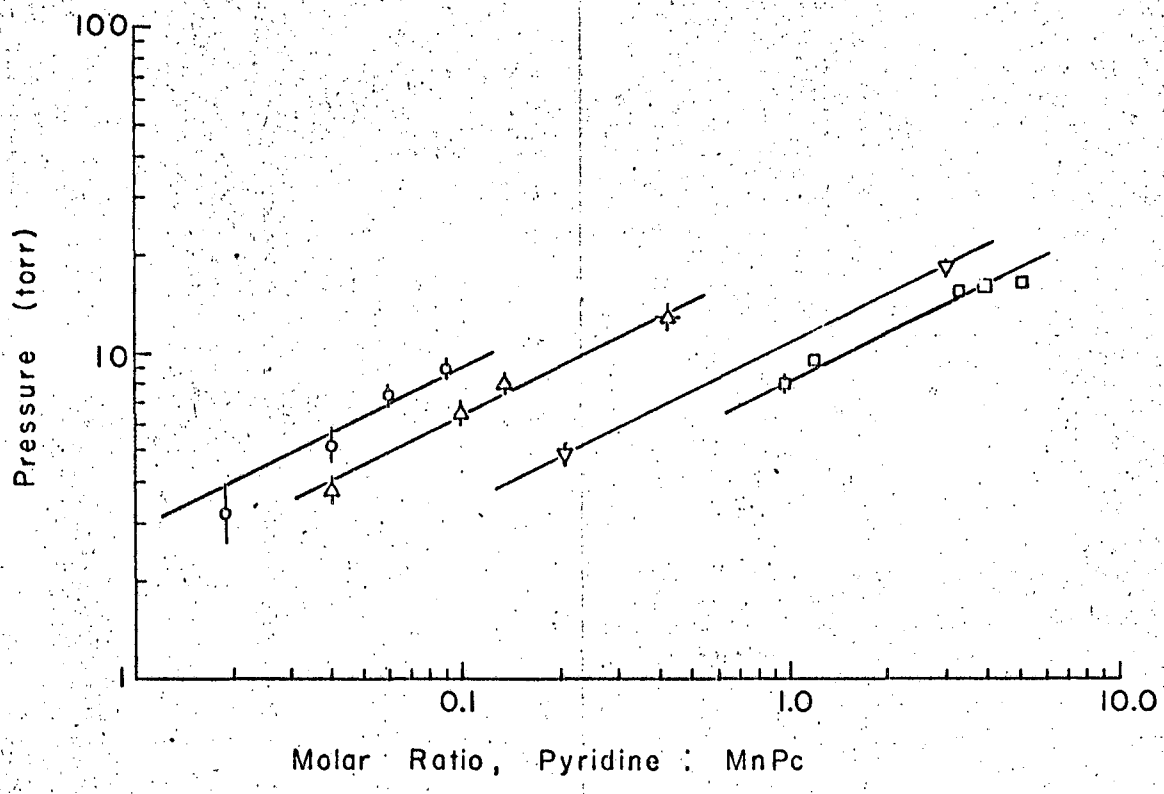

XBL 677-4532

Fig. V-6. Effect of pyridine pressure on the chemisorption of pyridine by phthalocyaninomanganese(II). The slope of each line, $\frac{P_2 - P_1}{Ratio_2 - Ratio_1} = 1/2$, corresponds to the reaction MnPc + 2 Py $\overset{K}{=}$ $MnPcPy_2$. For the samples illustrated here, the equilibrium constants are calculated as:

Symbol:	○	△	▽	□
K, atm^{-2}	3.5×10^2	7.1×10^2	2.5×10^3	4.5×10^3

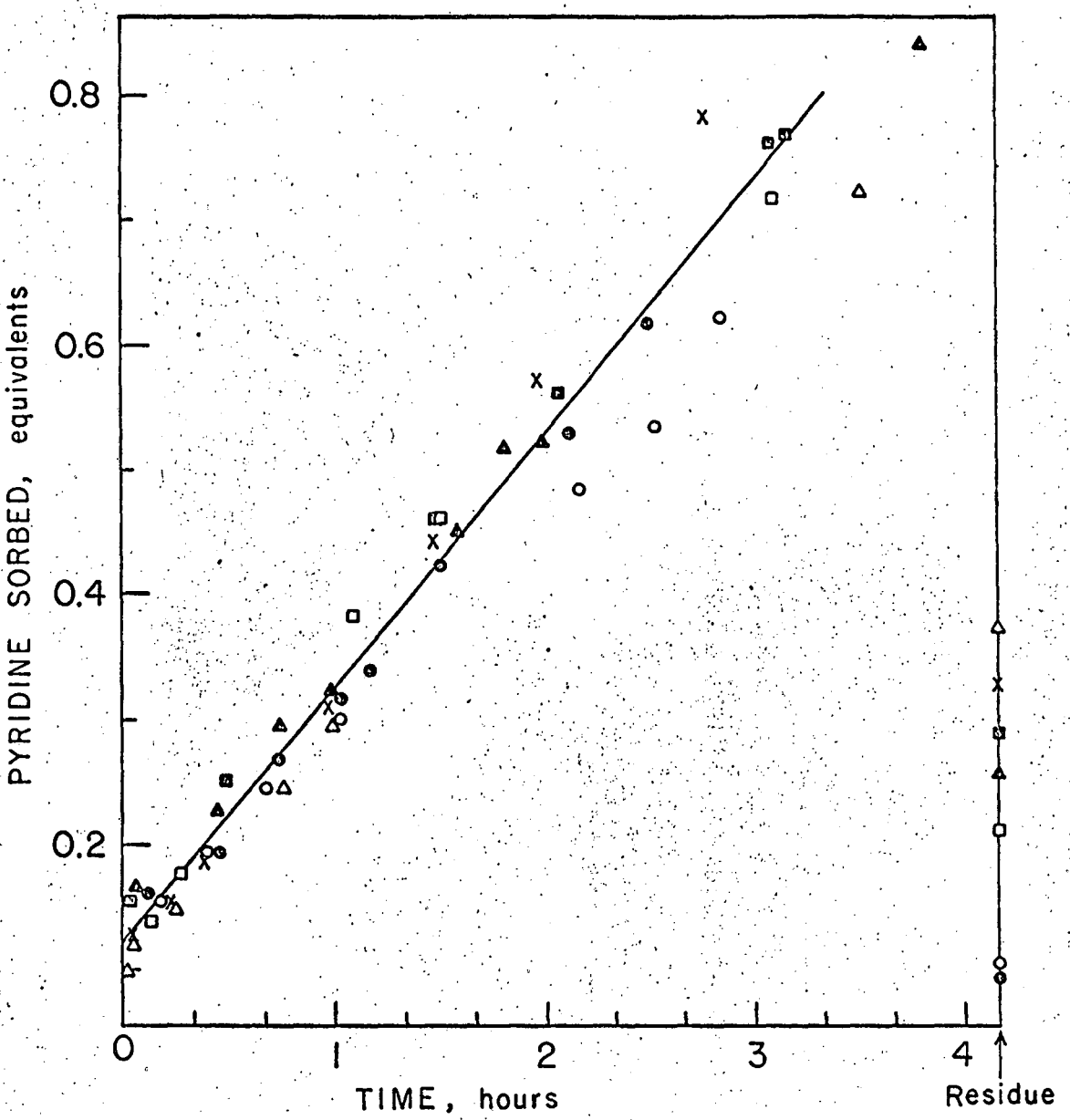

XBL 677-4525

Fig. V-7a. Physical and chemical sorption of pyridine by one sample of $Mn^{II}Pc$. Amounts shown above are the increments for each cycle; "Residue" refers to the pyridine remaining after evacuation to 10^{-5} torr, and thus represents chemisorption.

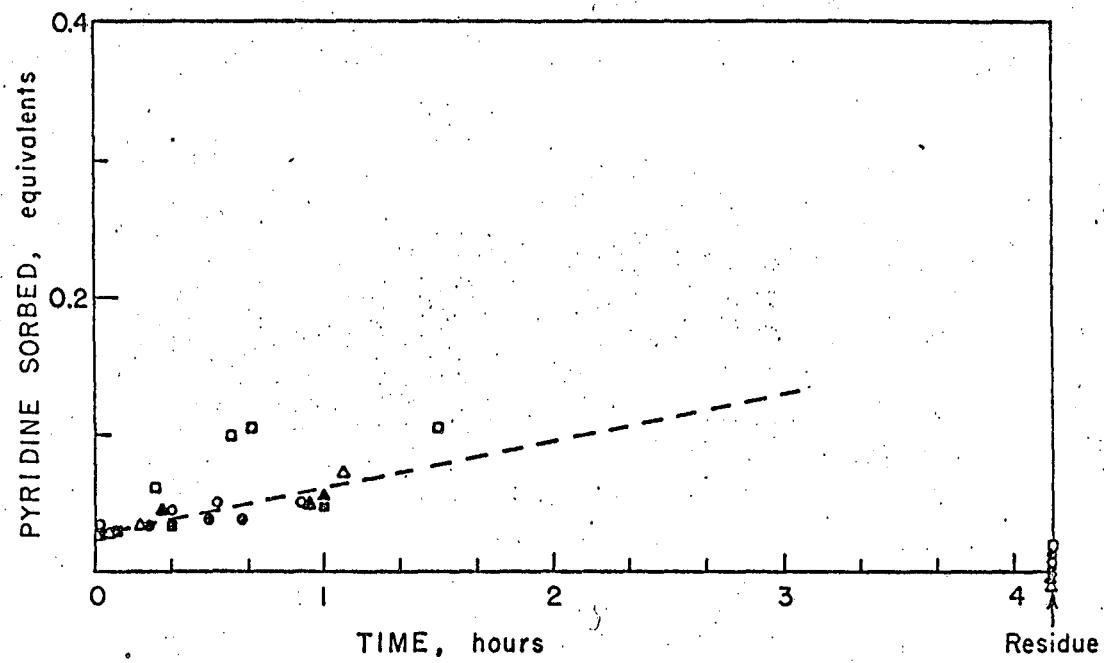

XBL 677-4526

Fig. V-7b. Blank runs: pyridine sorption on balance and aluminum sample pan, normalized to correspond to the sample in Fig. V-7a. One equivalent is 0.9 mg pyridine. Note that the blank adsorption is considerably less than sorption by the sample, and that no residue of pyridine remains on the empty balance in vacuum.

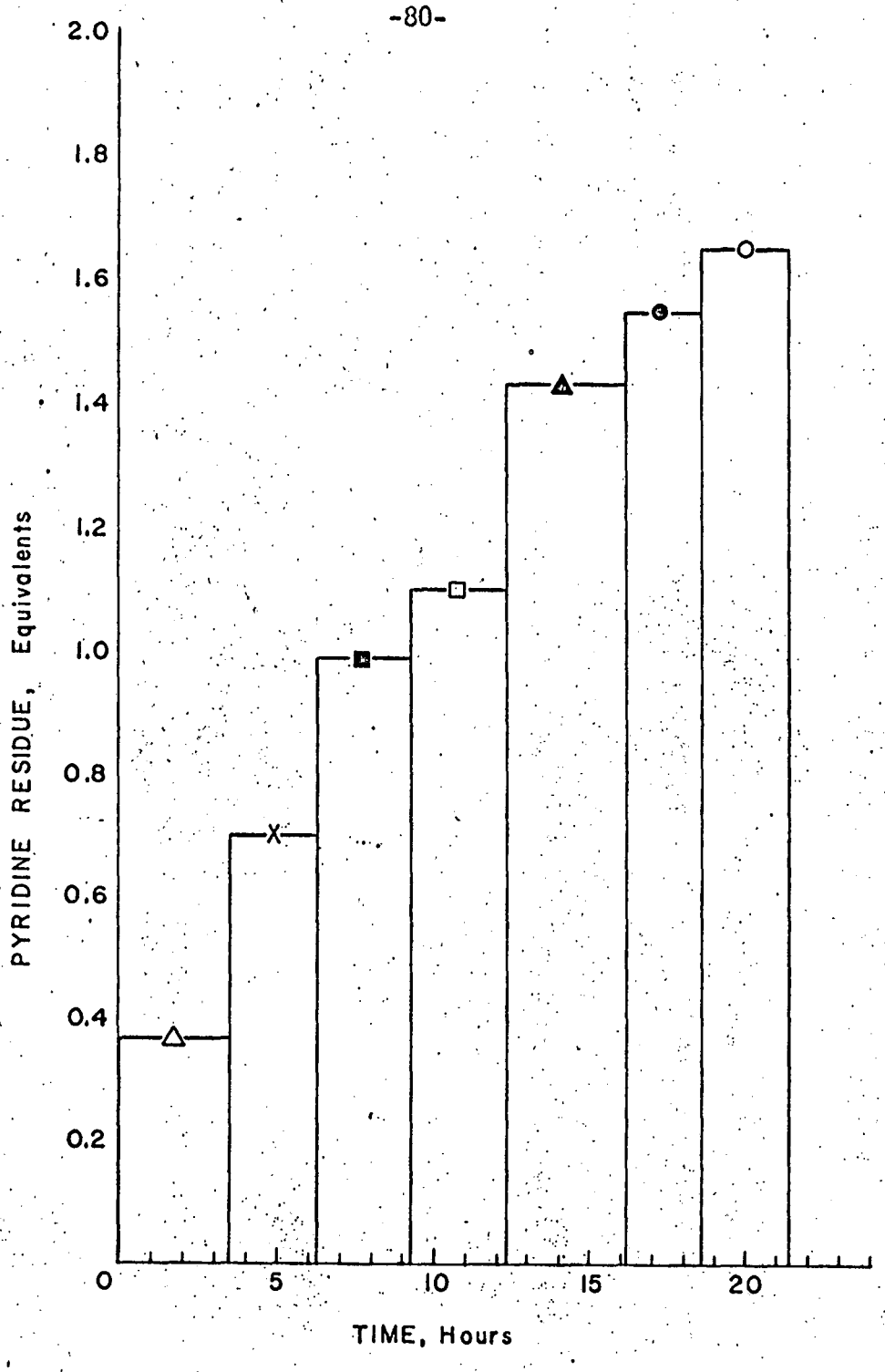

XBL 670-6203

Fig. V-8. Pyridine chemisorbed by MnPc during the experiment illustrated in Fig. V-7. The symbols correspond to those in Fig. V-7a. The total residue is plotted against time of exposure to pyridine vapor (approx. 15 torr).

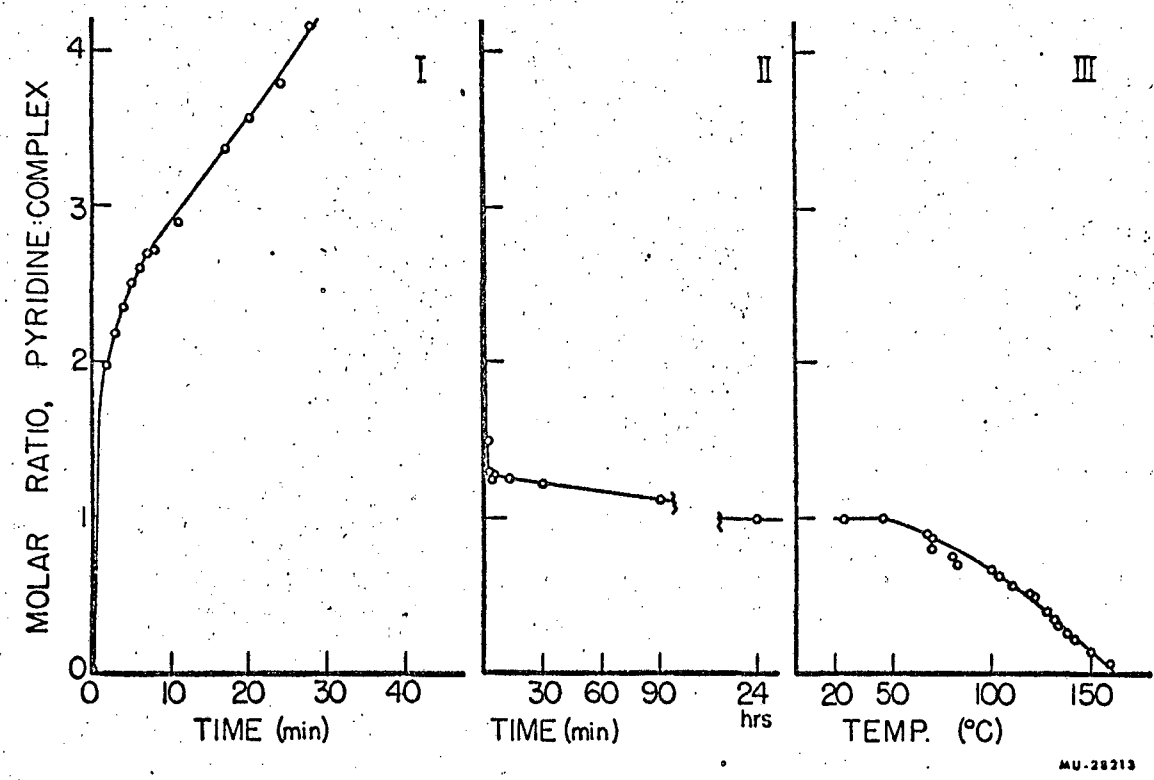

Fig. V-9. Sorption and desorption of pyridine by etioporphyrin I acetatomanganese(III). Molar ratio after sorption and evacuation, in subsequent experiments: 1,01, 1.00 (stage II).
I. Sorption of pyridine vapor (P = 18 torr). II. Evacuation at room temperature. III. Heating in vacuum.

absorbed, corresponding to the single axial position available for coordination:

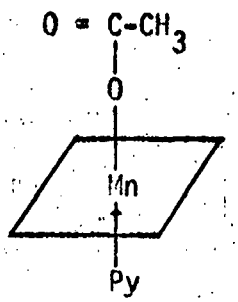

The rate of surface adsorption, in excess of the chemisorbed pyridine, varies among samples; however, both the approximate rate and the stoichiometry of the chemical absorption are reproducible. As with the phthalocyanine complexes, the coordinated pyridine can be removed by heating (Yamamoto, Phillips and Calvin).

2. Sorption of water. Since the manganese porphyrins have been proposed as model compounds for those involved in the photosynthetic production of oxygen from water, we have looked for formation of water adducts with these chelates. However, we have found no stable further complexes with water.

One sample of Mn^{III}Etp(OAc) absorbed 1.1 equivalent of water above the blank (Fig. V-9), which however came off immediately on evacuation. A second sample absorbed no water at all, even after 43 hours of exposure to water (P = ca. 23 torr), suggesting that the process is a surface phenomenon and involves no chemical bonding.

(Dimethylhematoporphyrin IX)chloromanganese(III) did not absorb water.

MnPc sorbed water in amounts which tended to increase with the pressure of the water vapor, although there was no straightforward pressure dependence. The sorbed water was released in vacuum. A

sample prepared by Vogt and purified by sublimation, on the other hand, sorbed little water above that observed for the balance and empty pan. Again we must conclude that there was no chemisorption.

3. Sorption of other gases. In contrast to its behavior with water, Vogt's sample of MnPc repeatedly gained (and lost on evacuation) about one equivalent of acetic acid above the blank, in an atmosphere of HOAc. Toluene, however, was not absorbed at all.

A specimen of MnPc was exposed to nitrogen gas at 18.5 and at 159 torr, at room temperature. There was no gain in weight.

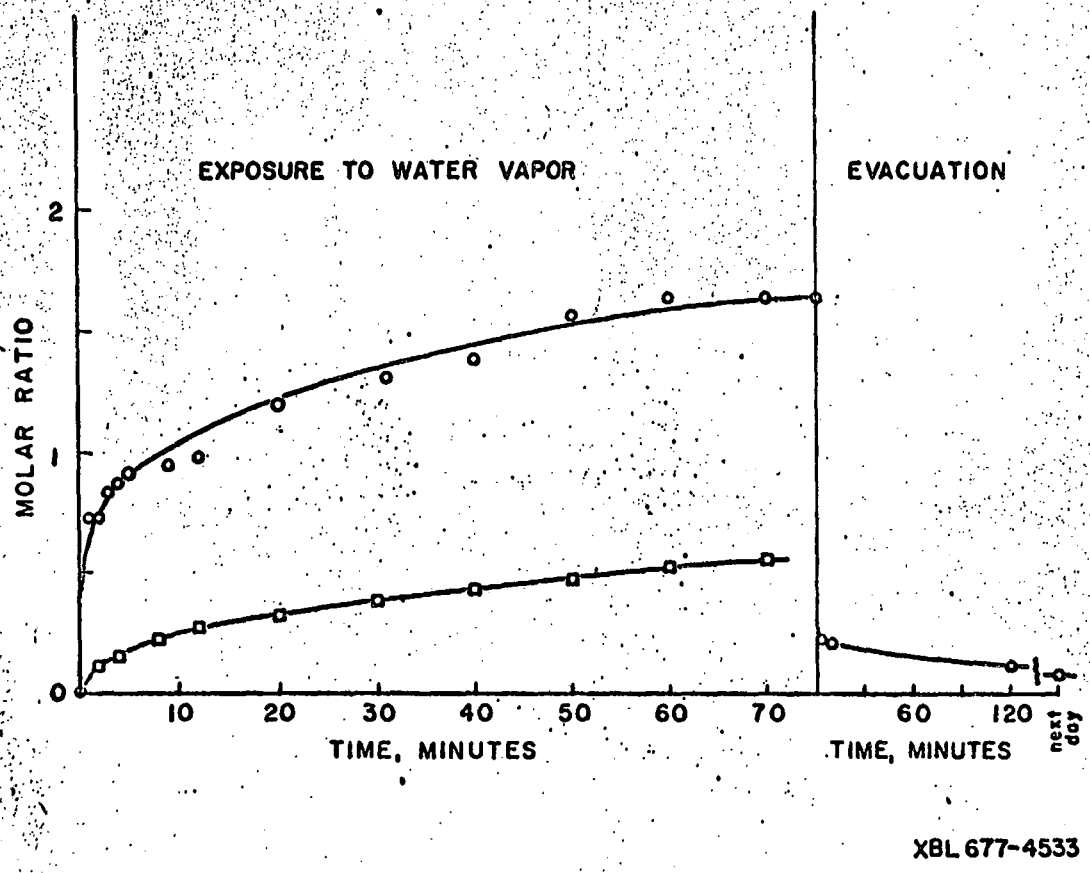

Fig. V-10. Sorption of water vapor by one sample of etioporphyrin I acetatomanganese(III). Molar ratio = moles water sorbed/moles MnEtp(OAc) in sample. $P(H_2O)$ was 19.0 torr. ○, Sample; □, Blank (normalized). One equivalent water = 0.28 mg.

VI. ELECTRON PARAMAGNETIC RESONANCE

The spin of an electron in a magnetic field can take on only two values: +1/2, "up"; or -1/2, "down". The energies of these two states depend strongly on the immediate environment of the electron, as well as on any external magnetic field. In many cases transitions between the spin states can be induced by a small magnetic field rotating at microwave frequencies, giving rise to the phenomenon known as electron paramagnetic resonance (EPR), or alternatively, as electron spin resonance (ESR). Because the transition energy is so sensitive to the electron's surroundings, EPR is an effective tool for studying the electronic structure of atoms or molecules containing unpaired electrons. In particular, a theorem due to Kramers states that in systems with an odd number of electrons, there must always be a degeneracy in spin states resolvable only by external magnetic field.* This degeneracy guarantees that in convenient magnetic fields, the transition in such systems will occur in the microwave energy region. For a free electron in a magnetic field of 3210 gauss, the transition energy is 0.3 cm^{-1} or 9000 mc/sec.

Since manganese(II) contains five d electrons, it can be studied by this technique. Unfortunately, while $Mn(H_2O)_6^{2+}$ gives a sharp and characteristic EPR signal, complexation with other ligands often broadens the signal so that it cannot be detected. Also, antiferro-

---

*For a general background on the theory and practice of EPR, the reader may wish to refer to a book such as Pake (1962) or Bersohn and Baird (1966).

magnetic interactions between manganese ions broaden the resonance in solid compounds.* Thus after several vain attempts in this laboratory to observe the EPR of phthalocyaninomanganese(II), the project was abandoned.

Earlier resonance studies of metal phthalocyanines are summarized by Lever (1965a). Apparently the only report on MnPc is that by Ingram and Bennett (1954), who reported simply that a powdered sample gave a 500 gauss wide signal at g = 2.0.

In an experimental survey of the paramagnetic resonance of various metallophthalocyanines in pyridine at liquid nitrogen temperature (Maksim and Phillips, 1964), Miss Ann Maksim inadvertantly included $Mn^{II}Pc$. A unique and complex spectrum appeared (Figure VI-2a). The several months of fascinating research recorded in this chapter stemmed directly from Miss Maksim's serendipity.

Since the paramagnetic resonance spectrum of MnPc is so complicated, we have developed a computer program which generates simulated EPR spectra. The calculations involve a semi-empirical spin Hamiltonian which assumes S = 1/2. The agreement between actual and simulated spectra indicates that the manganese(II) is in its rare spin-paired state.

We have observed the resonance signals of several other metal phthalocyanines, and our experimental findings are included in this chapter. The paramagnetic compounds and NiPc have been studied by others, and we shall compare our results with theirs. Although earlier workers have seen a free-radical signal in various impure

---

*Factors which influence the observability of spin transitions in general, and those of manganese in particular, are discussed by Ross (1966; p. 73ff, 86ff).

diamagnetic phthalocyanines, we have found another signal as well, which may be that of the phthalocyanine radical itself.

Sulfonated derivatives of the manganese and iron compounds were looked at; differences between the spectra of the sulfonated and unsubstituted chelates should be chiefly solvent effects.

Spectra of two manganese porphyrins are discussed briefly.

A. EXPERIMENTAL

An X-band spectrometer which operated near 9060 Mc/sec was used for all EPR spectra. The sample was placed in a quartz tube (3 mm bore) in the rectangular TE_{102} cavity (Varian V4531). The sample in the cavity could be cooled to about 90°K by a flow of cold nitrogen gas through a quartz cooling system (Varian V4547). The derivative of the absorption, obtained by phase-sensitive detection with 100-kc/sec field modulation, was recorded as a function of magnetic field. The field was measured by a gaussmeter and further checked by crystalline diphenylpicrylhydrazyl (DPPH), which gives an intense EPR signal at $g = 2.0036$.

Adaptations of sample tubes were similar to those on cuvettes for visible spectrophotometry (Section IV-A). Easily-oxidized samples were protected from air in tubes fitted with vacuum stopcocks or glass-sealed. Reactions could be carried out or visible spectra observed by a side-arm arrangement.

Samples kept for more than a day were stored in the dark; otherwise, no special precautions were taken to shield them from light. Although these compounds are light-sensitive (Chapter IV), there is little reaction unless the illumination is intense.

Pyridine (B&A, reagent grade) was distilled from BaO or KOH and stored over Linde molecular sieves which had been dried at 650°C; β-picoline was distilled from KOH. Dioxane was distilled immediately before use. Reagent grade toluene was stored over dried molecular sieves but was not purified further.

B. RESULTS

The six lines in the EPR spectrum of aqueous Mn^{2+} (Fig. VI-1b) are due to interactions between the electrons and the ^{55}Mn nucleus which has spin 5/2. At 100°K, the spectrum of $Mn(H_2O)_6^{2+}$ in a glass reveals additional structure: between each pair of hyperfine lines are two less intense peaks, which can be attributed to simultaneous nuclear and electron spin transitions (Fig. VI-1a). Characteristically, the paramagnetic resonance of Mn^{2+} is symmetric about the spectroscopic splitting factor g = 2 (close to the free-electron value), with hyperfine splitting A = 0.009 cm^{-1}, or about 95 gauss (Pake, 1962; pp. 183-185).

Phthalocyaninomanganese(II). MnPc dissolves sparingly at best in most solvents, and tends to precipitate out at the low temperatures at which paramagnetic resonance is observable. Spectra in frozen pyridine solution (Fig. VI-2a) exhibited bands with non-reproducible intensities and widths, which varied with concentration of MnPc and with rapidity of freezing. This is a symptom of solute aggregation during cooling (Ross, 1965). A spectrum in 1:1 pyridine-water and one in dioxane showed very low resolution, probably also because of aggregation. Any signals in the following solvents were hard to distinguish from noise: benzene, α-chloronaphthalene, acetone,

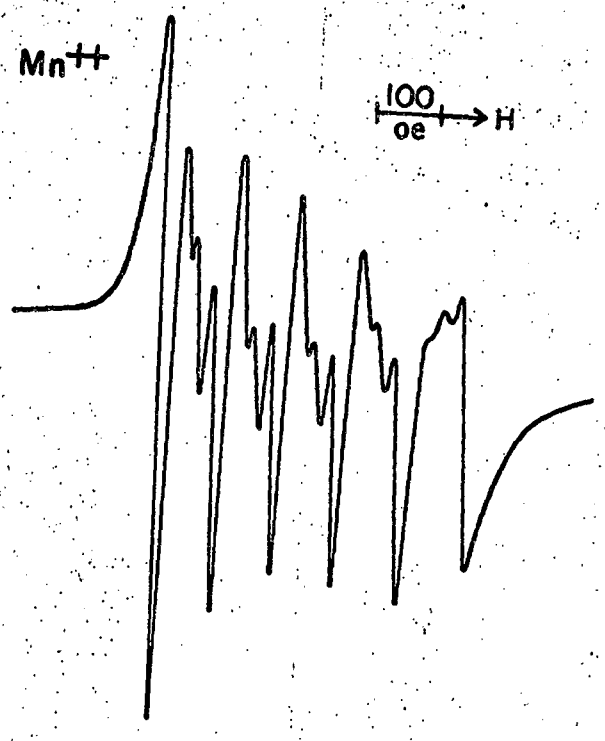

a) Aqueous solution at 100°K; 25 vol. % methanol added to the water to prevent aggregation of the solute.

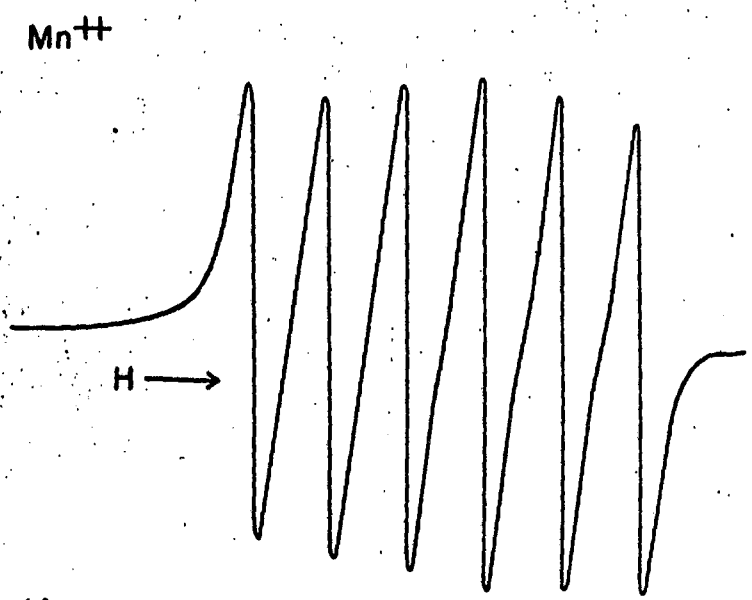

b) Aqueous solution at room temperature.

XBL 678-4687

Figure VI-1. Paramagnetic resonance spectra of $Mn(H_2O)_6^{2+}$. Figures from Ross (1966).

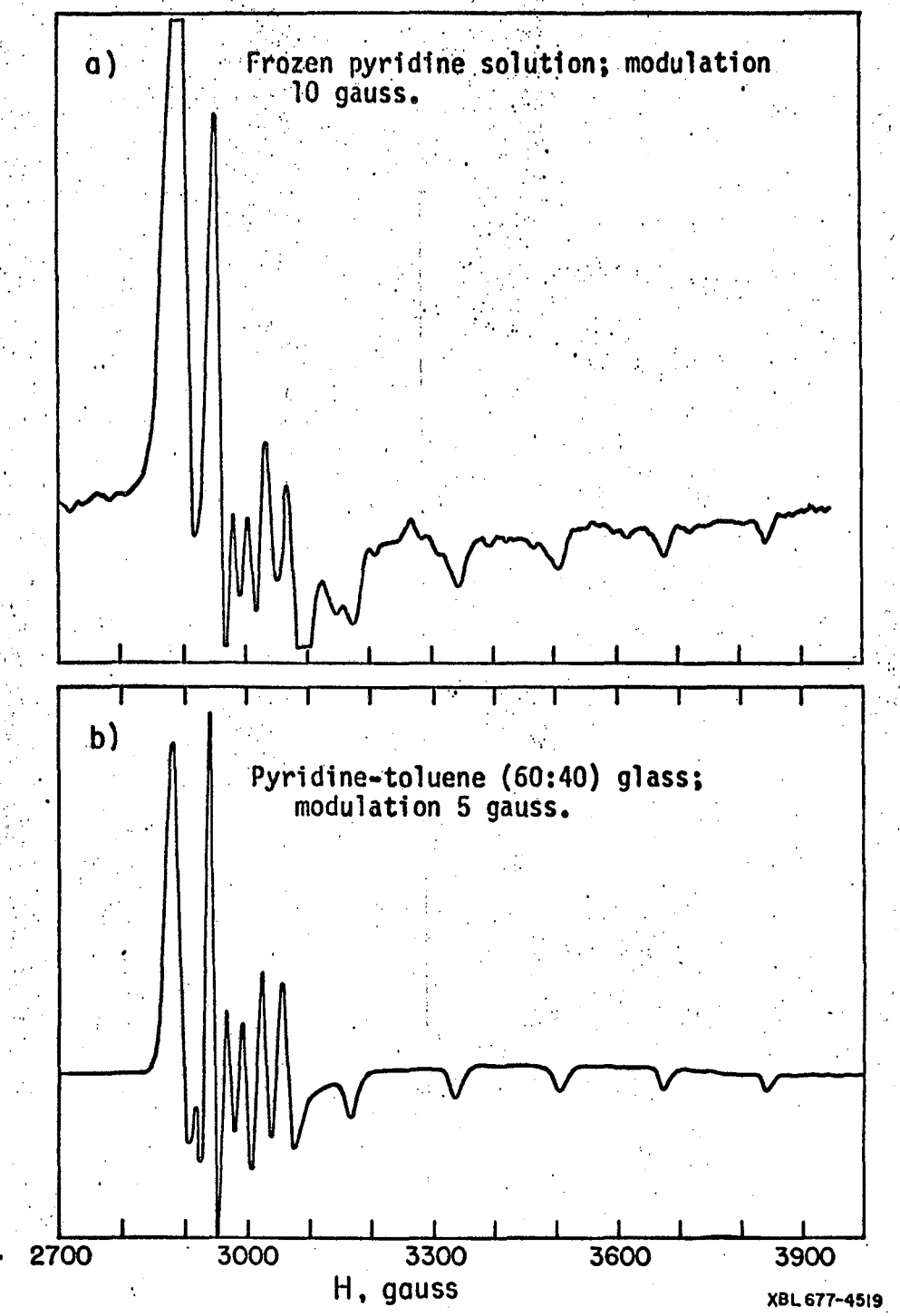

Figure VI-2. Phthalocyaninomanganese(II) paramagnetic resonance. Samples were under vacuum, and at about 90°K.

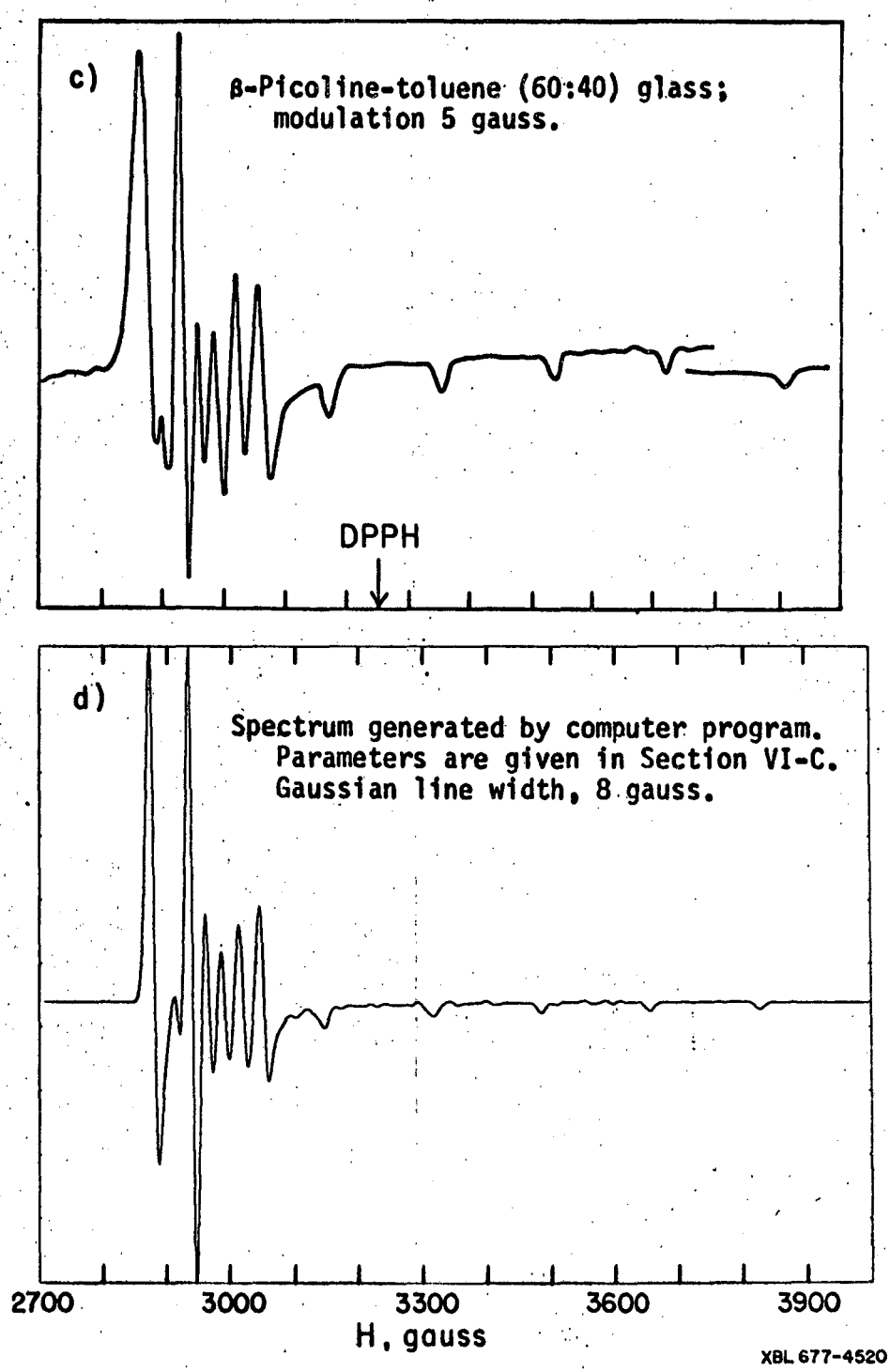

Figure VI-2 (continued).

tetrahydrofuran, glycerine, dimethylsulfoxide, or a DMSO-glycerine glass. A 60:40 mixture of pyridine or β-picoline with toluene forms a glass at low temperatures; formation of a satisfactory glass is aided by cooling rapidly, directly in liquid nitrogen. In these media phthalocyaninomanganese(II) showed a reproducible, well-resolved spectrum, similar to the clearest in pyridine alone (Fig. VI-2b,c).

Obviously in this compound manganese(II) is far from its usual state; the anisotropy of both $\underline{g}$ and $\underline{A}$ values is well outside the normal range for this ion. Data are summarized in Table VI-1.

Table VI-1

Paramagnetic resonance parameters of phthalocyaninomanganese(II) in various solvents

Solvent	$g_{\parallel}$	$g_{\perp}$	$\bar{g}$[b]	$A_{\parallel}$, cm^{-1}	$A_{\perp}$, cm^{-1}	Remarks
Pyridine	1.90	2.16	2.07	151×10^{-4}	25×10^{-4}	
Pyridine-toluene	1.90	2.16	2.07	151×10^{-4}	25×10^{-4}	(a)
β-Picoline-toluene	1.89	ca. 2.17	2.08	162×10^{-4}	ca. 28×10^{-4}	
Dioxane		ca. 2.15			ca. 37×10^{-4}	poor resolution
Acetone			2			single peak, width, 250 gauss
Pyridine-water, 1:1	1.95	2.16	2.09			poor resolution

(a) Values confirmed by computer analysis (see Section VI-C).

(b) $\bar{g} = \frac{1}{3}(2g_{\perp} + g_{\parallel})$.

On exposure to air, the $Mn^{II}Pc$ signal gradually disappears. A solution of $(MnPc)_2O$ (source: A. Yamamoto) in pyridine, in air, gave no detectable signal. On the other hand, a few of the samples of $Mn^{II}Pc$ dissolved in pyridine-toluene (60:40) under vacuum revealed two extra peaks: one at g = 1.89-1.91, the other at about g = 4.3. The latter tended to be quite broad and intense. These peaks behaved differently from those of $Mn^{II}Pc$: on oxidation, their intensity remained constant or even increased as the $Mn^{II}Pc$ signal faded (Fig. VI-3).

$(MnPc)_2O$ (source: L. Vogt) in pyridine-toluene under nitrogen atmosphere exhibited both the phthalocyaninomanganese(II) EPR spectrum and the two additional peaks (Fig. VI-4). When the solution was exposed to air, the $Mn^{II}Pc$ signal vanished, while the others decreased. It is curious that this supposedly oxidized species, when dissolved under an inert atmosphere, apparently contains a substantial amount of the manganese(II) species. The solution was blue-green rather than the true blue expected; at 100°K its color was green. Electronic spectra of a similar solution (Fig. VI-5) showed that in air the 716 nm and 620 nm species (and no other) were present, the former decreasing and the latter increasing with time.*

A low-field EPR peak has been observed in other compounds studied: etioporphyrin I manganese(III), (methylpheophorbide-a)manganese(III), metal-free phthalocyanine, and an oxidized form of etioporphyrin I zinc. Its cause is unknown. Nor has any explanation

---

*See Engelsma et al., 1962; Yamamoto, Phillips and Calvin. The process may be oxidation or dimerization.

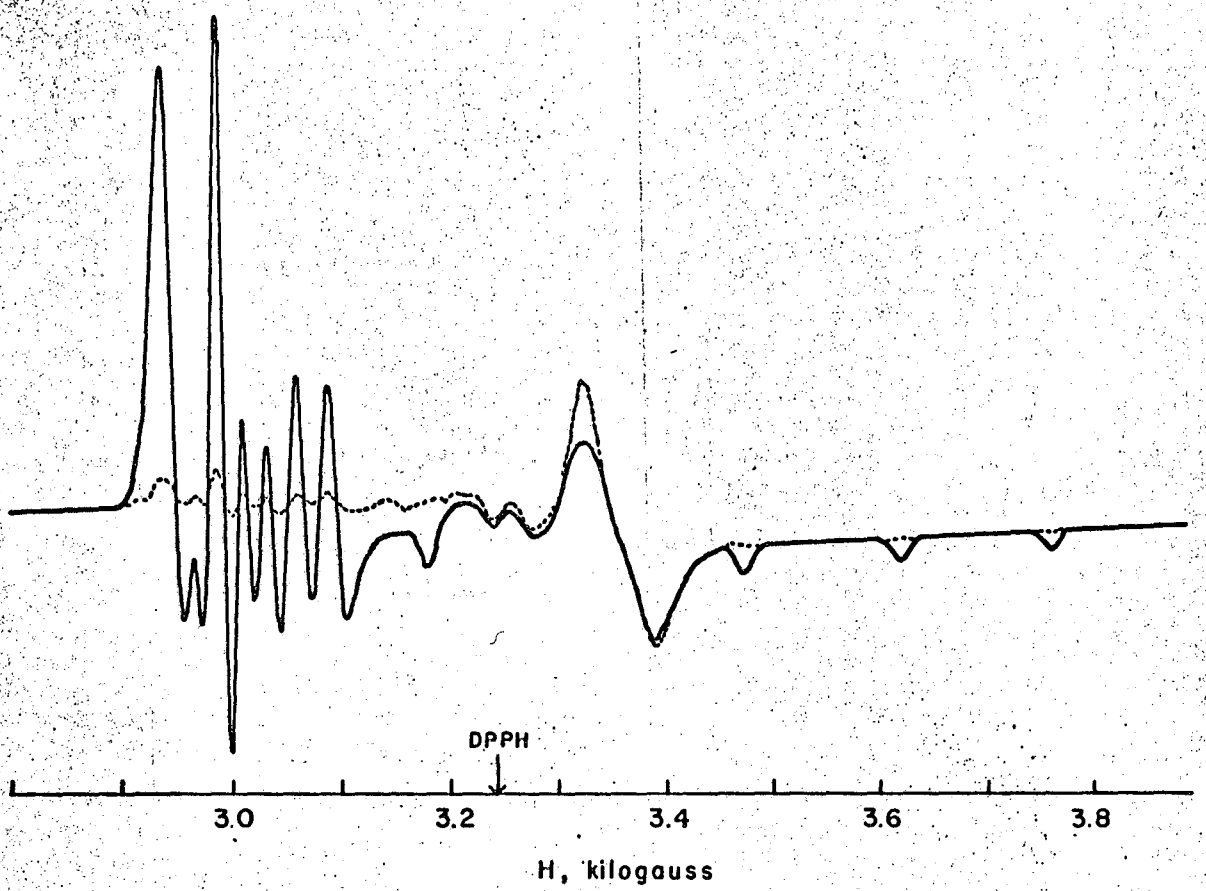

Figure VI-3. Behavior of "extra" EPR peaks in a phthalocyaninomanganese sample on oxidation by air. Spectra were taken at liquid nitrogen temperature; sample was warmed to 20°C to allow the reaction to proceed. The solvent was pyridine-toluene. Modulation 5 gauss. _____ , Solution freshly prepared in vacuum. --------- , After oxidation. The peak at g = 4.3 (cf. Fig. VI-4) remained constant in intensity.

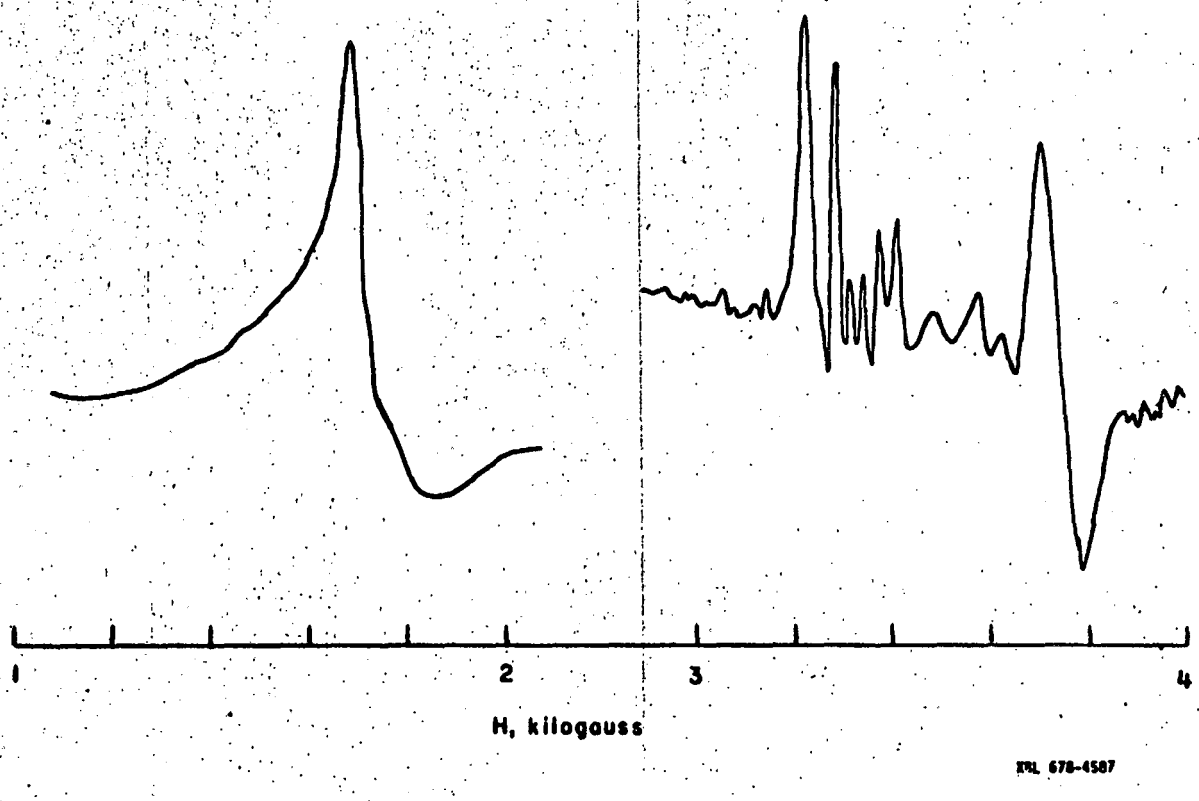

Figure VI-4. EPR spectrum of μ-oxobis(phthalocyaninomanganese) in pyridine-toluene glass. Temperature, 133°K; modulation, 3 gauss.

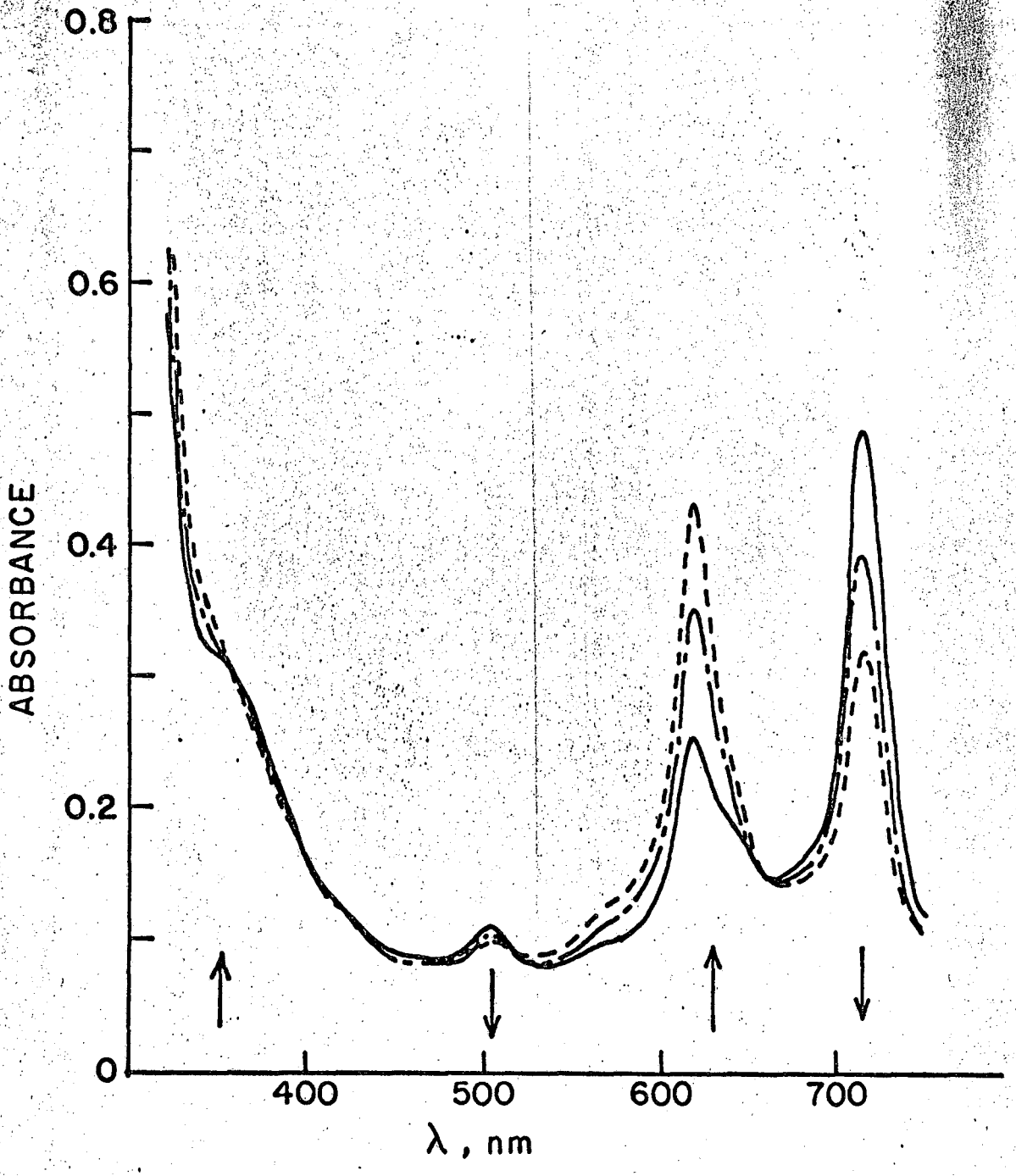

XBL 678-4589

Figure VI-5. Electronic spectra of a solution of μ-oxobis(phthalocyaninomanganese) in 60:40 pyridine-toluene, at room temperature. The solution was prepared in air, and a series of spectra were taken at invervals of a few minutes.

been found for the peak at g = 1.9, which has been seen only for phthalocyaninomanganese complexes dissolved in pyridine-toluene.

Tetrasulfophthalocyaninomanganese. This compound, examined in air, was almost certainly in its oxidized form. Solutions in water (2 M in $LiCl_2$; blue color) and in 1:1 water-ethanol (green) showed no EPR signal between 1000 and 4000 gauss. A sample freshly dissolved in 25% aqueous ethanol exhibited a weak spectrum of at least 16 resolved lines, with spacing about 50 gauss. Yamamoto (private communication) has observed a somewhat similar spectrum--even at room temperature--for powdered "MnPcO·2Py" (probably $(MnPcPy)_2O$). The intensity for Yamamoto's sample as compared with that of a known concentration of aqueous manganese^{2+}, was only 1/200 of that expected. The appearance of similar resonances for these two complexes suggests that the signal must be that of either the oxidized phthalocyaninomanganese moiety or a common impurity. The spectrum is unlike that for high-spin or low-spin manganese(II) or for $Mn^{II}Pc$; it is not due to the phthalocyanine free radical (see below). It is reproduced here in the hope that some reader may come up with a plausible explanation (Fig. VI-6a,b).

Phthalocyanine radical. An EPR signal at g = 2.0 has been observed in powdered samples of various phthalocyanines, usually those purified by sublimation (Ingram and Bennett, 1954; Lever, 1965a). The line has been attributed to a free radical, caused by decomposition of the phthalocyanine ring during sublimation or due to absorption of oxygen (Harrison and Assour, 1964). Apparently previous investigators have seen only the single peak, which we shall refer to as I.

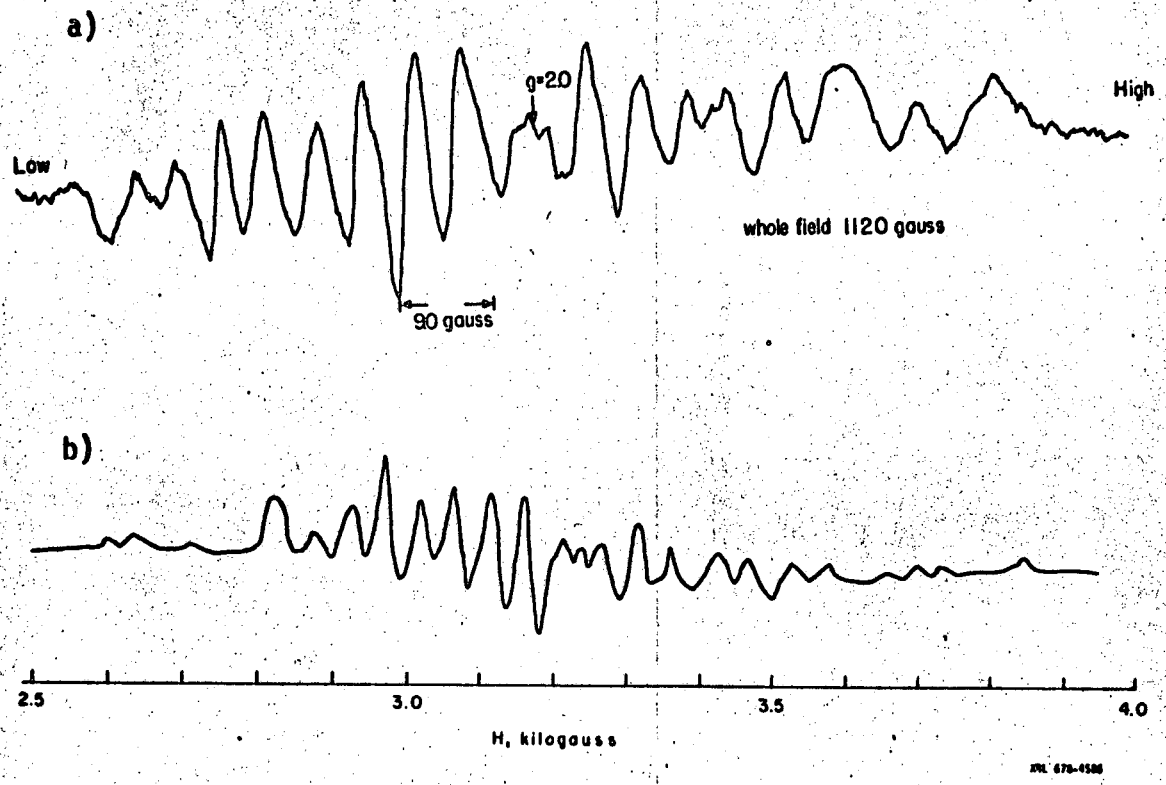

Figure VI-6. Electron paramagnetic resonance spectra of oxidized phthalocyaninomanganese species.

a) Powdered $(MnPcPy)_2O$ (Yamamoto, work done in this laboratory).

b) Tetrasulfophthalocyaninomanganese in 25% ethanol, in air, 90°K (oxidation state unknown).

In addition to the very strong free-radical peak, we have found a series of at least 15 much weaker lines also centered about g = 2, with spacing approximately 15-19 gauss (Fig. VI-7). The spectrum appears in the two diamagnetic compounds studied: phthalocyaninozinc and metal-free phthalocyanine. The splitting is the right magnitude for hyperfine structure of a radical containing nitrogen; if all eight nitrogens in the molecule were equivalent, we would expect 2I+1 = 17 hyperfine lines. Relative intensities of the absorption lines should correspond to the appropriate coefficients in the binomial expansion. The disagreement of the intensities of these derivative peaks with any reasonable pattern (including the possibility that the groups above and below g = 2 arise from separate transitions) may be due to distortion by the overwhelming peak (I).

Thus the spectrum in Fig. VI-7, excluding the intense peak, is tentatively considered that of the true phthalocyanine radical.

Phthalocyaninocobalt(II). The EPR spectrum of a pyridine solution of $Co^{II}Pc$ at liquid nitrogen temperature (Maksim and Phillips, 1964) is rich in structure (Fig. VI-8a). There are eight lines arising from hyperfine interaction with the ^{59}Co nucleus (I = 7/2); on each of these is superimposed five extrahyperfine lines from the nitrogens (I=1) on two axial pyridines. As with $Mn^{II}Pc$, $g_{\parallel} \neq g_{\perp}$. We estimate $g_{\parallel} = 2.03$, $g_{\perp} = 2.24$; $A_{\parallel} = 74$, $A_{\perp} = 61$, $A_N = 12 \times 10^{-4}$ cm^{-1}.

When the CoPc solution was allowed to stand in air, the signal appeared to coalesce into a single band of about 150 gauss width, much greater in intensity. The change is probably caused by oxidation to $Co^{III}Pc$, which should be diamagnetic; the intense signal is the

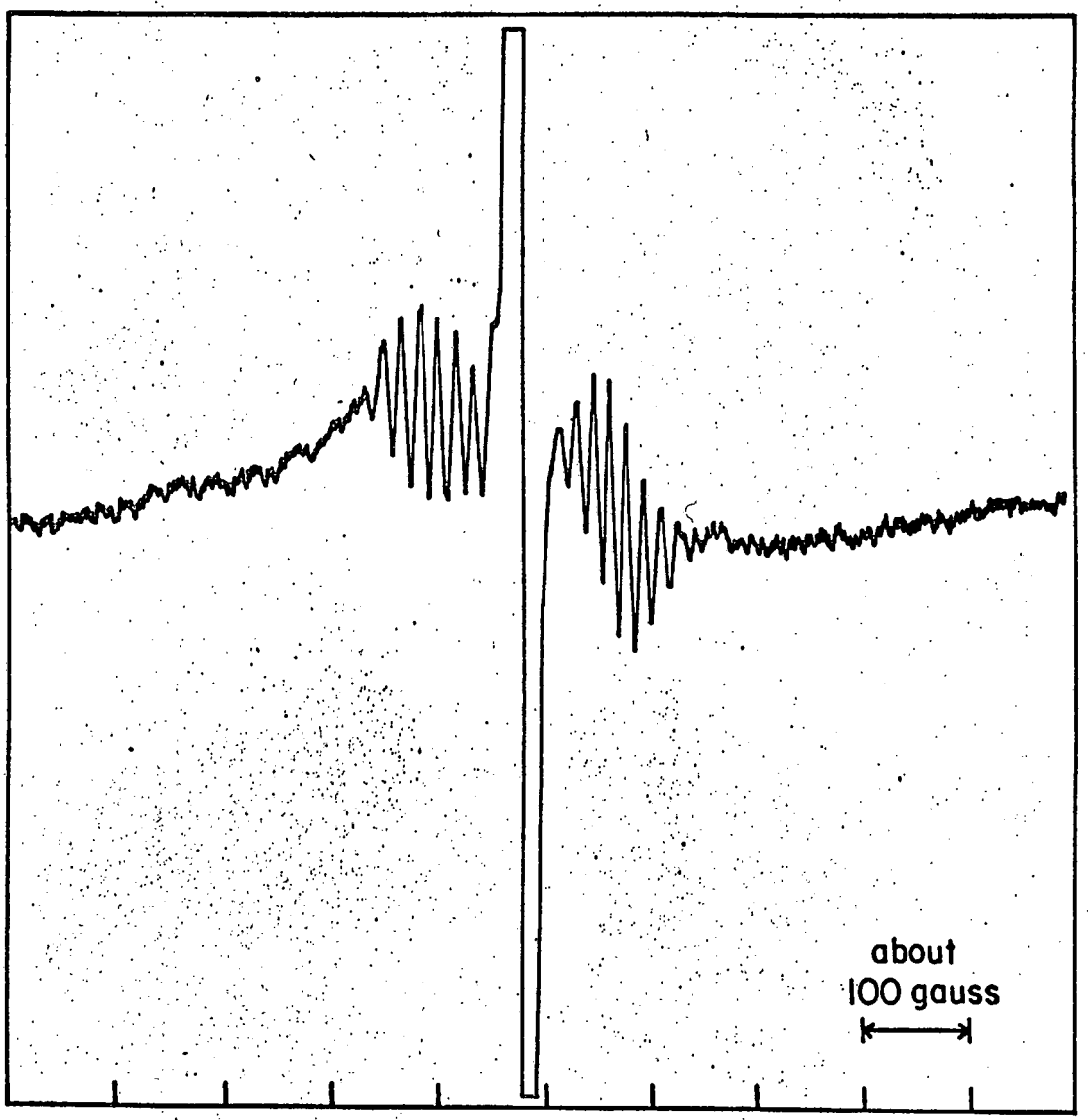

XBL677-4521

Figure VI-7. Phthalocyaninozinc(II), crystalline, sublimed. Temperature about 90°K; modulation 5 gauss (optimum for the weaker signal). The intense peak at g = 2.0 is referred to in the text as (I); the other lines may be due to a phthalocyanine free radical.

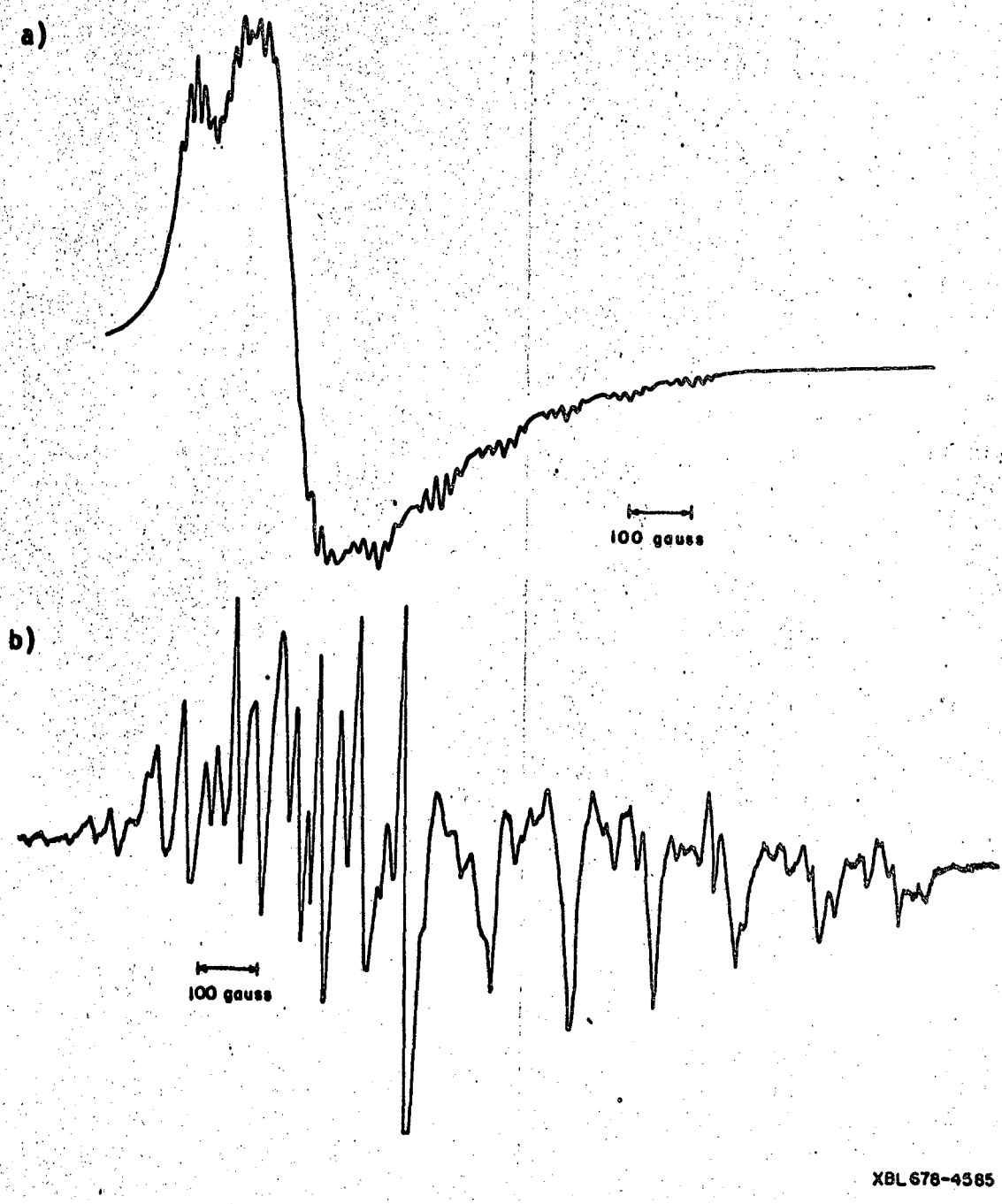

Figure VI-8. Phthalocyaninocobalt(II) paramagnetic resonance spectra at about 90°K.

a) Pyridine solution; modulation 3 gauss.

b) Tetrahydrofuran solution; modulation 10 gauss.

free radical (I) discussed above.

The phthalocyaninocobalt(II) spectrum in pyridine agrees with that reported by Assour (1965c). It is surprisingly like that of coenzyme B_{12} (reduced form) in water at 108°K: $g_{\perp} = 2.2$, $g_{\parallel} = 1.96$ (Hogenkamp et al., 1963). Normal coenzyme B_{12} contains cobalt(III); the EPR signal vanishes on oxidation. The oxidized form is diamagnetic.

Since the unpaired electron in $Co^{II}Pc$ is in the d_{z2} orbital (Assour, 1965c), its paramagnetic resonance is affected by the solvent. This is dramatically illustrated by the difference between spectra in pyridine and in tetrahydrofuran (Fig. VI-8a,b). The latter is so complicated that we have not even guessed at the usual parameters. Analysis of the spectrum in THF would be a real test for the computer program which will be described in Section VI-C. The signal disappears on oxidation by air.

Phthalocyaninonickel(II). This diamagnetic compound gave only the free radical signal (I). The sample was a pyridine solution.

Phthalocyaninocopper(II) in pyridine displayed a single broad, assymetric band, width about 120 gauss peak-to-peak in the derivative presentation, at approximately g = 2.04. Since an earlier report (Maksim and Phillips, 1964) erroneously included the signal of an internal DPPH standard as part of the CuPc spectrum, the correct spectrum is reproduced in Fig. VI-9. It is rather surprising that we observed no hyperfine structure from either the Cu (I = 3/2) or its surrounding nitrogens. The hyperfine structure is well-resolved when CuPc is dissolved in sulfuric acid or diluted in H_2Pc crystals; it has been thoroughly discussed by Harrison and Assour (1964).

Figure VI-9. EPR spectrum of phthalocyaninocopper, probably polymeric, in pyridine at about 90°K. Modulation 3 gauss.

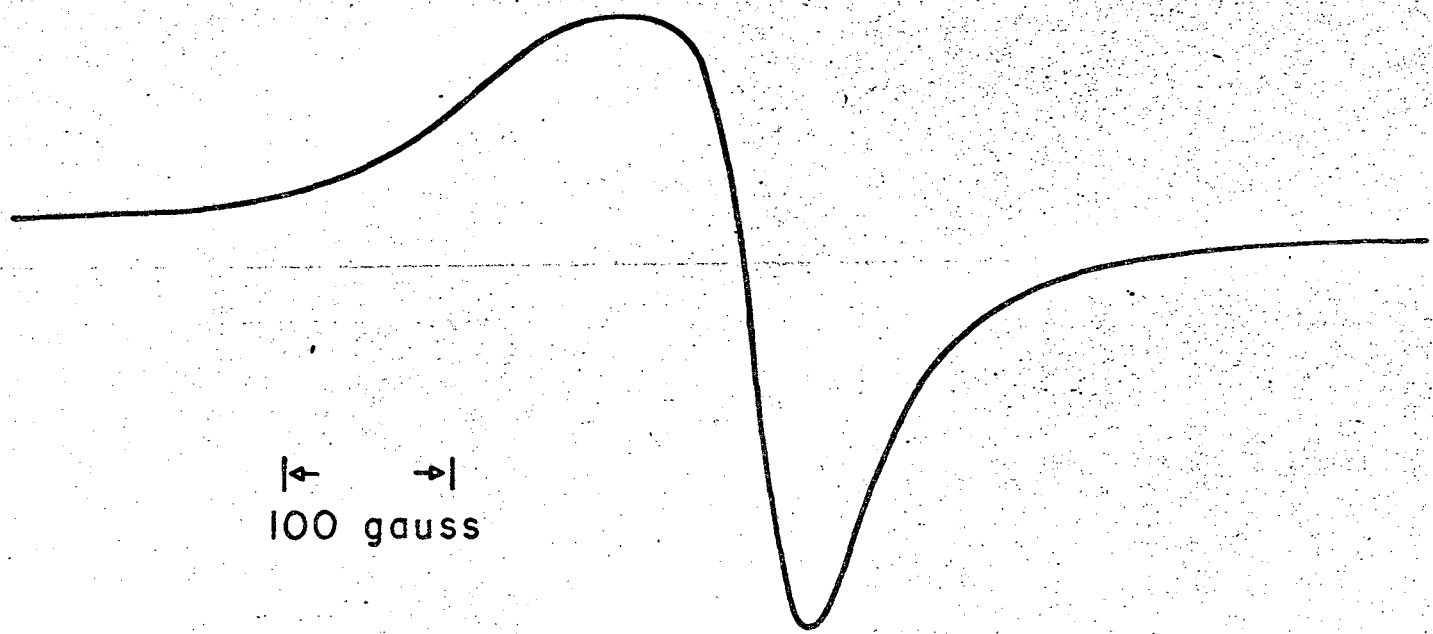

XBL 678-6124

The complex is only slightly soluble in pyridine; the lack of structure in the EPR spectrum indicates that the pyridine solution may contain polymers rather than monomers.

Phthalocyaninochloroiron(III), as a pyridine solution, exhibited two structured peaks near g = 2 (Fig. VI-10). Because ^{56}Fe has no nuclear moment, the structure is unexpected. The intensities are such that earlier (Maksim and Phillips, 1964) we assigned $g_{\parallel} = 2.2$, $g_{\perp} = 2.0$. However, the perpendicular value must be represented by a peak found at g roughly 4. The latter appeared more intense in a sample from which air had been removed.

Our results, though surprising, agree with the observation of Ingram and Bennett (1954) that iron phthalocyanine gives a broad absorption with g = 3.8 and 2.0, with weaker side lines.

Tetrasulfophthalocyaninoiron(III), in a 25% MeOH solution prepared in air, had an EPR spectrum rather similar to that of FePcCl, with the low-field peak at g = 4.3, and a main high-field peak at g = 2.0 plus some structure including a small peak at g about 2.2 (Fig. VI-11a). After 16 days the spectrum of this sample had not changed.

Powdered $Fe^{III}PTS$ (the anion was probably hydroxide) under nitrogen gave no EPR signal. When the same sample was dissolved (still under nitrogen atmosphere) in 25% methanol, a spectrum similar to that above appeared. The following day two new peaks had grown in at approximately g = 2.11 and 2.17. The only immediate effect of exposure to air was to decrease the intensity of the low-field peak; after ten days in air, however, both original peaks had diminished and the new ones predominated (Fig. VI-11b).

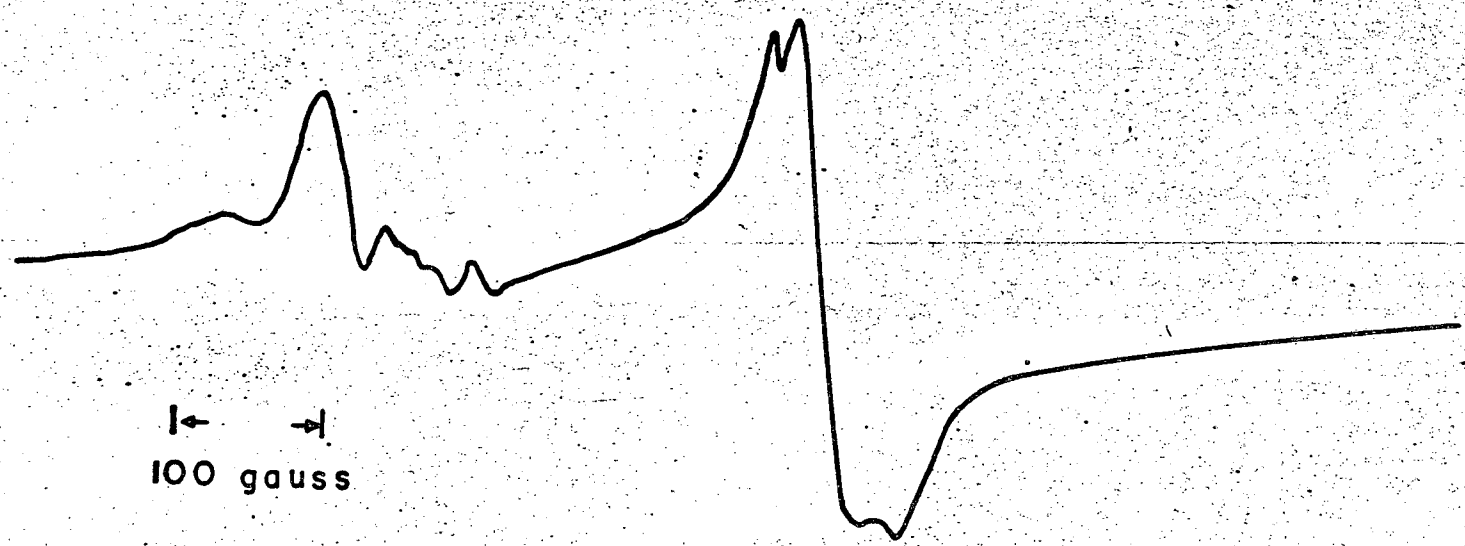

XBL 678-6123

Figure VI-10. Frozen pyridine solution of phthalocyaninochloroiron(III). EPR spectrum in the region approximately 2700-3700 gauss. Modulation 3 gauss.

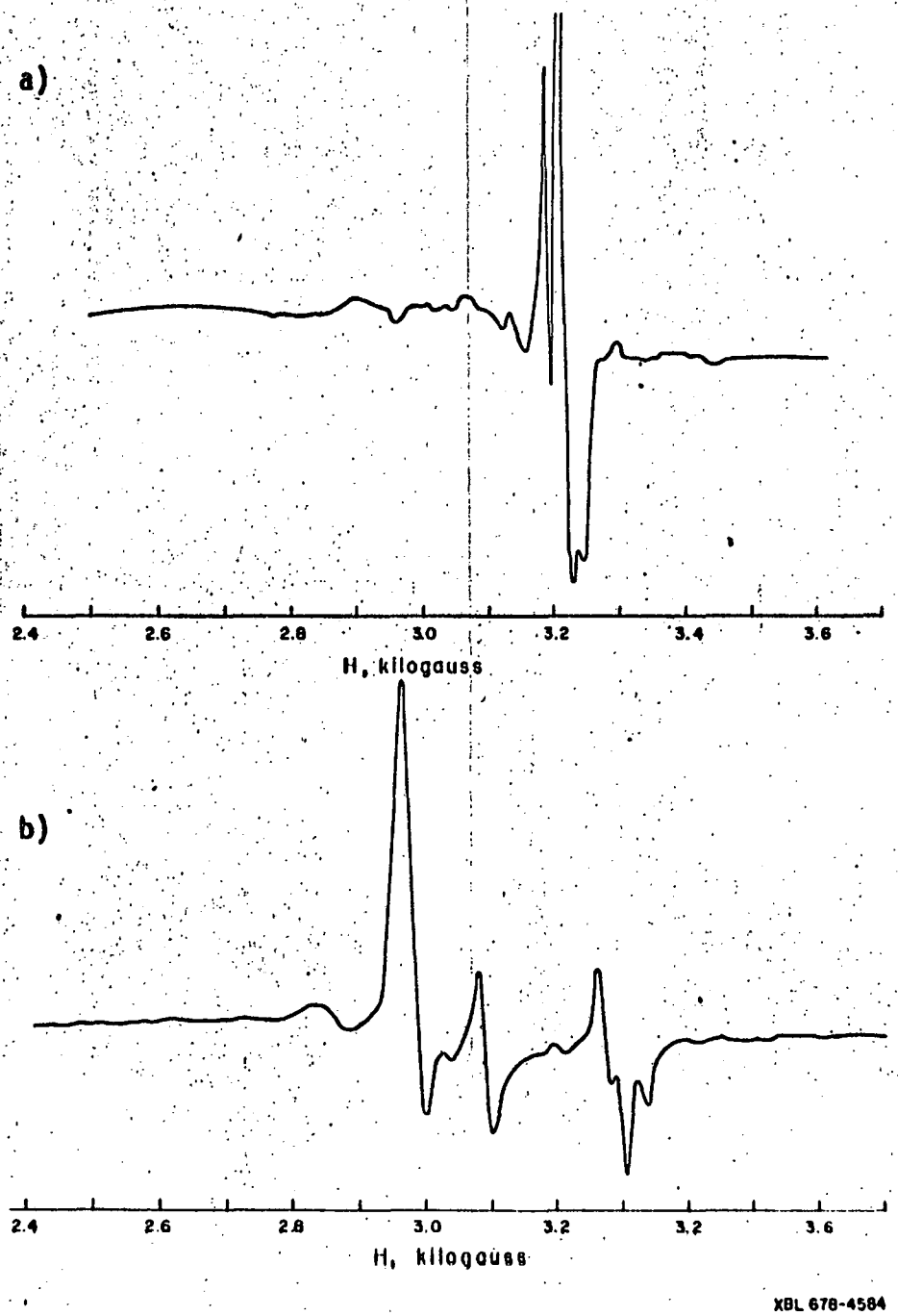

Figure VI-11. Paramagnetic resonance spectra of two different samples of tetrasulfophthalocyaninoiron(III), in water-methanol glass.

a) Sample I. When freshly prepared, Sample II showed a similar but less well-resolved spectrum. The peak at g = 4.3 is not shown.
b) Sample II, after long exposure to air. Modulation in each case, 10 gauss.

(Methyl pheophorbide-a)manganese. In the Mn^{II} or the Mn^{III} form, this compound yielded either no EPR signal or that of uncomplexed manganese^{2+} (Fig. VI-1b). However, in one sample which exhibited the Mn^{2+} signal, there was in addition a peak at g = 4.4; the solvent was $CDCl_3$-CD_3OD (70:30) for this sample. No evidence was seen* for a signal unambiguously due to Mn^{II}Pheo, nor for a free radical connected with Mn^{III}Pheo.

(Etioporphyrin I)manganese(III) in syrupy phosphoric acid showed a very weak Mn^{2+} signal, and an intense, broad signal at low field, with a minimum at 1670 gauss. Again, no free radical signal was seen. (For a discussion of the reasons the free radical signal was sought, see Section III-A.)

C. ANALYSIS OF DATA

The effective magnetic field seen by an electron in a molecule depends on the molecule's orientation with respect to the external magnetic field. Energies of the electron spin states, and hence that of the observed transition, are proportional to the effective field. Substances whose transitions are strongly orientation-dependent (anisotropic) have traditionally been studied in single crystals which can be positioned at will. In contrast, our investigations have been on glasses, in which the molecules are randomly oriented. The same information is present in either case, even though the EPR spectrum from a glass is an average over all possible

*As we mentioned at the beginning of this chapter, the paramagnetic resonance of manganese(II) is often broadened in high-spin complexes. Thus the lack of a signal attributable to Mn^{II}Pheo--which is probably high-spin (see Section III-A.3)--is not surprising.

molecular orientations,* and so may be more difficult and tedious to interpret. Experimentally, the easier method is often the glass.

Phthalocyanine can be thought of as a square surrounding the metal ion in the $\underline{x},\underline{y}$ plane (Fig. VI-12). The effective field should be the same for any direction within the $\underline{x},\underline{y}$ plane, while its value along the normal $\underline{z}$ may be far different. We speak of "perpendicular" and "parallel" transitions, referring to the angle between $\underline{z}'$ (external field H) and the molecular axis $\underline{z}$. Because $\underline{x}$ and $\underline{y}$ are equivalent, the intensity observed for perpendicular transitions is greater than that for parallel transitions. Thus in Fig. VI- 2 we can immediately see that the lower-field lines are associated with the perpendicular orientation.

The theory of paramagnetic resonance of transition metal ions has been discussed extensively (see, for example, Pake, 1962; Abragam and Pryce, 1951). It is convenient to analyze EPR spectra by a phenomenological spin Hamiltonian

$$\mathcal{H}(\text{spin}) = \beta \underset{\sim}{g}\cdot\underset{\sim}{S}\cdot\underset{\sim}{H} + \lambda \underset{\sim}{L}\cdot\underset{\sim}{S} + \underset{\sim}{A}\cdot\underset{\sim}{I}\cdot\underset{\sim}{S} \qquad (1)$$

$$= \beta(g_x\cdot S_x\cdot H_x + g_y\cdot S_y\cdot H_y + g_z\cdot S_z\cdot H_z) + D(S_z^2 - 1/3\ S(S+1)) + E(S_x^2 - S_y^2) + (A_x\cdot I_x\cdot S_x + A_y\cdot I_y\cdot S_y + A_z\cdot I_z\cdot S_z) \qquad (2)$$

Here the first term is related to the effect of the external magnetic field on the energy of an electron with spin "up" or "down"; in a 3210-gauss field, the $S = 1/2$ state of a free electron is raised and the $S = -1/2$ state is lowered by 0.15 cm^{-1}, so that the transition between them occurs at 0.3 cm^{-1}. The second term is the spin-

*Pure solvents seldom form glasses, and the solute may tend to crystallize during freezing. The extra hash in Fig. VI-2a is due to nonrandom orientation of the MnPc.

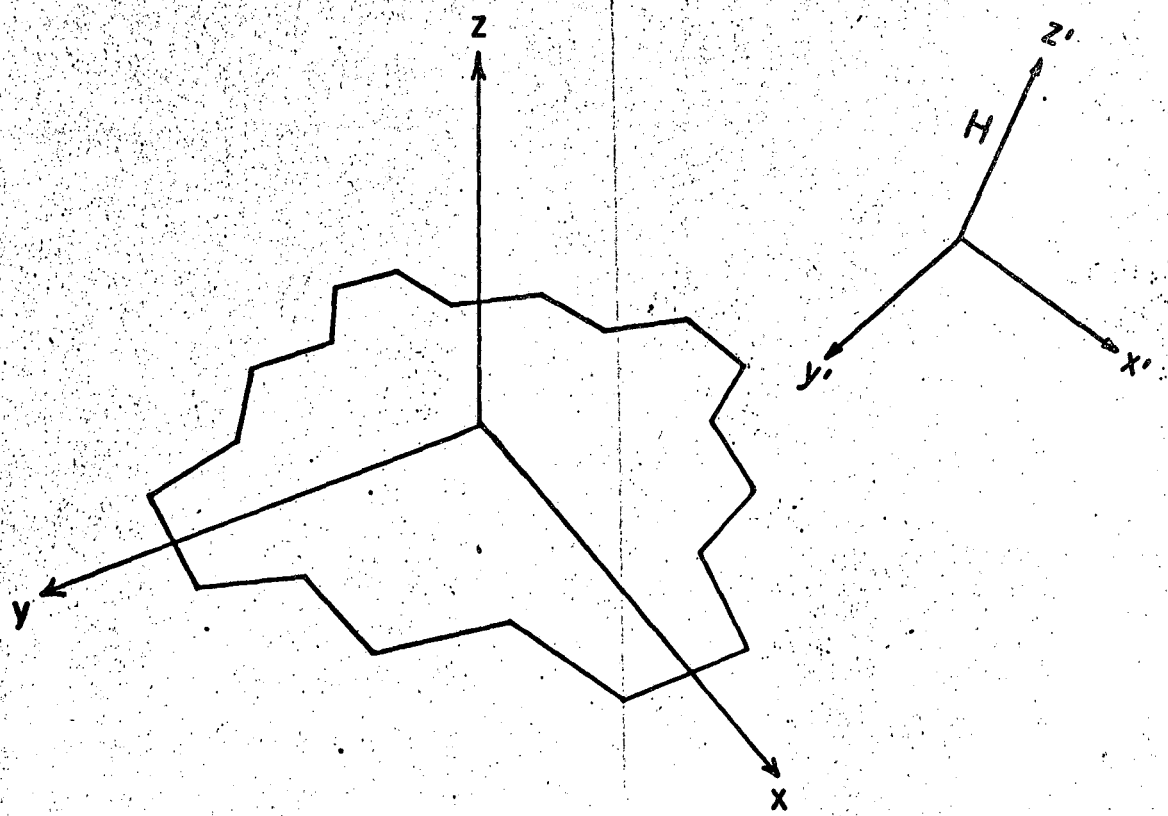

XBL 677-4517

Figure VI-12. Coordinate system for a metal phthalocyanine or porphyrin complex in an external magnetic field. x,y,z are the molecular coordinates; x',y',z' are fixed in the laboratory, with magnetic field H along z'.

orbit interaction--coupling between the spin and orbital angular momenta; in equation (2), it is expanded to second order in the parameters $\underline{D}$ and $\underline{E}$ used to describe crystal fields of lower than octahedral symmetry. $\underline{\lambda}$ is more or less constant for a given ion. For free Mn^{2+}, $\lambda = 347\ cm^{-1}$ (Griffith, 1961); in manganese(II) compounds, $\underline{D}$ is usually less than $0.04\ cm^{-1}$, and $\underline{E}$, less than $0.01\ cm^{-1}$ and often too small to be observed (Pake, 1962, p. 183-5).* The hyperfine splitting, or interaction between the electronic and nuclear spins, comprises the third term; for manganese(II), $|\underline{A}|$ is ordinarily near $0.009\ cm^{-1}$ and isotropic (Pake, op. cit.).** A similar term can be included to describe interaction of the electron spin with another nucleus: extrahyperfine splitting. Other effects, such as quadrupole coupling between nucleus and electrons, might be expected to contribute to the Hamiltonian. However, the observed phthalocyaninomanganese(II) spectra can be well fitted by equation (1), indicating either that further terms are smaller than the experimental resolution, about $4 \times 10^{-4}\ cm^{-1}$; or that transitions arising from them have very low intensity.

The paramagnetic resonance of $Mn^{II}Pc$ was analyzed by calculating a spectrum from the spin Hamiltonian, and comparing this with the observed spectrum. We assumed that $S = 1/2$ so that terms in D and E do not occur. Angular averaging over the first and third terms in equation (2) gives (Bleaney, 1951):

**Often the sign of A cannot be directly determined from experiments.

*Although the relative sizes of D and E depend on the coordinate system, usually coordinates are chosen so that D>>E.

$$h\nu = g\beta H_o + Km_I + \frac{A_\perp^2}{4g\beta H_o}\left(\frac{A_\parallel^2 + K^2}{K^2}\right)[I(I+1) - m_I^2]$$

$$+ \frac{1}{2g\beta H_o}\left(\frac{A_\parallel^2 - A_\perp^2}{K}\right)\frac{g_\parallel g_\perp}{g^2}\sin^2\theta\cos^2\theta\, m_I^2 \qquad (3)$$

where $g_\perp^2 = g_x^2\cos^2\phi + g_y^2\sin^2\phi$

$A_\perp^2 = \frac{1}{2}(A_x^2 + A_y^2)$

$K^2g^2 = A_\parallel^2 g_\parallel^2\cos^2\theta + A_\perp^2 g_\perp^2\sin^2\theta$

and $g^2 = g_\parallel^2\cos^2\theta + g_\perp^2\sin^2\theta$.

The last term in equation (3) is important only for strongly anisotropic A values, such as those found in the metal phthalocyanines, where it may become very large.

A computer program (Phillips, Ross and Blumberg, 1965) using equation (3) is included as an Appendix. The calculated values which best fit the data for $Mn^{II}Pc$ are:

$g_\parallel = 1.90$ $\qquad$ $A_\parallel = 151 \times 10^{-4}\ cm^{-1}$

$g_\perp = 2.16$ $\qquad$ $A_\perp = 25 \times 10^{-4}\ cm^{-1}$

D. DISCUSSION

Phthalocyaninomanganese(II). Since manganese(II) possesses a half-filled d shell, its electron distribution in the ground state is spherically symmetric: orbital angular momentum L = 0. The five unpaired electrons lead to a multiplicity of 2S + 1 = 6, hence the ground state is ^6S. To first order, L·S = 0, so that there should

be no spin-orbit coupling. In fact, the $\underline{D}$ value for Mn^{2+} in $(NH_4)_2Zn(SO_4)_2 \cdot 6H_2O$ is only 0.024 cm^{-1}, while that for Ni^{2+} in the same salt is -2.24 cm^{-1}. The electrons are supposed to be in pure $\underline{d}$ orbitals, which have nodes at the nucleus; thus coupling between electron spins and the ^{55}Mn nuclear spin of 5/2 should also be small. The famous 'anomalous' hyperfine splitting seen in the experimental EPR spectrum (Fig. VI-1) is explained qualitatively (if not quantitatively) by spin polarization of the $\underline{s}$ electrons by the unpaired $\underline{d}$ electrons. Note that the $\underline{g}$ and $\underline{A}$ tensors are very nearly isotropic and that $\underline{g}$ is close to the free-electron value--properties of almost all manganese(II) compounds for which they have been measured.

Instead of the characteristic isotropy, the EPR of $Mn^{II}Pc$ displays two separate groups of lines, each group having its own $\underline{g}$ and $\underline{A}$ values. Just as surprising, the spectrum agrees with one generated by equation (3) and shown in Fig. VI-2d, which includes only terms in $\underline{g}$ and $\underline{A}$. There is no need to include terms in D or E, though their effects are often observable in high-spin Mn^{2+}.

Obviously, the environment of the manganese is highly tetragonal; that is, the phthalocyanine plane is very different from the $\underline{z}$ direction. This we could surmise from molecular structure; but it is also clear from the magnetic anisotropy. However, a spin 5/2 ion in a strong tetragonal field should have $g_\perp = 6$ (Griffith, 1957); a spin 3/2 ion should have $g_\perp = 4$, both with $g_\parallel$ about 2. Either would lead to an EPR spectrum entirely different from the one seen.*

---

*The EPR signal with $g_\perp = 4.3$, $g_\parallel = 1.9$, which is occasionally seen (Fig. VI-3, VI-4) may well be that of a spin 3/2 species. Lack of hyperfine structure indicates, however, that manganese is not responsible. Possibly iron(III) is present as a contaminant.

Another factor to consider is the magnetic susceptibility. This has never been measured for phthalocyaninomanganese(II) in pyridine solution, but Weber and Busch (1965) have reported that tetrasulfophthalocyaninomanganese(II) in water has a single unpaired electron, μ_{eff} = 1.94 B.M. With the more strongly-bonding axial ligand pyridine, spin-pairing is also likely.

Thus the evidence points to low-spin manganese(II), which only the most powerful ligands, for instance cyanide, can produce. Solid $Mn^{II}Pc$ apparently has three unpaired electrons (Lever, 1965a), so that perhaps axial ligands in addition to the phthalocyanine are required for full spin-pairing. Theoretical considerations (Gouterman, private communication) suggest that structural changes may be involved, with the manganese in the phthalocyanine plane in one spin state, but not the other.

Where is the unpaired electron of $Mn^{II}Pc$? The tetragonal ligand field imposed by phthalocyanine will split the manganese d orbitals so that only the d_{xz}, d_{yz} orbitals remain degenerate. The $d_{x^2-y^2}$ orbital, with its densest regions close to the bonding pyrrole nitrogens, is expected to be highest in energy. Ordering of the other levels cannot be determined a priori; it may vary with the axial ligands, and depends on such effects as pi-bonding between metal and ligands. The bridge nitrogens (see Fig. I-3) lie along the lobes of the d_{xy} orbital, at 3.38 Å; the pyridines are 2.15 Å from the manganese, along the d_{z^2} orbital. Only d_{xz}, d_{yz} are of the proper symmetry (E_g) to participate in pi-bonding with certain phthalocyanine molecular orbitals.

Either of two orderings of energy levels seems reasonable:

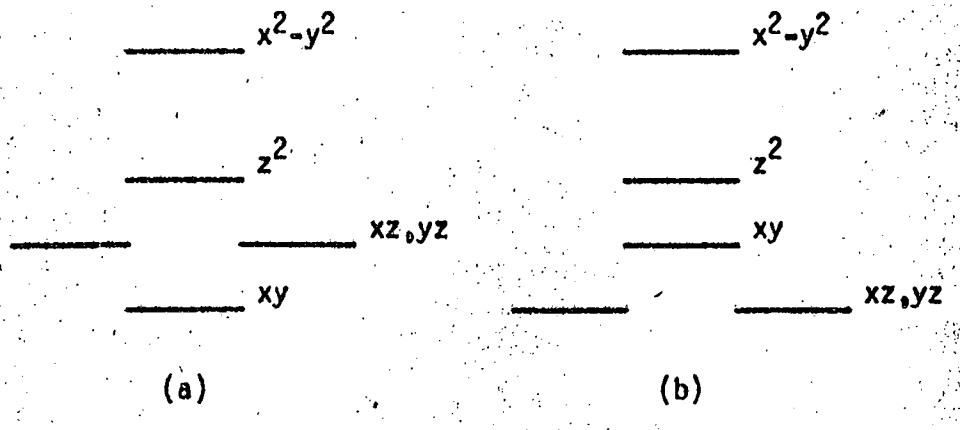

Griffith has proposed (1961) that scheme (a) holds for all porphyrin and phthalocyanine complexes. The relative energy of d_{z^2} will depend on the axial ligands. Griffith adds a note of caution: "...it is almost impossible to produce a logically compelling interpretation [of resonance data on these compounds] because there are so many unknown parameters in the theory."

If the levels in MnPc follow scheme (a), there must be either three or one electrons in d_{xz}, d_{yz} --the latter if d_{z^2} falls below d_{xz}, d_{yz} in energy. The spatial degeneracy leads to $\underline{g}$ values near $g_{\parallel} = 4$, $g_{\perp} = 0$. Thus our experimental results rule out this scheme.

If d_{xz}, d_{yz} lie lowest, the ordering of d_{xy} and d_{z^2} is again a question. A single electron in either of these orbitals will have $g_{\parallel}$ and $g_{\perp}$ near 2, as observed. Phthalocyaninocobalt(II), with its unpaired electron located in d_{z^2}, exhibits nicely resolved extra-hyperfine interaction with solvent nitrogens (Fig. VI-8a). Its $\underline{g}$ and $\underline{A}$ values are quite sensitive to solvent: in pyridine $g_{\perp} = 2.268$, in β-picoline, 2.326--a shift of about 75 gauss. $A_{\perp}$ is usually greater than $A_{\parallel}$.

The EPR spectra of vanadyl porphyrins, on the other hand, are rather indifferent to solvent or diluent; $A_{\parallel}$ is larger than $A_{\perp}$; and extrahyperfine interactions with the surrounding nitrogen nuclei are at the most 2.6×10^{-4} cm^{-1}, below our limits of resolution (Kivelson and Lee, 1964). The low-spin $Mn(CN)_5NO^{2-}$ has $A_{\parallel} = 151$ cm^{-1}; $A_{\perp} = 36.2$ cm^{-1}, which are close to the values found for MnPc, although this compound also shows quadrupole effects of ^{55}Mn and extrahyperfine splitting due to the nitrogen on the strongly electron-attracting NO^{+}. In both VOPc and $Mn(CN)_5NO^{2-}$ the unpaired electron is assigned to d_{xy}; according to Fortman and Hayer (1965) scheme (b) applies to the pentacyanonitrosyl complexes.

We can test the ordering of orbitals by calculating the energy differences between them, as well as two other parameters: K, the Fermi contact term, depends on the electron density at the nucleus; P is a dipole coupling term, $P = 2\beta_0\beta_N\gamma \langle r^{-3} \rangle$. β_0 and β_N are the Bohr and nuclear magnetons respectively, γ is the magnetic moment of the nucleus--here ^{55}Mn--and $\langle r^{-3} \rangle$ is taken over the occupied orbital. For Mn^{2+}, K is experimentally near 0.6 (Abragam and Pryce, 1951); Fortman and Hayes find for $Mn(CN)_5NO^{2+}$ that P is 0.0126 cm^{-1}.

Following Assour and co-workers (1965a,b) we use for the unpaired electron in the d_{z2} level:

$$g_{\parallel} = g_0 - 3\left(\frac{\lambda}{\Delta}\right)^2$$

$$g_{\perp} = g_0 + 6\left(\frac{\lambda}{\Delta}\right) - 6\left(\frac{\lambda}{\Delta}\right)^2$$

$$A_{\parallel} = P\left(-\frac{4}{7} - K - \frac{18}{7}\frac{\lambda}{\Delta}\right)$$

$$A_{\perp} = P\left(-\frac{2}{7} - K + \frac{51}{7}\frac{\lambda}{\Delta}\right)$$

where Δ is the energy difference, $E(z^2) - E(xz,yz)$; $g_o = 2.0023$; and λ is the spin-orbit coupling of Mn^{2+}, for which the free-ion value is $-350\ cm^{-1}$.

For a singly occupied d_{xy} orbital,

$$g_{\parallel} = g_o\ (1 - [4\lambda\alpha^2\ \beta^2/\Delta_{\parallel}])$$

$$g_{\perp} = g_o\ (1 - [\lambda\delta^2\ \beta^2/\Delta_{\perp}])$$

$$A_{\parallel} = P\ (-\tfrac{4}{7}\beta^2 - K + [g_{\parallel} - g_o] + \tfrac{3}{7}[g_{\perp} - g_o])$$

$$A_{\perp} = P\ (\tfrac{2}{7}\beta^2 - K + \tfrac{11}{14}[g_{\perp} - g_o])$$

where $\Delta_{\parallel} = E(xy) - E(x^2-y^2)$; $\Delta_{\perp}$ d_{xy} and $d_{xz,yz}$; and α, β, δ are the bonding coefficients of $d_{x^2-y^2}$, respectively. A bonding coefficient of 1 signifies that the electron is isolated in the metal d orbital. Assour and co-workers estimate $\alpha = 0.85$, and $\beta = 1$ in the phthalocyanine complexes. δ may be considerably less than 1, showing delocalization of d_{xz}, d_{yz} into the pi system.

From the values observed for $Mn^{II}Pc$ in pyridine-toluene (Table VI-1), and recalling that the signs of $A_{\parallel}$ and $A_{\perp}$ are unknown, we obtain for the unpaired electron in d_{z^2} the result that $\Delta = 5840\ cm^{-1}$, that is, d_{z^2} will as required lie above $d_{xz,yz}$. However,

$P = \pm .0472\ cm^{-1}$, $K = .097$ for $A_{\parallel}$ and $A_{\perp}$ of the same sign;

$P = \pm .066\ cm^{-1}$, $K = .19$ for $A_{\parallel}$ and $A_{\perp}$ of different signs.

The values of P and K seem unreasonable.

If the electron is in d_{xy}, then $\Delta_{\parallel} = -19{,}800$ and $\Delta_{\perp} \leq 4430\ cm^{-1}$ (the value of $\Delta_{\perp}$ will be reduced if $\delta<1$).

$P = \mp .0128\ cm^{-1}$, $K = .58$ for $A_{\parallel}$ and $A_{\perp}$ both $\begin{cases} >0 \\ <0 \end{cases}$

$P = \mp .0173\ cm^{-1}$, $K = .27$ for $A_{\parallel}$ and $A_{\perp}$ of opposite signs. Not only do we calculate that as anticipated, d_{xz}, d_{yz} lie lower in energy than d_{xy}, while $d_{x^2-y^2}$ lies higher, but for $A_{\parallel}$ and $A_{\perp}$ of the same sign, the values of P and K are just those found in other manganese(II) compounds.

Thus from the lack of extrahyperfine splitting, the values of $A_{\parallel}$ and $A_{\perp}$ and their insensitivity to solvent, and the sizes of derived parameters, we conclude that in $Mn^{II}Pc$ the occupation and approximate* energies of the manganese d orbitals are:

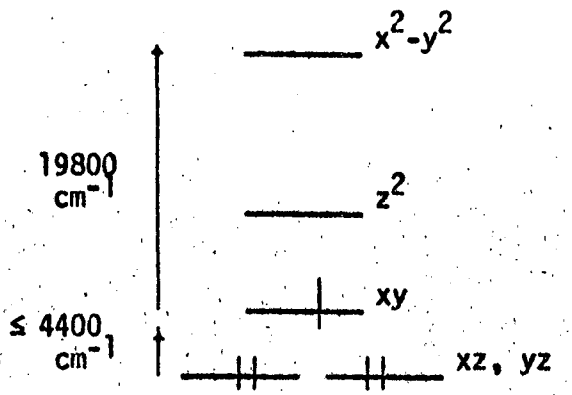

We must caution against assuming that the ordering found in phthalocyaninomanganese holds also for the manganese porphins and chlorins. For these, a simplified theoretical model predicts different ordering, as discussed in Section III-A.3.

*Only upper limits can be found for the energy differences both because of the uncertainty in δ, and because λ is likely to be smaller than its free-ion value which was used in the calculations.

VII. SUMMARY

We have explored some aspects of the redox and coordination properties and the electronic structure of manganese porphyrin complexes. The techniques used have ranged from a simple quartz spring balance, through visible and infrared spectrophotometry, to electron paramagnetic resonance.

The manganese ion within the complex can, under the proper conditions, be oxidized or reduced either by chemical agents or by exposure to light, without destruction of the ligand. In some compounds the manganese has been observed in its 2+, 3+, and 4+ oxidation states; the most stable state is generally 3+ for these complexes. The methyl pheophorbide-a chelate was studied as a possible model for photosynthetic oxygen production, but no formation of free oxygen was seen.

Because of the geometry of the porphyrins, their metal chelates must be nearly square planar. The tendency of manganese ions to from octahedral or near-octahedral complexes is shown by its ready coordination of additional ligands in the axial positions. This further coordination has been examined mainly by measuring weight changes of the solid manganese porphyrin complexes on exposure to ligands in the gas phase. The stoichiometry agrees with proposed oxidation states and structures of the various species.

Paramagnetic resonance spectra have been observed for several phthalocyanine derivatives, of which the most interesting is $Mn^{II}Pc$. Data on this compound has been analyzed by the aid of

a specially developed computer program, and has enabled us to determine the spin state and probable electronic structure of the manganese.

Some insight has been gained as well into the electronic structure of the manganese porphin and chlorin complexes. The similarity of the infrared spectrum of etioporphyrin I manganese(III) to those of other etioporphyrin I derivatives, and the absence of a free radical EPR signal in Mn^{III}Pheo or Mn^{III}Etp, are in accord with theoretical calculations which indicate that this species is not a stable porphyrin radical. The "resonance" explanation advanced by Gouterman to explain the anomalous electronic spectra of these compounds might have interesting implications for their redox behavior. The area deserves further study.

REFERENCES

Abragam, A., and M.H.L. Pryce (1951), Proc. Roy. Soc. (London) A205, 135;

Assour, J. M., J. Goldmacher, and S. E. Harrison (1965a), J. Chem. Phys. 43, 159.

Assour, J. M. (1965b), J. Chem. Phys. 43, 2477.

Assour, J. M. (1965c), J. Am. Chem. Soc. 87, 4701; J. M. Assour and W. K. Kahn, Ibid. 87, 207.

Bellamy, L. J. (1958), "The Infra-red Spectra of Complex Molecules", Second Edition (Wiley, New York).

Bersohn, M., and J. Baird (1966), "An Introduction to Electron Paramagnetic Resonance", (W. A. Benjamin Co., New York).

Bleaney, G. (1951), Phil. Mag. 42, 441.

Borg, D. C., and G. C. Cotzias (1958), Nature 182, 1677.

Calvin, M. (1965), Rev. Pure and Appl. Chem. 15, 1.

Czanderna, A. W. (1961), in M. J. Katz (op. cit.), p. 129 ff.

Elvidge, J. A., and A.P.B. Lever (1959), Proc. Chem. Soc. (London), 195.

Engelsma, G., A. Yamamoto, E. Markham, and M. Calvin (1962), J. Phys. Chem. 66, 2517.

Falk, J. E. (1964), "Porphyrins and Metalloporphyrins", (Elsevier, New York, N. Y.).

Fortman, J. J., and R. G. Hayes (1965), J. Chem. Phys. 43, 15.

Glikman, T. S., M. E. Podlinyaeva, and B. Ya. Dain (1959), J. Gen. Chem. USSR 29, 1785; Consultants Bureau translation, p. 1758.

Gouterman, M. (1961), J. Mol. Spec. 6, 138.

Griffith, J. S. (1957), Proc. Roy. Soc. (London) A235, 23.

Griffith, J. S. (1961), "Theory of the Transition Metal Ions" (Cambridge University Press).

Hamor, T. A., W. S. Caughey, and J. L. Hoard (1965), J. Am. Chem. Soc. 87, 2305.

Harrison, S. E., and J. M. Assour (1964), J. Chem. Phys. 40, 365.

Hoard, J. L., M. J. Hamor, T. A. Hamor, and W. S. Caughey (1965), J. Am. Chem. Soc. 87, 2312.

Hogenkamp, H.P.C., H. A. Barker, and H. S. Mason (1963), Arch. Biochem. Biophys. 100, 353.

Honig, J. M. (1961), in M. J. Katz (op. cit.), p. 55 ff.

Ingram, D.J.E., and J. E. Bennett, (1954), J. Chem. Phys. 22, 1136.

Katz, M. J. (1961), ed., "Vacuum Microbalance Techniques", Vol. 1 (Plenum Press, Inc., New York).

Kivelson, D., and S. K. Lee (1964), J. Chem. Phys. 41, 1896.

Kobayashi, H., Y. Torii, and N. Fukada (1960), Nippon Kagaku Zasshi 81, 694; UCRL translation 1318. (Several other papers by Fukada's group are also available as UCRL translations.)

Lever, A.B.P. (1965a), The Phthalocyanines, in "Advances in Inorganic Chemistry and Radiochemistry", Vol. 7, Emeleus and Sharpe, editors (Academic Press, New York), pp. 27-114.

Loach, P. A., and M. Calvin (1963), Biochem. 2, 361.

Loach, P. A., and M. Calvin (1964a), Biochem. Biophys. Acta 79, 379.

Loach, P. A., and M. Calvin (1964b), Nature 202, 343.

Maksim, A., and L. K. Phillips (1964), LCBQ-4, p. 78.

Martell, A. E., and M. Calvin (1952), "Chemistry of the Metal Chelate Compounds" (Prentice-Hall, Inc., Englewood Cliffs, N. J.).

Mason, S. F. (1958), J. Chem. Soc. (London), 976.

Miller, J. R., and G. D. Dorough (1952), J. Am. Chem. Soc. 74, 3977.

Nakamoto, K. (1963), "Infrared Spectra of Inorganic and Coordination Compounds" (John Wiley & Sons, New York).

Oster, G., J. S. Bellin, and S. B. Broyde (1964), J. Am. Chem. Soc. 86, 1313.

Pake, G. E. (1962), "Paramagnetic Resonance" (W. A. Benjamin, New York).

Park, R. B., and J. Biggins (1964), Science 144, 1009.

Phillips, L. K., R. T. Ross, and W. E. Blumberg (1965), LCBQ-5, 75.

Robertson, J. M. (1936), J. Chem. Soc. (London), 1195.

Ross, R. T. (1965), J. Chem. Phys. 42, 3919.

Ross, R. T. (1966), Ph.D. Thesis, Department of Chemistry, University of California, Berkeley.

Sidorov, A. N., and A. N. Terenin (1961), Optics and Spectry. 11, 175.

Tanner, H. A., T. E. Brown, C. Eyster, and R. W. Treharne (1960), Ohio J. Sci. 60, 231.

Thomas, D. W., and A. E. Martell (1959), J. Am. Chem. Soc. 81, 5111.

Vogt, L. H., Jr., A. Zalkin, and D. H. Templeton (1966), Science 151, 569.

Vogt, L. H., Jr., A. Zalkin, and D. H. Templeton (1967), Inorg. Chem. 6, 1725.

Waters, P. M., ed. (1965), "Vacuum Microbalance Techniques," Vol. 4 (Plenum Press, New York).

Webb, L. E., and E. B. Fleischer (1965), J. Chem. Phys. 43, 3100.

Weber, J. H., and D. H. Busch (1965), Inong. Chem. 4, 469.

Yamamoto, A., L. K. Phillips, and M. Calvin, to be published.

Zeiger, G., and H. T. Witt (1961), Z. phys. Chem. (Frankfurt) (N.F.) 28, 286.

Zerner, M., and M. Gouterman (1966), Theoret. chim. Acta (Berl.) 4, 44.

Zerner, M., M. Gouterman, and H. Kobayashi (1966), Ibid. 6, 363.

APPENDIX

A COMPUTER PROGRAM FOR SIMULATING GLASS OR POWDER EPR SPECTRA

Electron paramagnetic resonance spectra are generally obtained in derivative form. For a transition metal ion with nuclear spin, in a polycrystalline or glassy sample, interpretation of the spectra by inspection may become impossible. Overlapping absorption bands give unusual relative intensities of derivative bands, and even spurious peaks. Second-order effects may cause variable hyperfine splittings, particularly if the crystal field is strongly anisotropic. The computer program described here (Phillips, Ross, and Blumberg, 1965) was written to aid in analyzing such complicated spectra.

This program is particularly applicable to spin 1/2 transition metal ions in an axial or nearly axial environment, and with any value of nuclear spin. The spectrum is averaged over all angles, corresponding to powdered or glassy materials; the angular integral is approximated by a finite sum. In the axial case (x and y axes equivalent) 500 values of θ are taken in the averaging. Originally a 90-point average was used, but the infinite series converges rather slowly so that small spurious peaks appear when only 90 values of θ are included. For nonequivalent x and y axes, 300 values of θ, ϕ are taken.

The variable parameters are g_x, g_y, g_z; the components of the hyperfine interaction tensor A_x, A_y, A_z; extrahyperfine splittings and amplitudes; and line width. In practice these parameters are estimated from the experimental spectrum, then varied by the programmer to give

the best output "spectrum". Absorption bands are assumed to be gaussian. The primary output is in derivative form, but an option is provided for absorption curves as well. Output is always in the form of a graph. A plot on the regular output paper is provided for users who are impatient and who expect slowly-varying, uncomplicated spectra; others may choose an elegant Cal-Comp plot.

The phenomenological Hamiltonian, by which transition energies are found, is defined in equation (3), Chapter VI. It imposes several restrictions: total electronic spin is limited to 1/2. Nuclear quadrupole interaction is not considered, nor is interaction between two paramagnetic centers.

The program was written in Fortran IV for the IBM 7094 computer at the Lawrence Radiation Laboratory, University of California, Berkeley.

The program MAGRES consists of the main deck ESR and three subroutines: GDPLOT, QKPLOT, and CONST.

QKPLOT compresses field and amplitude into a 100 x 50 grid, with field running across the page. Amplitude is normalized. CONST defines the graph symbols and must be included with QKPLOT. CONST is written in MAP language rather than Fortran. It should be fairly easy to substitute for these subprograms a vertical plot (H running down one page and onto the next) without touching the main deck. However, the user should remember the label and normalization contained in QKPLOT, as well as various COMMON variables which must be included. I would like to know about any improvements the reader may make in QKPLOT, since it is not very useful in its present form.

GDPLOT normalizes spectral intensity and produces a titled Cal-Comp graph and printed label. Under option IEXPT, data points are

normalized and plotted on the same graph.

The following data cards are needed, in the order listed:

1. TITLE--72 characters allowed.
2. HRANGE, HMIN, HFINE, IEXPT, IQK, IGD, IABSOR, INUCL, ISHFS (Format 2F6.0, F7.1, I5, 5I6).
3. JSHFS(I), I = 1,24 (Format 24 I3). This card should be present only if ISHFS is nonzero.
4. NEXPT, HINC, (FMT(I), I = 1,9) (Format I6, F6.2, 6X, 9A6). This card is included only if IEXPT is nonzero.
5. A set of cards containing experimental data: NEXPT data points taken at magnetic field increments HINC. Data is punched in format FMT.
6. GZ, GX, GY, AZ, AX, AY, WIDTH, FRQ, ASHFS (Format 6 F12.4; 2 cards).

Parameters beginning with I denote program options; when the option is used the parameter is nonzero; otherwise it is zero.

Parameter	Option
IEXPT	Experimental points will be plotted on same scale as calculated spectrum. This option requires cards (4), (5).
IQK	A crude derivative plot will be executed by the printer. IQK must be <10,000.
IGD	A Cal-Comp plot will be provided (spectrum in derivative form). If desired, both IGD and IQK may be chosen.
IABSOR	An absorption spectrum will be provided, either "good" or "quick" as chosen.
INUCL	Nuclear spin. INUCL should be the actual nuclear spin, in units of 1/2. For instance, given a nucleus of spin 5/2, INUCL = 5. This is the only option whose value has a meaning.

ISHFS — Extrahyperfine interaction will be included in the calculation. Choice of this option requires card (3), which gives the relative amplitudes of the extrahyperfine lines. ASHFS must be included on card (6): it is the isotropic SHF splitting.

The meanings of the remaining parameters are as follows:

HRANGE is the range of magnetic field examined, with minimum field HMIN. The computation increment is HFINE. If a transition falls outside the permitted field range, an overflow message is printed.

JSHFS(I) are the relative amplitudes of extrahyperfine peaks. For example, interaction with two nitrogens (each $I = 1$, $I_{total} = 2$) requires the JSHFS vector 1, 4, 6, 4, 1. Up to $I_{total} = 11$ can be handled.

GZ, GX, GY; AZ, AX, AY, ASHFS are the spectroscopic and hyperfine splittings estimated from experiment. The A parameters are in megacycles.

WIDTH is linewidth, in gauss. FRQ is the measured microwave frequency of the resonance, in megacycles/sec.

Cards (6) ONLY may be repeated as many times as wished, so that the effect of varying g and A parameters and width can be studied. A new computation and plot will be done for each card set (6) included: two cards per set. Although the plot itself is allowed only one title per run, a numbered label is printed for each Cal-Comp graph.

Figure VI-2d, drawn by Cal-Comp, has the following parameters:

GZ = 1.9000	AZ = 452.0	FRQ = 9050.0	HMIN = 2700
GX = 2.1610	AX = 76.0	WIDTH = 8.0	HRANGE = 1500
GY = 2.1610	AY = 76.0		HFINE = 2.0
	ASHFS = 0.		

```
C  POLYCRYSTALLINE ESR FOR SPIN 1/2
C
      DIMENSION EXDATA(1050), EXGAUS(1050), DISTR(1000), ABSORP(1000),
     1 BROAD(200), DERIV(1000), GAUSS(1000), TITLE(12), FMT(9),JSHFS(24)
      COMMON /CCPOOL/ XMIN,XMAX,YMIN,YMAX,CCXMIN,CCXMAX,CCYMIN,CCYMAX
      COMMON TITLE, FRQ, WIDTH, GZ, GX, GY, AZ, AX, AY, ASHFS, HRANGE,
     1 HMIN, NSLOT, IEXPT, NEXPT
      READ (2,1001) (TITLE(I),I=1,12)
 1001 FORMAT (12A6)
      READ (2,1000) HRANGE, HMIN, HFINE, IEXPT, IQK, IGD, IABSOR,
     1 INUCL, ISHFS
 1000 FORMAT (2F6.0,F7.1,I5,5I6)
C  THE DECIMAL POINTS OF H PARAMETERS ARE IN 6,12,18. THE I PARAMETERS
C  ARE IN 24,30,36,42,48,54.
C  HRANGE IS RANGE OF FIELD FROM HMIN UP. HFINE IS THE COMPUTATION IN-
C  CREMENT. THE I PARAMETERS ARE NON ZERO IF THESE OPTIONS ARE TO BE
C  USED. INUCL IS IN UNITS OF SPIN 1/2.
      IF(ISHFS) 6, 5, 6
 6    READ (2,1004) (JSHFS(I),I=1,24)
 1004 FORMAT (24I3)
C  THE JSHFS ARE THE SUPERHYPERFINE LINE AMPLITUDES.
C  SHFS AMPLITUDES END IN 3,6,9, ETC.
 5    CONTINUE
      IF(IEXPT) 1, 10, 1
 1    READ (2,1002) NEXPT, HINC, (FMT(I),I=1,9)
 1002 FORMAT (I6, F6.2, 6X, 9A6)
C  NEXPT IS NUMBER OF POINTS TO BE READ ENDING IN 6. HINC IS THE
C  INCREMENT WITH DECIMAL IN 10. FMT BEGINS IN 19.
      READ (2,FMT) (EXDATA(I),I=1,NEXPT)
      DO 2 I=1,NEXPT
      FI = I
      EXGAUS(I) = HMIN + HINC*FI
 2    CONTINUE
C  ECHO CHECK
      WRITE (3,1005) (I,EXGAUS(I),EXDATA(I), I = 1,NEXPT)
 1005 FORMAT (1H ,2(3X,1HI,4X,6HEXGAUS,5X,6HEXDATA,13X)/(1H ,2(I6,F10.1,
     1 F12.5,10X)))
      IF(IQK) 3, 4, 3
 3    CALL QKPLOT (EXGAUS, EXDATA)
 4    CONTINUE
C  NOW PROCEED TO HAMILTONIAN.
 10   READ (2,1003) GZ, GX, GY, AZ, AX, AY, WIDTH, FRQ, ASHFS,
 1003 FORMAT (6F12.4)
C  THESE HAVE DECIMAL POINTS IN 6,18,30,42,54,66 AND 6,18,30 ON NEXT CD.
C  A PARAMETERS AND FRQ ARE IN MEGACYCLES. WIDTH IS IN GAUSS.
      NSLOT = HRANGE/HFINE
C  HRANGE/HFINE MUST BE LESS THAN 1001.
      IF (NSLOT - 1000) 9, 9, 68
 9    IHYP = INUCL + 1
      DO 41 M=1,1000
      DISTR(M) = 0.
 41   DERIV(M) = 0.
      ZMAX = IHYP
      DO 11 M=1,IHYP
      FM = M
      ZCOMP = (ZMAX - 1.)/2. - FM + 1.
 101  IF (GX-GY) 13, 14, 13
 14   IF (AX-AY) 13, 15, 13
 15   NPHI = 1
      NTHETA = 600
      ANGINC = 0.15
```

```
      THETA = 0.075
      GO TO 16
 13   NPHI = 20
      NTHETA = 15
      ANGINC = 0.298
      THETA = 0.3
 16   CONTINUE
      RTHETA = THETA*0.0174533
C   THETA IS THE INCLINATION ANGLE IN DEGREES.
      DO 12 I=1,NTHETA
      DO 17 L=1,NPHI
      FL = L
      PHI = 9.*ABS(FL-11.)
      RPHI = PHI*0.0174533
C   PHI IS THE AZIMUTHAL ANGLE IN DEGREES.
      STHETA = SIN(RTHETA)
      CTHETA = COS(RTHETA)
      GZC = GZ*CTHETA
      GXC = GX*STHETA*COS(RPHI)
      GYC = GY*STHETA*SIN(RPHI)
      GEFF = SQRT(GZC*GZC + GXC*GXC + GYC*GYC)
      IF(INUCL) 200, 201, 200
 201  CONTINUE
      FIELD = FRQ/1.4/GEFF
      GO TO 202
 200  CONTINUE
C   HYPERFINE CALCULATION
      AGEFF = SQRT(AZ*AZ*GZC*GZC + AX*AX*GXC*GXC + AY*AY*GYC*GYC)
      TROUBL =(AZ*AZ - 0.5*(AX*AX + AY*AY))/(AGEFF/GEFF)
      FIELD = FRQ/1.4/GEFF - ZCOMP*AGEFF/GEFF**2/1.4
     1 -((ZMAX**2 - 1.)/4. - ZCOMP**2)*(AX*AX + AY*AY)*
     2 (AZ*AZ*GEFF**2/AGEFF**2 + 1.)/(11.2*FRQ*GEFF)
     3-TROUBL**2/(2.8*FRQ*GEFF)*STHETA**2*CTHETA**2*ZCONP**2
C   THE 'TROUBL' TERM IS IMPORTANT ONLY WHEN AZ - APERP IS LARGE.
 202  CONTINUE
      IF(ISHFS) 18, 19, 18
 18   DO 20 K=1,24
C   SUPERHYPERFINE CALCULATION
      IF(JSHFS(K)) 21, 22, 21
 21   KMAX = K
 20   CONTINUE
 22   CONTINUE
      HSHFS = ASHFS/1.4/GEFF
      FKMAX = KMAX
      DO 23 K=1,KMAX
      FK = K
      FSHFS = JSHFS(K)
       J = (FIELD + HSHFS*((FKMAX+1.)/2.-FK) - HMIN)/HFINE
      IF (J) 98,98,25
 25   IF(J - NSLOT) 26, 26, 98
 98   WRITE (3,1010) J
C   PRINT ERROR MESSAGE.  J INDICATES FIELD POSITION OF UNPLOTTED
C   TRANSITION.
 1010 FORMAT (47H TRANSITION OUTSIDE ESTIMATED FIELD RANGE.  J=  I5)
      GO TO 24
 26   IF (L - 1) 29,29,28
 28   IF (L - 11) 27,29,27
  27  DISTR(J) = DISTR(J) + FSHFS*STHETA
  29 'DISTR(J) = DISTR(J) + FSHFS*STHETA
 24   CONTINUE
 23   CONTINUE
```

```
      GO TO 40
 19   J = (FIELD - HMIN)/HFINE
      IF (J) 99,99,35
 35   IF (J - NSLOT) 36,36,99
 99   WRITE (3,1010) J
      GO TO 34
 36   IF (L - 1) 39,39,38
 38   IF (L - 11) 37,39,37
 37   DISTR(J) = DISTR(J) + STHETA
 39   DISTR(J) = DISTR(J) + STHETA
 34   CONTINUE
 40   CONTINUE
      THETA = THETA + ANGINC
      RTHETA = THETA*0.0174533
 17   CONTINUE
 12   CONTINUE
 11   CONTINUE
C  NOW PROCEED TO THE CONVOLUTION.  RESULT IS THE DERIVATIVE
C   OF A GAUSSIAN
      NBROAD= 2*(NSLOT/10) + 1
C  THE MAXIMUM BREADTH CALCULATED FOR ANY ONE SPIN IS 1/5 HRANGE.
      NMID = NBROAD/2 +1
      BROAD(NMID) = 0.
      ALPHA = HFINE/WIDTH
      DO 50 I=2,NMID
      FI = I - 1
      K = I + NMID - 1
      BROAD(K) = -FI*EXP(-.693*FI*FI*ALPHA*ALPHA)
      J = NMID - I + 1
      BROAD(J) = -BROAD(K)
      IF (BROAD(J) + .01) 51,51,50
C  THE BROADENING FUNCTION IS COMPUTED TO .01 OF MAXIMUM HEIGHT.
 50   CONTINUE
 51   CONTINUE
      DO 52  J = 1, NSLOT
      FJ = J
      GAUSS(J) = HFINE*FJ + HMIN
      DO 53 I=1,NBROAD
      IF(BROAD(I)) 54, 53, 54
 54   K = J + NMID - I
      IF(K) 53, 53, 55
 55   IF(K - NSLOT) 56, 56, 53
 56   IF(DISTR(K)) 53, 53, 57
 57   DERIV(J) = DERIV(J) + DISTR(K)*BROAD(I)
 53   CONTINUE
 52   CONTINUE
      IF(IABSOR) 59, 61, 59
C  INTEGRATE DERIV TO GET ABSORP.
 59   ABSORP(1) = 0.
      DO 60 J=2,NSLOT
      ABSORP(J) = ABSORP(J-1) + DERIV(J-1)
 60   CONTINUE
 61   CONTINUE
C  COMPUTATION IS FINISHED. PROCEED TO PLOT.
      IF(IQK) 62, 63, 62
 62   CALL QKPLOT(GAUSS, DERIV)
      IF (IABSOR) 64, 63, 64
 64   CALL QKPLOT(GAUSS, ABSORP)
 63   CONTINUE
      IF(IGO) 65, 66, 65
 65   CALL GDPLOT (GAUSS, DERIV, EXGAUS, EXDATA)
      IF(IABSOR) 67, 66, 67
 67   CALL GDPLOT (GAUSS, ABSORP, EXGAUS, EXDATA)
 66   CONTINUE
      IF(IQK-10000) 10, 68, 68
 68   STOP
      END
      END
```

```
$IBFTC QKPLOT  LIST,REF
      SUBROUTINE QKPLOT(P,Q)
C  THIS SUBROUTINE WILL COMPRESS THE MAIN PROGRAM ARRAY (P,Q),
C  DIMENSIONS UP TO 1050 X 1050, INTO A 100 X 50 GRID.
C  ONLY SLOWLY VARYING FUNCTIONS ARE HANDLED WELL.
C
      DIMENSION P(1),Q(1),XGRID(11),YGRID(11),GRID(101),TITLE(12),
     1  X(1050),Y(1050)
      COMMON /CCPOOL/ XMIN,XMAX,YMIN,YMAX,CCXMIN,CCXMAX,CCYMIN,CCYMAX
      COMMON TITLE, FRQ, WIDTH, GZ, GX, GY, AZ, AX, AY, ASHFS, HRANGE,
     1 HMIN, NSLOT, IEXPT, NEXPT
      IF(ISTART) 301,302,301
  301 ISTART = 0
      IF(IEXPT) 310,311,310
  310 ITITLE = 1
      GO TO 312
  302 CONTINUE
  311 ITITLE = 0
  312 CONTINUE
      IF(ITITLE)151,151,150
  150  WRITE (3,123) TITLE
  123  FORMAT (1H1,12A6/20H EXPERIMENTAL CURVE      )
C  TITLE AND CURVE DESIGNATION WILL BE WRITTEN AT THE TOP OF THE PAGE.
      NUM = NEXPT
      GO TO 153
  151  WRITE (3,128) TITLE, GZ, GX, GY, AZ, AX, AY, WIDTH, FRQ, ASHFS
  128 FORMAT(1H1,12A6/6X,2HGZ,1OX,2HGX,10X,2HGY,10X,2HAZ,10X,2HAX,10X,2H
     1AY,9X,5HWIDTH,5X,9HFREQUENCY,5X,5HASHFS/1H ,9F12.4//)
      NUM = NSLOT
  153  CONTINUE
      XMIN = HMIN
      XMAX = HMIN + HRANGE
C  THE ARRAY (P,Q) IS DUPLICATED BY (X,Y), WHICH IS THEN SORTED
C  IN ORDER OF DESCENDING Y.
      DO 205 M = 1, NUM
      X(M) = P(M)
      Y(M) = Q(M)
  205 CONTINUE
      NM = NUM - 1
      DO 15 J = 1, NM
      IND = 0
      K = NUM - J
      DO 10 I = 1, K
      IF (Y(I).GE.Y(I+1)) GO TO 10
      S = Y(I)
      T = X(I)
      Y(I) = Y(I + 1)
      X(I) = X(I + 1)
      Y(I + 1) = S
      X(I + 1) = T
      IND = 1
   10 CONTINUE
      IF (IND.EQ.0) GO TO 20
   15 CONTINUE
   20 T1 = (XMAX - XMIN) / 10.
      YMAX = Y(1)
      YMIN = Y(NUM)
      T2 = (YMAX - YMIN) / 10.
      XGRID(1) = XMIN
      YGRID(1) = YMAX
      DO 25 I = 2, 11
      XGRID(I) = XGRID(I - 1) + T1
   25 YGRID(I) = YGRID(I - 1) - T2
      BLNK = BLANK(D)
```

XBL 670-5037

```
      DO 40 I = 1,2
   40 WRITE (3, 45)
   45 FORMAT (20X, 1H*, 10(9X, 1H*))
      L = 1
      M = 1
      DO 65 K = 1, 10
      DO 50 I = 1, 101
   50 GRID(I) = BLNK
      A = FLOAT(M)
      Q = (YMAX * (51. - A) + YMIN * (A - 1.))/ 50.
      DO 53 IL = 1, NUM
      IF (ABS(Q - Y(IL)) - (YMAX - YMIN) / 100.) 41, 53, 53
   41 IXP = 100. * (X(IL) - XMIN) / (XMAX - XMIN) + 1.5
   51 GRID(IXP) = XXXXX(D)
   53 CONTINUE
   52 WRITE (3,75) YGRID(L),(GRID(I), I = 1, 101)
      N = M + 1
      M = N + 3
      DO 60 J = N, M
      DO 55 I = 1, 101
   55 GRID(I) = BLNK
      A = FLOAT(J)
      Q = (YMAX * (51. - A) + YMIN * (A - 1.))/ 50.
      DO 57 IL = 1, NUM
      IF (ABS(Q - Y(IL)) - (YMAX - YMIN) / 100.) 46, 57, 57
   46 IXP = 100. * (X(IL) - XMIN) / (XMAX - XMIN) + 1.5
   56 GRID(IXP) = XXXXX(D)
   57 CONTINUE
   60 WRITE (3,76)(GRID(I), I = 1, 101)
      M = M + 1
   65 L = L + 1
      DO 66 I = 1, 101
   66 GRID(I) = BLNK
      DO 72 IL = 1, NUM
      IF (ABS(YMIN - Y(IL)) - (YMAX - YMIN) / 100.) 69, 72, 72
   69 IXP = 100. * (X(IL) - XMIN) / (XMAX - XMIN) + 1.5
   70 GRID(IXP) = XXXXX(D)
   72 CONTINUE
   71 WRITE (3,75) YGRID(11),(GRID(I), I = 1, 101)
   75 FORMAT (6X,F12.6,2X,101A1)
   76 FORMAT (20X, 101A1)
      DO 80 I = 1,2
C  THESE FORMATS EXTEND THE GRAPH 3 LINES BEYOND USUAL PAGE OVERFLOW.
C  THE LRL 7094 ALLOWS THIS, BUT OTHER MACHINES MAY REQUIRE
C  OVERFLOW CONTROL.
   80 WRITE (3, 45)
      WRITE (3,85) (XGRID(I), I = 1, 11)
   85 FORMAT (14X, 11(F9.2, 1X)/1H1)
      RETURN
      END
$IBMAP CONST
C  THESE CONSTANTS (BLANK AND XXXXX),WRITTEN IN MAP LANGUAGE,
C  MUST BE INCLUDED WITH QKPLOT.
      ENTRY BLANK
      ENTRY XXXXX
BLANK SAVE
      CLA =0606060606060
      RETURN BLANK
XXXXX SAVE
      CLA =0676767676767
      RETURN XXXXX
      END
```

XBL 670-5038

```
$IBFTC GDPLOT  LIST,REF
      SUBROUTINE GDPLOT (X,Y,U,V)
C
      DIMENSION X(1000), Y(1000), U(1050), V(1050), TITLE(12)
      COMMON /CCPOOL/ XMIN,XMAX,YMIN,YMAX,CCXMIN,CCXMAX,CCYMIN,CCYMAX
      COMMON TITLE, FRQ, WIDTH, GZ, GX, GY, AZ, AX, AY, ASHFS, HRANGE,
     1 HMIN, NSLOT, IEXPT, NEXPT
      IF(IPLOT) 10, 11, 10
 10   NPLOT = 0
      IPLOT = 0
      CALL CCRGN
 11   NPLOT = NPLOT + 1
      XMIN = HMIN
      XMAX = HMIN + HRANGE
      YMAX = Y(1)
      YMIN = Y(1)
      DO 1 J = 2,NSLOT
      IF(Y(J) - YMAX) 5, 5, 6
 6    YMAX = Y(J)
 5    IF(Y(J) - YMIN) 7, 1, 1
 7    YMIN = Y(J)
 1    CONTINUE
      YLO = YMIN
      YHI = YMAX
      CCXMAX = 1570./1024.
      CALL CCLTR(0.,.02,0.2,NPLOT,6)
      CALL CCLTR(.2,.02,0.2,TITLE,48)
      CALL CCGRID(1,15,1,6HNOLBLS,1,10,1)
      CALL CCPLOT(X,Y,NSLOT,4HJOIN)
      IF(IEXPT) 16, 15, 16
 16   IF(NPLOT-1) 80, 80, 81
 80   CONTINUE
      VMAX = V(1)
      VMIN = V(1)
      DO 71 J = 2,NEXPT
      IF(V(J) - VMAX) 75, 75, 76
 76   VMAX = V(J)
 75   IF(V(J) - VMIN) 77, 71, 71
 77   VMIN = V(J)
 71   CONTINUE
 81   CONTINUE
      YMAX = VMAX
      YMIN = VMIN
      CALL CCPLOT(U,V,NEXPT,6HNOJOIN,8,1)
 15   CONTINUE
      CALL CCNEXT
      WRITE(3,100) NPLOT,TITLE,GZ,FRQ,GX,WIDTH,GY,YLO,AZ,YHI,AX,HMIN,
     1             AY,XMAX,ASHFS,NSLOT
 100  FORMAT (1H1,A6/1H ,12A6/4H GZ=,F12.4,6X,6H FREQ=,F10.4/
     1  4H GX=,F12.4,6X,7H WIDTH=,F9.4/4H GY=,F12.4,6X,3H Y=,F13.6/
     2  4H AZ=,F12.4,6X,4H  TO,F12.6/4H AX=,F12.4,6X,6H HMIN=,F10.4/
     3  4H AY=,F12.4,6X,6H HMAX=,F10.4/
     4  7H ASHFS=,F9.4,6X,11H NUM SLOTS=,I4///)
      RETURN
      END
```

XBL 670-5039